

NONCLASSICAL PROPERTIES FROM FREQUENCY MODULATION IN TRAPS AND OF MICROMASER FIE

A Thesis submitted for the degree of
Doctor of Philosophy

by
S. Arun Kumar



School of Physics
University of Hyderabad
Hyderabad - 500 046
INDIA
August 1995

DECLARATION

I hereby declare that the matter embodied in this Thesis is the result of investigations carried out by me in the School of Physics, University of Hyderabad, Hyderabad - 500 046, under the supervision of Professor G.S. Agarwal.

Place: Hyderabad

Date: 31.08.1995




(S. Arun Kumar)


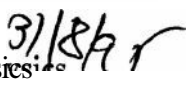
CERTIFICATE

This is to certify that the work contained in this thesis entitled, "Nonclassical properties from frequency modulation in traps and of micromaser field", has been carried out by Mr. S. Arun Kumar, under my supervision for the full period prescribed under Ph.D. ordinances of the University and the same has not been submitted for the award of research degree of any University.

Place:Hyderabad

Date:31.08.95


Thesis supervisor


Dean

School of Physics
University of Hyderabad,
Hyderabad - 500 046, INDIA.

ACKNOWLEDGEMENTS

It gives me great pleasure to thank Professor G.S. Agarwal for his guidance and patient teaching. He has been extremely kind and understanding. His dedication and efficiency in work has been a great inspiration for me. I am greatly indebted to him.

I would like to thank Professors V. Srinivasan, S. Chaturvedi, S.P. Tewari, Drs. S. Dutta Gupta, D. Narayana Rao and all the faculty of the School who have taught me and helped me. I wish to thank Drs. Ashok Chatterjee and Prashanth Panigrahi for giving me the much needed encouragement and enthusiasm. I am thankful to all my teachers and friends of my school and college days. I would also like to thank the Dean, School of Physics, for allowing me to use all the facilities available at the School. I also wish to thank the authorities of the University of Hyderabad, for providing various facilities.

I am very grateful to all my colleagues and friends, especially Rajan, Tara, Jyotsna, Mandaar, Ashoka, Nirmal, Gautam, Harsha, Murali, R.P. Singh, Biplab, Shanta, Hari, Jolly, Soma, Ramana and a long list of friends for their constant support, understanding and friendship. I also wish to thank my seniors Drs. M. Sanjay Kumar, G.V. Varada and M. Krishna Kumari for their help and guidance during the initial stages.

I thank the Physical Research Laboratory, Ahmedabad, for providing computer and other facilities during the final stages of writing of the thesis. Especially, I would like to thank Dr. Arul Laxminarayan and Mr. Santhanam for their help during my stay at PRL.

I thank the Department of Science and Technology (DST), the Council of Scientific and Industrial Research (CSIR) and the National Laser Programme (NLP) for providing me with financial support during the tenure.

I thank my parents for their love, sacrifice and good wishes. I thank my brother, Arvind, my cousins Kiran and Rashmi and my aunt and uncle for their help. Finally, I wish to thank my wife, Anupama, who has been a great support inspite of enormous hardships she had to put up with during the writing of this thesis.

CURRICULUM - VITAE

Name : S. ARUN KUMAR

Date of Birth : 20-June-1965

Nationality : Indian

Marital status : Married

Educational Qualifications

Ph.D. : submitted thesis in August 1995
School of Physics, University of Hyderabad
Hyderabad, India

Master's Degree : May 1989, M.Sc. in Physics
University of Hyderabad, Hyderabad, India.

Bachelor's Degree ; May 1987, B.Sc.Ed.
Regional College of Education, University of Mysore,
Mysore, India.

List of Publications

1. "Exact Quantum-Statistical Dynamics of an Oscillator with Time-Dependent Frequency and Generation of Nonclassical states", Phys. Rev. Lett. 67, 3665 (1991).
2. "Squeezed and Nonclassical states due to Frequency changes in Harmonic Oscillators", *Recent Developments in Quantum Optics*, Proceedings of the International Conference on Quantum Optics held at Hyderabad, edited by Ramarao Inguva (Plenum, New York, 1993) p 269.
3. "Quantised Motion of an ion in a Paul Trap", Proceedings of National Laser Symposium", I.I.T., Madras, February 17-19, 1993, p 191.

4. "Intensity-intensity correlations for the micromaser Spectral and antibunching characteristics", Phys. Rev. A 50, 680 (1994).

Talks delivered

1. "Squeezing due to Time Dependent Frequency in Harmonic Oscillators" in LAMP seminar conducted during "Topical Workshop on Coherent Atom-Radiation Interactions", held at the International Centre for Theoretical Physics, Trieste, Italy, February 24 to March 6, 1992.
2. "Quantised Motion of an ion in a Paul Trap" in "Coherent States: New Developments and Perspectives", held at the University of Hyderabad, Hyderabad, India, October 29-31, 1993.
3. "Production of Nonclassical Radiation by Moving Mirrors" in "Discussion Meeting on Nonclassical Aspects of Radiation", held at the Indian Institute of Science, Bangalore, India, January 10-12, 1994.
4. "Generation of Nonclassical Light by Moving Mirrors" in "National Workshop on Recent Advances in Quantum Optics", held at the Centre for Advanced Technology, Indore, India, March 7-10, 1994,

Conferences, Symposia and Workshops attended

1. "Second IPA/DST Symposium on Lasers and Applications", held at The Benaras Hindu University, Varanasi, India, December 11-15, 1989.
2. "Workshop on Geometric Phases in Physics", held at the Institute of Mathematical Sciences, Madras, India, October 7-11, 1990.
3. "Tutorial School on Modern Developments in Optics", held at the Indian Institute of Science, Bangalore, India, June 18-30, 1990.

4. "International Workshop on Lasers and their Applications", held at the Centre for Advanced Technology, Indore, India, November 12-30, 1990.
5. "International Conference on Quantum Optics", held at the University of Hyderabad, Hyderabad, India, January 5-10, 1991
6. "Third Training College on Physics and Technology of Lasers and Optical Fibres", held at the International Centre for Theoretical Physics, Trieste, Italy, January 27 to February 21, 1992.
7. "Topical Workshop on Coherent Atom-Radiation Interactions", held at the International Centre for Theoretical Physics, Trieste, Italy, February 24 to March 6, 1992.
8. "National Laser Symposium", held at the Indian Institute of Technology, Madras, India, February 17-19, 1993.
9. "Hyderabad Symposium on Recent Advances in Quantum Optics", held at the University of Hyderabad, Hyderabad, India, March 19-20, 1993.
10. "Coherent States: New Developments and Perspectives", held at the University of Hyderabad, Hyderabad, India, October 29-31, 1993.
11. "Discussion Meeting on Nonclassical Aspects of Radiation", held at the Indian Institute of Science, Bangalore, India, January 10-12, 1994.
12. "National Workshop on Recent Advances in Quantum Optics", held at the Centre for Advanced Technology, Indore, India, March 7-10, 1994.

Table of Contents

| | |
|--|------------|
| List of Figures | xii |
| Abstract | xv |
| 1 Introduction | 1 |
| 1.1 Photon antibunching | 9 |
| 1.2 Sub-Poisson photon statistics | 11 |
| 1.3 Squeezing | 13 |
| References | 17 |
| 2 Generation of nonclassical states by time-dependent perturbations on oscillator | 20 |
| 2.1 Exact analytical approach | 21 |
| 2.2 Linear sweep of ω^2 , a specific case. | 29 |
| 2.3 Numerical approach. | 31 |
| 2.4 Demonstration of nonclassical properties. | 32 |
| 2A Calculation of the matrix element $\langle n S m \rangle$ | 39 |
| References | 42 |
| 3 Quantised motion of an ion in a Paul trap | 44 |
| 3.1 Paul trap. | 45 |
| 3.1.1 Secular approximation | 48 |
| 3.1.2 Floquet solution. | 49 |

| | | |
|-----------|---|------------|
| 3.2 | Quantum dynamics | 52 |
| 3.3 | Dynamics in the Schrodinger picture. | 55 |
| 3.4 | External perturbations and the transitions caused by the electromagnetic field. | 58 |
| 3A | Scaling of Gaussians | 64 |
| | References | 66 |
| 4 | Nonclassical light generation in a cavity of variable length | 68 |
| 4.1 | The model | 69 |
| 4.2 | Specific case: demonstration of squeezing. | 74 |
| 4A | Derivation of α_{nk} and β_{nk} | 80 |
| | References | 82 |
| 5 | Intensity-Intensity Correlations for Micromaser | 83 |
| 5.1 | Micromaser | 84 |
| 5.2 | Two-photon intensity-intensity correlations for the micromaser field .. . | 89 |
| 5.2.1 | Calculation of G | 90 |
| 5.2.2 | Calculation of I | 92 |
| 5.3 | Numerical results for different types of two-photon correlations. | 92 |
| 5.4 | Probe of the intensity correlations for the micromaser field | 101 |
| 5A | Eigenvalue method | 106 |
| 5B | Green's function approach | 108 |
| | References | 111 |
| 6 | Quasiprobability distributions for the micromaser field | 113 |
| 6.1 | Quasiprobability distributions. | 113 |

| | | |
|------------|---|------|
| 6.1.1 | Q-function | .111 |
| 6.1.2 | Wigner function | .115 |
| 6.1.3 | Glauber-Sudarshan P -function | .115 |
| 6.2 | Trapping states and quasiprobability distributions for the micromaser field | 116 |
| References | | 128 |

List of Figures

| | | |
|-----|---|----|
| 1.1 | A typical Hanbury Brown-Twiss type setup. | 9 |
| 1.2 | The family of minimum uncertainty states. | 14 |
| 2.1 | Form of the function $\beta(t)$. The sudden limit corresponds to $\lim_{T \rightarrow 0}$ and the adiabatic limit to $\lim_{T \rightarrow \infty}$ | 29 |
| 2.2 | The variance of the quadrature \hat{X} versus time, τ for an oscillator initially in the ground state. The parameters are: $\beta_0 = 1$ and $\omega T = (a)10^{-3}, (b)1, (c)3$ and $(d)10^3$. The cases (a) and (d) correspond, respectively, to sudden and adiabatic limits. | 34 |
| 2.3 | Same as Fig.2.2, but with the oscillator initially in a squeezed coherent state $ \alpha, \zeta\rangle$ with $a = 1$ and $\zeta = 0.5e^{i\pi}$ | 35 |
| 2.4 | The phases of u (curve (a)), v (curve (b)) and μ (curve (c)) versus time, τ corresponding curve (6) of Fig.2.2. As the phases are non-zero for most of the time, the quadratures X and P are correlated most of the time. . . | 36 |
| 2.5 | Wigner function $\Phi(\alpha, \alpha^*, \tau)$ with $a = (X) + i(P)$ for the system initially in vacuum state for $\omega T = 10^{-3}$, $\beta_0 = 1$ and $\tau = 1.1$ which corresponds to the minimum in Fig.2.2. Squeezing in the quadrature X can be seen in the inset which shows contours of constant values of the Wigner function. . . | 37 |
| 2.6 | Mandel's Q -parameter as a function of t for the case of an oscillator initially in a coherent state $ \alpha\rangle, \alpha = 1$. The parameter ωT has been chosen as $(a)10^{-3}, (b)1, (c)3$ and $(d)10^3$ | 38 |
| 3.1 | A schematic of a Paul trap | 47 |
| 3.2 | Stability regions for the Mathieu equation | 61 |

| | | |
|-----|--|----|
| 3.3 | The uncertainty in the position of the ion as a function of time. The corresponding parameters are $a = 0.04, q = 0.2$ and $\frac{\omega_0}{\Omega} =$ (a) 1, (b) 0.5, (c) 0.1, (d) 0.01. The initial state is the vacuum. | 62 |
| 3.4 | Wigner function at a later time when the initial state (at $\tau = 0$) is a coherent state with $a = 1, a = 0.04, q = 0.2$ and $\omega_0/\Omega = 0.1$ | 63 |
| 4.1 | An "in-out" motion. | 70 |
| 4.2 | Trajectory of the mirror corresponding to $R_{in}(\zeta)$ given by (4.29). | 77 |
| 4.3 | Spectrum of photons created due to the mirror motion. | 78 |
| 4.4 | Demonstration of squeezing in the cavity. | 79 |
| 5.1 | A typical micromaser setup. | 86 |
| 5.2 | Normalised spectrum $\mathcal{G}(\omega - \omega_c)/\mathcal{G}(0)$ as a function of $(\omega - \omega_c)/\gamma$ for $N = 20, n_b = 1$ and for (a) $g\tau = 0.3, (b) g\tau = 1$ and (c) $g\tau = 3$ | 93 |
| 5.3 | Exact numerical linewidth D/γ as a function of the pump parameter $\theta = \sqrt{N}g\tau$ for $N = 20$ and $n_b = 1$ | 94 |
| 5.4 | Real part of the first five eigenvalues of (5.18) corresponding to the correlation function $\mathcal{G}(t)$ (5.23) as a function of the pump parameter $\theta = \sqrt{N}g\tau$ for $N = 20$ and $n_b = 1$ | 96 |
| 5.5 | Weights ($ W_a $) of the eigenvalues contributing to the spectrum $G(\omega - \omega_c)$ for $N = 20, n_b = 1, (a) g\tau = 0.3, (b) g\tau = 1, (c) g\tau = 3$ and (d) $g\tau = 7$ | 97 |
| 5.6 | Time dependence of the logarithm of the correlation function $\mathcal{G}(t)$ for $N = 20, n_b = 1$ and $g\tau = 1$. The dashed curves correspond to the two eigenvalues (cf Fig. 5.5(b)). | 98 |
| 5.7 | Comparison between the exact linewidth D/γ (solid curve) and the approximate analytical expression (5.40) (dashed curve), for $N = 50$ and $n_b = 10^{-4}$ | 99 |

- 5.8 Time dependence of the quantity $[\mathcal{I}(t), \mathcal{I}(0)] - 1$ for $N = 200$, $n_b = 0.1$ and $\theta = 1.5p$. Inset shows the Mandel's Q-parameter, $Q = (\langle \hat{a}^\dagger \hat{a}^2 \rangle - \langle \hat{a}^\dagger \hat{a} \rangle^2) / \langle \hat{a}^\dagger \hat{a} \rangle$, plotted as function of the pump parameter q for the same parameters N and n_b 100
- 5.9 Same as Fig.5.4, but corresponding to the correlation function $\mathcal{I}(t)$ (5.24). 102
- 6.1 Mean photon number $\langle n \rangle$ versus the pump parameter θ in units of p for $n_b = 0.1$ and $N = 200$. Inset shows the photon number distribution, p_n for values of the pump parameter corresponding to the labels a , ($\theta = 2.14$) and b , ($\theta = 3.88$) in the main figure 118
- 6.2 Mandel's Q-parameter (solid curve) and the A_3 parameter (dashed curve) as functions of the pump parameter θ with $n_b = 1$ and $N = 100$ 121
- 6.3 Normalised mean value of the photon number versus the pump parameter. The pump parameter is varied through N . The dashed curve is from the semi-classical theory and the solid curve is from the micromaser theory calculated for $g = 18$ kHz and $\tau = 35$ ms 124
- 6.4 The Q-function (dashed curve) and the Wigner function (solid curve) corresponding to the three points (marked a , b , c) of Fig.6.3 125
- 6.5 Normalised mean value of the photon number versus the pump parameter for a range which shows the trapping states ($n_b = 10^{-4}$, $N = 100$). Inset shows the phase transition region, a magnification of the boxed portion of which is shown in the main figure. The dashed curves are calculated from the semi-classical theory. 126
- 6.6 The Q-function (dashed curve) and the Wigner function (solid curve) as functions of $|\alpha|^2$, and p_n as a function of n (dotted curve) for various points indicated by the labels ($a-i$) in the Fig.6.4. To highlight the peaks corresponding to the trapping state with $q = 1$, five times the value of the photon number distribution, p_n is plotted in plots (a) and (i). 127

ABSTRACT

The production and properties of nonclassical states continues to be of great interest. Nonclassical properties like antibunching, sub-Poissonian photon counting statistics and squeezing have been studied and experimentally observed in many systems. Central to these concepts is the quantum harmonic oscillator. In the second quantisation formalism of the electromagnetic field, it is seen that the electromagnetic field is a collection of harmonic oscillators. The main aim of this thesis is to study the generation of nonclassical states and their properties in the generic system of a quantum harmonic oscillator. A harmonic oscillator whose frequency is time dependent is considered which is then shown to manifest nonclassical properties. The results are then applied to specific quantum systems for which the harmonic oscillator forms a representative. Two specific systems are studied: (a) the quantised motion of an ion in a Paul trap and (b) production of photons in a one-dimensional cavity, one boundary of which executes an "in-out" motion.

Another fundamental system of great current interest and activity is that of a micromaser. The micromaser field exhibits many novel features which are not seen in conventional masers and lasers. The micromaser field is also rich in exhibiting nonclassical features. An extensive study of these properties of the micromaser field is carried out.

The outline of the thesis is as follows:

To begin with in the first chapter, the meanings of classicality and nonclassicality are defined, following which an introduction and overview of the nonclassical properties of radiation like antibunching, sub-Poissonian photon-counting statistics and squeezing is provided.

In the second chapter, a linear system with externally controllable parameters is considered. The system consists of a quantum harmonic oscillator Hamiltonian with its frequency being time dependent. The time dependence of the frequency is achieved through the restoring force being time dependent. The Heisenberg equations of motion for the quadrature operators X and P are solved and the *exact analytical solutions* for the

time dependence of the operators are obtained. The time dependence of the annihilation and creation operators defined in terms of the quadratures X and P is then determined. It is found that the time dependence of the annihilation and creation operators defines a Bogoliubov transformation, the coefficients of which are functions of time. Using this Bogoliubov transformation, the time evolution operator and the time dependence of the density matrix are obtained. The probability of the system to make a transition to the state $|n\rangle$ at time t given that at time $t = 0$ the system was in state $|m\rangle$ is calculated from the time evolution operator.

The quantum statistical characteristics of a system are also studied by quasiprobability distributions. A very large class of states of the harmonic oscillator have a Gaussian form for the Wigner function. The time evolution of the Wigner function of the system is obtained by using the Bogoliubov transformation. It is found that the Gaussian nature of the Wigner function remains intact even if the frequency of the oscillator is changed. The major finding of this study is that the system exhibits strong nonclassical nature when the frequency of the oscillator is changed suddenly, whereas, for adiabatic changes of the frequency there is no appreciable nonclassical nature. A linear sweep of the restoring force is considered and is solved as an example.

In the third chapter, as an application of the above generic system to a specific situation, the quantised motion of an ion in a Paul trap is considered. Paul trap is a device to trap ions in an effective attractive potential that is formed with a combination of a high frequency rf field and a dc field. The quantised motion of the ion in a Paul trap is described by an equation that is classically a Mathieu equation. By an exact solution of the Heisenberg equations of motion for the position and momentum of the ion, the time evolution operator, the density matrix and the Wigner function are determined. Explicit forms of the wave functions for the ground and excited harmonic oscillator states in the co-ordinate representation are also obtained. It is found that various initial states, as they evolve in time, show nonclassical properties like squeezing of fluctuations in the quadratures. It is shown that this approach is also useful in determining the strengths of

the sidebands in the fluorescence spectrum of the trapped ion. They are calculated from the consideration of Raman transitions in which the centre of mass motion is excited to a higher level by an external electromagnetic field.

Another related problem that is considered is that of the production of particles in the vicinity of a moving mirror. This problem has received considerable attention in the recent past in the context of particle creation. The present aim is to study the quantum statistical properties of the field so produced due to accelerated mirror motion and to look for nonclassical nature of the field. Thus in the fourth chapter, a simple model which consists of a quantised scalar field in a region bounded by two mirrors, one of which has an "in-out" motion is considered. Nonclassical properties of the field so produced inside such a cavity are studied. The field so produced shows squeezing and the modes inside the cavity are found to be correlated.

In the fifth chapter, a simple but extremely important and practically viable quantum system — a micromaser is considered. The micromaser is a practical realisation of the simplest model in Quantum Optics, viz., the Jaynes-Cummings Model (JCM). The field produced in a micromaser is highly nonclassical. The sub-Poissonian nature of the field was theoretically predicted and was later experimentally verified. The experimental observation of collapse and revival phenomena has also been reported. The phase sensitive properties of the micromaser field also shows very many interesting features. Recently a proposal has been made regarding the measurement of the linewidth of the micromaser field. In this chapter the intensity-intensity correlations of the micromaser field are calculated. Two types of intensity-intensity correlation functions are defined and then using the steady state photon statistics of the micromaser field and the quantum regression theorem these functions are calculated. These functions are also obtained numerically by using the standard continued-fraction method and by an equivalent eigenvalue approach. It is found that the two-photon linewidth increases as a function of the pump parameter and after a certain value starts decreasing. It also shows resonances which are associated with the existence of trapping states for those pump parameter values. From the

eigenvalue approach it is found that various eigenvalues contribute to the linewidth. In particular, the multi-exponential character of the correlation function and the antibunching character of the micromaser field are demonstrated. Finally, a proposal as to how one can probe such intensity-intensity correlations in a typical micromaser setup is given.

In the sixth and final chapter, a short description of quasiprobability distributions is given. Quasiprobability distributions, in addition to being computational tools, also provide insight into the quantum statistical aspects of a system. Two of the most important quasiprobability distributions, viz., the Q -function and the Wigner function are calculated for the micromaser field. Contrary to the equally important Glauber-Sudarshan P -function, these two distributions always exist as ordinary functions for any state of the system. Further, the Q -function has the property that it is strictly positive definite for any state. The Wigner function does not, however, share this property. Since the micromaser field density matrix remains diagonal the off-diagonal density matrix elements are zero. Hence the Q - and the Wigner functions are phase independent.

The micromaser has an unique feature unlike conventional masers and lasers. In addition to the initial maser transition the micromaser shows many abrupt jumps at approximately integer multiples of 2π of the pump parameter. The initial maser transition shows the characteristics of a continuous (second-order) phase transition whereas the subsequent transitions have the characteristics of a first-order phase transition. In these regimes the micromaser has very interesting bistable and hysteretic nature. The quasiprobability distributions are studied for the first order phase transition regimes of the micromaser. The very low temperature behaviour of the micromaser exhibits very sharp resonances due to the occurrence of trapping states. Following a brief description on trapping states the quasiprobability functions are studied for the pump parameter values corresponding to these trapping states.

Chapter 1

Introduction

The invention of the laser in the early sixties has spawned the birth of new fields such as nonlinear optics, laser spectroscopy and quantum optics- In a parallel development, the concept of coherence has evolved quite a bit and considerable effort has been expended to evolve a complete statistical description of any optical field. The theory of optical coherence basically deals with the statistical description of fluctuations, which are an inherent part of any field. Initially by coherence of a radiation only correlations between the electric field amplitude at two space-time points was implied. The classical theory of optical coherence based on the two-point correlations or the correlation measurements between field quantities which depend linearly on the field was sufficient to explain all interference and diffraction phenomena known at that time.

The importance of the study of higher-order correlation effects was realised after the experiments performed by R. Hanbury Brown and R.Q. Twiss [1], Light from a narrow-band thermal source was split by a beam-splitter and the split beams were made to be incident on two photomultiplier detectors. The coincidence rate in the detection of light in the two photomultipliers was then plotted as a function of the time delay introduced in one of the detector. If the light from the source was a stable wave with no intensity fluctuations, then one expects the coincidence rate to be independent of the time delay introduced. But it was found that there was an enhancement of correlated photocounts around zero time delay. This observation was explained by considering quantities which depend quadratically on the field variables. A general theory of coherence was then developed, applying the theory of stochastic processes and by considering higher-order

correlation functions [2-4].

Eventhough the importance of higher-order coherence functions was realised, the entire theory was done only in the classical footing, viz., by giving a classical description of the field. In 1963, Glauber introduced the quantum theory of optical coherence [5-7]. In the quantised picture of the electromagnetic field, the field is no longer a c-number, but is an operator satisfying certain commutation relations. In such a system, in addition to the conventional sources of noise, there is the unavoidable quantum noise arising basically due to the non-commutativity of the field operators. Glauber showed that, in addition to correct description of all classical phenomena, like Young's interference experiment and higher-order effects like the Hanbury Brown-Twiss experiment, new phenomena which cannot be described by classical description of fields can manifest.

In the second quantisation formalism, free electromagnetic field can be represented as a collection of uncoupled quantum harmonic oscillators, and the field Hamiltonian is

$$H = \sum_{\mathbf{k}} \hbar \omega_{\mathbf{k}} (\hat{a}_{\mathbf{k}}^{\dagger} \hat{a}_{\mathbf{k}} + \frac{1}{2}). \quad (1.1)$$

Here the operators $\hat{a}_{\mathbf{k}}$ and $\hat{a}_{\mathbf{k}}^{\dagger}$ are the annihilation and creation operators for the k th mode of the field. Thus the Hamiltonian for a single mode of angular frequency ω is

$$H = \hbar \omega (\hat{a}^{\dagger} \hat{a} + \frac{1}{2}). \quad (1.2)$$

The connection between the annihilation and creation operators and the position and momentum operators of the oscillator is

$$\begin{aligned} \hat{a} &= \sqrt{\frac{\omega}{2\hbar}} \hat{x} + i \sqrt{\frac{1}{2\hbar\omega}} \hat{p} \\ \hat{a}^{\dagger} &= \sqrt{\frac{\omega}{2\hbar}} \hat{x} - i \sqrt{\frac{1}{2\hbar\omega}} \hat{p}, \end{aligned} \quad (1.3)$$

where the Hamiltonian interms of the 'position', \hat{x} and 'momentum', \hat{p} , operators is

$$\hat{H} = \frac{\hat{p}^2}{2} + \frac{\omega^2 \hat{x}^2}{2}. \quad (1.4)$$

The mass m of the oscillator is taken to be unity. The operators a and a^\dagger satisfy the Bosonic commutation relation

$$[a, a^\dagger] = 1. \quad (1.5)$$

From elementary quantum mechanics we know that the operator $a^\dagger a$ corresponds to the number operator and the eigen states of which are the number states or the Fock states, $|n\rangle$. Thus,

$$\begin{aligned} H|n\rangle &= \hbar\omega\left(a^\dagger a + \frac{1}{2}\right)|n\rangle = E|n\rangle \\ &= \hbar\omega\left(n + \frac{1}{2}\right)|n\rangle. \end{aligned} \quad (1.6)$$

The Fock states form a complete set of states and any state of the Hilbert space of states of the oscillator can be represented in terms of the Fock states. The action of the annihilation (or lowering) operator is to lower the state $|n\rangle$ to $|n-1\rangle$ and that of the creation (or raising) operator is to raise the state $|n\rangle$ to $|n+1\rangle$. Thus,

$$a|n\rangle = \sqrt{n}|n-1\rangle \quad (1.7)$$

$$a^\dagger|n\rangle = \sqrt{n+1}|n+1\rangle \quad (1.8)$$

$$a|0\rangle = 0. \quad (1.9)$$

The states $|n\rangle$ are obtainable from $|0\rangle$ by the action of the creation operator, a^\dagger :

$$|n\rangle = \frac{(a^\dagger)^n}{\sqrt{n!}}|0\rangle. \quad (1.10)$$

In the Heisenberg picture the operators a and a^\dagger satisfy the equations of motion

$$\begin{aligned} i\hbar \frac{d\hat{a}(t)}{dt} &= [\hat{a}(t), \hat{H}] \\ i\hbar \frac{d\hat{a}^\dagger(t)}{dt} &= [\hat{a}^\dagger(t), \hat{H}], \end{aligned} \quad (1.11)$$

which have as solutions

$$\begin{aligned} \hat{a}(t) &= e^{-i\omega t}\hat{a}(0) \\ \hat{a}^\dagger(t) &= e^{i\omega t}\hat{a}^\dagger(0). \end{aligned} \quad (1.12)$$

Consider a quantised electromagnetic field of a single (angular) frequency, ω . The electric field operator, \mathbf{E} , can be represented in terms of the positive and negative frequency parts as

$$\mathbf{E}(t) = A(\hat{\mathbf{a}}e^{-i\omega t} + \hat{\mathbf{a}}^\dagger e^{i\omega t}), \quad (1.13)$$

where A is a constant (containing spatial dependence). We can define quadrature operators, \hat{X} and \hat{P} such that

$$\begin{aligned} X &= \frac{1}{2}(\hat{\mathbf{a}} + \hat{\mathbf{a}}^\dagger) \\ P &= \frac{i}{2}(\hat{\mathbf{a}}^\dagger - \hat{\mathbf{a}}). \end{aligned} \quad (1.14)$$

These operators satisfy the commutation relation

$$[\hat{X}, \hat{P}] = i. \quad (1.15)$$

In terms of the quadrature operators, (1.13) can be expressed as

$$\mathbf{E} = 2A(X \cos(\omega t) + P \sin(\omega t)). \quad (1.16)$$

For a quantised system, the measurable quantities like the electric field correlation between two space-time points are averages of relevant operators. This averaging is done with respect to a particular statistical state of the field. The state of the field is given by the density operator ρ and the average of a field quantity represented by the field operator O is given by

$$\langle \hat{O}(\hat{\mathbf{a}}, \hat{\mathbf{a}}^\dagger) \rangle = \text{Tr}\{\rho \hat{O}\}, \quad (1.17)$$

where the symbol $\langle \bullet \bullet \bullet \rangle$ represents the expectation value in the state ρ and "Tr" represents the tracing operation. The density operator approach facilitates the cases when the state is not pure, but is mixed. When the field is in a particular state, ρ , the uncertainty in the quadrature X is given by the square root of the variance

$$\langle (\Delta \hat{X})^2 \rangle = \langle (\hat{X} - \langle \hat{X} \rangle)^2 \rangle. \quad (1.18)$$

Let A and B be two **operators** whose commutator is non-zero. Let us define the deviations $\Delta A = A - \langle A \rangle$ and $\Delta B = B - \langle B \rangle$. The product of the **uncertainties** in the two operators, according to **Heisenberg** uncertainty principle is

$$\langle (\Delta \hat{A})^2 \rangle \langle (\Delta \hat{B})^2 \rangle \geq \frac{1}{4} |\langle [\hat{A}, \hat{B}] \rangle|^2. \quad (1.19)$$

A more general form of this uncertainty product exists, called the Schrodinger uncertainty relation [8,9]:

$$\langle (\Delta \hat{A})^2 \rangle \langle (\Delta \hat{B})^2 \rangle > \frac{1}{2} |\langle [\hat{A}, \hat{B}] \rangle|^2 + \frac{1}{4} \langle \Delta \hat{A} \Delta \hat{B} + \Delta \hat{B} \Delta \hat{A} \rangle^2 \quad (1.20)$$

$$> \frac{1}{2} |\langle [\hat{A}, \hat{B}] \rangle|^2 (1 + r^2), \quad (1.21)$$

where $r = \frac{\langle \Delta \hat{A} \Delta \hat{B} + \Delta \hat{B} \Delta \hat{A} \rangle}{\langle [\hat{A}, \hat{B}] \rangle}$ is called the correlation **co-efficient**. The Schrodinger uncertainty relation (1.20) is more general in the sense that in addition to non-commutativity of the operators it also takes into consideration the correlations between the two operators. In the classical limit, when the commutator of the two operators vanishes, the uncertainty product corresponds to the definition of covariance. On the other hand, when the two observables are uncorrelated, then the Schrodinger uncertainty relation reduces to that of the Heisenberg uncertainty relation.

In 1926, Schrodinger studied the conditions in which a quantum state of a system most closely corresponds to a classical state. In such a state we expect the uncertainties in $\hat{x}(t)$ and $\hat{p}(t)$ to be independent of time and be equally distributed between the position and momentum of the oscillator. To determine such a state, let us define operators $\Delta \hat{a}(t)$ and $\Delta \hat{a}^\dagger(t)$ as

$$\begin{aligned} \Delta \hat{a}(t) &= \hat{a}(t) - \langle \hat{a}(t) \rangle \\ \Delta \hat{a}^\dagger(t) &= \hat{a}^\dagger(t) - \langle \hat{a}^\dagger(t) \rangle. \end{aligned} \quad (1.22)$$

They satisfy the same commutation relations as a and a^\dagger . If we now determine the variances in the quadratures X and P , and the correlations between them, then

$$\langle (\Delta \hat{X}(t))^2 \rangle = \frac{1}{2} \{ \langle (\Delta \hat{a}(0))^2 \rangle e^{-2i\omega t} + \langle (\Delta \hat{a}^\dagger(0))^2 \rangle e^{2i\omega t} \}$$

$$\begin{aligned}
& + \langle \Delta \hat{a}^\dagger(0) \Delta \hat{a}(0) + \Delta \hat{a}(0) \Delta \hat{a}^\dagger(0) \rangle, \\
\langle (\Delta \hat{P}(t))^2 \rangle &= -\frac{1}{2} \{ \langle (\Delta \hat{a}(0))^2 \rangle e^{-2i\omega t} + \langle (\Delta \hat{a}^\dagger(0))^2 \rangle e^{2i\omega t} \\
& - \langle \Delta \hat{a}^\dagger(0) \Delta \hat{a}(0) + \Delta \hat{a}(0) \Delta \hat{a}^\dagger(0) \rangle \}
\end{aligned} \tag{1.23}$$

and

$$\frac{1}{\hbar} \langle \Delta \hat{X}(t) \Delta \hat{P}(t) + \Delta \hat{P}(t) \Delta \hat{X}(t) \rangle = \frac{i}{4} \{ \langle (\Delta \hat{a}^\dagger(0))^2 \rangle e^{2i\omega t} - \langle (\Delta \hat{a}(0))^2 \rangle e^{-2i\omega t} \}, \tag{1.25}$$

where the solutions (1.12) are used. If the uncertainties are to be time independent, then we require that both $\langle (\Delta \hat{a})^2 \rangle$ and $\langle (\Delta \hat{a}^\dagger)^2 \rangle$ be zero. The requirement that the dispersions in the two quadratures \hat{X} and \hat{P} be minimal then would demand a minimisation of the quantity $\langle \Delta \hat{a}^\dagger \Delta \hat{a} + \Delta \hat{a} \Delta \hat{a}^\dagger \rangle$. Since the operators $(\Delta \hat{a})$ and $(\Delta \hat{a}^\dagger)$ have identical commutation relations as \hat{a} and \hat{a}^\dagger , the operator $(\Delta \hat{a}^\dagger)(\Delta \hat{a}) + (\Delta \hat{a})(\Delta \hat{a}^\dagger)$ is isospectral to $\hat{a}^\dagger \hat{a} + \hat{a} \hat{a}^\dagger$, having an eigenvalue proportional to $(n + \frac{1}{2})$. Thus the quantity $\langle \Delta \hat{a}^\dagger \Delta \hat{a} + \Delta \hat{a} \Delta \hat{a}^\dagger \rangle$ will have its minimum value with $n = 0$. In this state, which gives the minimum uncertainty in the quadratures, we thus have

$$\Delta \hat{a} | \rangle \equiv (\hat{a} - \langle \hat{a} \rangle) | \rangle = 0. \tag{1.26}$$

If we define the expectation value of the operator \hat{a} as, $\langle \hat{a} \rangle = a$, then we find that the state which minimises the quadrature uncertainties is an eigenstate of the annihilation operator:

$$\hat{a} | \rangle = \alpha | \rangle. \tag{1.27}$$

The eigenstates of the annihilation operator \hat{a} play a very fundamental role in quantum optics as well as in many other fields [10]. They were first introduced and studied extensively by Glauber [5,6]. The minimum uncertainty state in (1-27) is written as $|\alpha\rangle$ and is called *coherent state* as the wavepacket corresponding to this state ‘coheres’ or maintains its shape [11]. Thus,

$$\begin{aligned}
\hat{a} |\alpha\rangle &= \alpha |\alpha\rangle \\
a &= \alpha_x + i\alpha_y, \quad \alpha_x, \alpha_y \in \mathbb{R}.
\end{aligned} \tag{1.28}$$

The coherent states, $|\alpha\rangle$, can be obtained by the action of the displacement operator, defined as $D(\alpha) = \exp(\alpha\hat{a}^\dagger - \alpha^*\hat{a})$, on the vacuum state, $|0\rangle$

$$D(\alpha)|0\rangle = \exp(\alpha\hat{a}^\dagger - \alpha^*\hat{a})|0\rangle = |\alpha\rangle. \quad (1.29)$$

Thus, we have

$$|\alpha\rangle = \exp(-\frac{1}{2}|\alpha|^2) \sum \frac{\alpha^n}{\sqrt{n!}} |n\rangle. \quad (1.30)$$

The coherent states are not orthogonal and they satisfy the completeness relation

$$1 = \int \frac{d^2\alpha}{\pi} |\alpha\rangle\langle\alpha|, \quad (1.31)$$

where $d^2\alpha = d\alpha_x d\alpha_y$ and the integration is over the whole of the α -plane.

One can express these averages of operators in terms of averages of classical functions by resorting to a particular operator ordering prescription [12,13]. When the operators are ordered in *normal* order, all creation operators are arranged to the left of all annihilation operators. Frequently, a set of colons are used to enclose operators to imply that the enclosed operator should be arranged in normal order. It should be noted that when this colon symbol is used, creation operators are all arranged to the left of annihilation operators, *with complete disregard* to the commutation relation between them. For example,

$$<:(\hat{a}^\dagger\hat{a})^2:> = \langle\hat{a}^{\dagger 2}\hat{a}^2\rangle \quad (1.32)$$

Anti-normal ordering of operators corresponds to arranging all creation operators to the *right* of all annihilation operators. *Symmetric* ordering of operators corresponds to the average of all possible ways of ordering operators.

Often it is useful to represent states and operators in terms of coherent states. If one represents the density operator of the field, ρ , in the "diagonal" coherent state representation (Glauber-Sudarshan P-representation) [6,14],

$$\rho = \int P(\alpha) |\alpha\rangle\langle\alpha| d^2\alpha, \quad (1.33)$$

Chapter 1. Introduction

using the "optical equivalence theorem" [14,15] one can then cast the average (1.17) of an operator O expressed in normal order as

$$\langle O \rangle = \int d^2\alpha O(\alpha, \alpha^*) P(\alpha). \quad (1.34)$$

For example,

$$\begin{aligned} \langle : (\hat{a}^\dagger \hat{a})^m : \rangle &= \langle \hat{a}^{\dagger m} \hat{a}^m \rangle \\ &= \int d^2\alpha P(\alpha) \alpha^{*m} \alpha^m \end{aligned} \quad (1.35)$$

Thus, the operator average of normally ordered products of operators is given by simple moments of the distribution $P(\alpha)$. Equation (1.34) has a formal resemblance to the evaluation of averages in classical statistics with $P(\alpha)$ taking the role of a phase space distribution. By definition, a classical phase space distribution is positive definite and non-singular. There are fields for which the distribution $P(\alpha)$ is strictly positive and non-singular. Such fields can be described by a classical description of the field and noise properties can be described by the application of classical statistics over an ensemble of classical fields. Such fields are said to have classical analogues. But, for some fields, the quantity $P(\alpha)$ in the diagonal coherent state representation of the state $\hat{\rho}$, is not positive or may be highly singular, more **singular** than a tempered distribution. In such a situation $P(\alpha)$ will be violating the requirements of classical statistics that the phase space distribution be positive definite and non-singular, and hence cannot be considered as a classical phase space distribution. Thus, states of the quantised field for which $P(\alpha)$ is non-positive or singular, are called non-classical states, as they have no classical analogues. A host of review articles have appeared on the topics of nonclassical light and squeezed states [16-26].

There are three ways in which the nonclassical nature of a field manifests, viz.,

1. photon antibunching
2. sub-Poissonian photon counting statistics, and

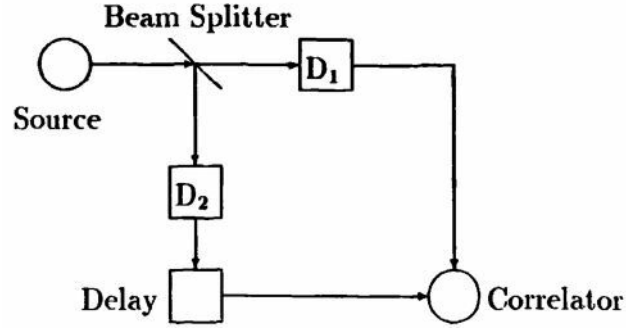


Figure 1.1: A typical Hanbury Brown-Twiss type setup

3. squeezing.

Let us now consider them one by one.

1.1 Photon antibunching

The phenomenon of photon antibunching was the first of the manifestations of the non-classical nature of radiation to be observed experimentally. Consider an experimental setup essentially similar to the Hanbury Brown-Twiss setup (see Fig. 1.1). Such a setup measures the quantity

$$G^{(2)}(t + \tau) = \langle : \hat{I}(t + \tau) \hat{I}(t) : \rangle \quad (1.36)$$

where

$$I(t) = \bar{E}^-(t) \bar{E}^+(t). \quad (1.37)$$

Thus,

$$G^{(2)}(t + \tau) = \langle \bar{E}^-(t) \bar{E}^-(t + \tau) \bar{E}^+(t + \tau) \bar{E}^+(t) \rangle. \quad (1.38)$$

If we have classical fields we can write (1.38) as

$$G^{(2)}(t + \tau) = \int dI_2 I_2(t + \tau) \int dI_1 I_1(t) P(I_2(t + \tau) I_1(t)), \quad (1.39)$$

where $P(I_2(t + \tau)I_1(t))$ is the probability that a photodetection event for I_2 occurs at $t + \tau$ given that a detection of I_1 occurs at t . With the application of Cauchy-Schwarz inequality ($|z_1 z_2| \leq |z_1| |z_2|$), we have

$$\int dI_2 \int dI_1 I_2(t + \tau) I_1(t) P(I_2(t + \tau) I_1(t)) < \sqrt{\int dI_2 I_2^2 P(I_2(t + \tau))} \sqrt{\int dI_1 I_1^2 P(I_1(t))} \quad (1.40)$$

where, $P(I(t))$ is the marginal distribution. In the steady state, we have

$$P(I) = \lim_{t \rightarrow \infty} P(I(t + \tau)) = \lim_{t \rightarrow \infty} P(I(t)) \quad (1.41)$$

and

$$G^{(2)}(\tau) = \lim_{t \rightarrow \infty} G^{(2)}(t + t) \quad (1.42)$$

and hence (1-40) can be written as

$$G^{(2)}(\tau) < G^{(2)}(0), \quad (1.43)$$

where $G^{(2)}$ is the steady state correlation function the slope of which is negative. Thus the photons tend to arrive in bunches and hence this is called bunching. All natural sources (chaotic) satisfy this inequality and any quantum field exhibiting this property has a classical analogue.

On the other hand, in the stationary condition if we have a field which violates the inequality (1-43) and has a positive slope, then

$$G^{(2)}(\tau) > G^{(2)}(0); \quad (1.44)$$

such an inequality will not be satisfied by any classical field and any field which satisfies (1.44) is genuinely quantum mechanical and does not have a classical analogue. From (1.44) it is evident that the probability of detecting coincident pair of photons is less than that from a fully coherent light field with Poissonian distribution of photons. In other words, the photons tend to arrive separate from one another and hence this effect is called *antibunching*. Thus any field exhibiting antibunching is a nonclassical field.

Antibunching is also referred to as violations of the Cauchy-Schwarz inequality in the literature, as the inequality (1.43) basically follows from the Cauchy-Schwarz inequality.

As an example of the situation where the nonclassicality of the field involved manifests antibunching, consider the phenomenon of resonance fluorescence from a single atom, which gave the first evidence of nonclassical nature of light. It was first pointed out by H. Carmichael and D.F. Walls [27,28] that such a field would exhibit strong antibunching and it was first experimentally demonstrated by H.J. Kimble et al. [29-31] and later by Cresser et al. [32].

In single-atom resonance fluorescence, radiation from an external source excites a single atom. When the atom has relaxed back to its ground state radiatively, it can radiate no further. Hence, if we perform a delayed coincidence experiment we would see the phenomenon of antibunching.

1.2 Sub-Poisson photon statistics

Another manifestation of nonclassical character is sub-Poissonian photon counting statistics. As against the situation for antibunching, instead of measuring the time intervals between the detection of photons, one can also encounter nonclassical nature in the direct photon detection experiments.

Consider the probability, $p(n)$, of recording n photocounts in a time interval t and $t + T$ with a detector of small area A , and quantum efficiency η , [33,34,7]

$$p(n) = \langle : \frac{W^n}{n!} e^{-W} : \rangle \quad (1.45)$$

where

$$W = \eta A \int_t^{t+\tau} \hat{I}(t') dt' \quad (1.46)$$

and

$$I(t) = \hat{E}^{(-)}(t) \hat{E}^{(+)}(t). \quad (1.47)$$

For very short counting times τ such that τ is much smaller than the coherence time and

Chapter 1. Introduction

and for a stationary field, we have

$$\langle (\Delta \hat{n})^2 \rangle = \langle \hat{n} \rangle + \eta^2 \mathcal{A}^2 \tau^2 \langle (\Delta \hat{I})^2 \rangle. \quad (1.48)$$

For the case of a classical field the ordering prescription in the second term is redundant and hence is always non-negative. Thus for fields which have classical analogues, the following inequality holds

$$\langle (\Delta \hat{n})^2 \rangle > \langle \hat{n} \rangle. \quad (1.49)$$

The equality in (1.49) implies that the photon number distribution is Poissonian. It holds for a coherent state, and is called the shot-noise level. Any field whose photon number distribution is *less* than the shot-noise level, then necessarily violates the inequality (1.49). This would mean that $\langle (\Delta \hat{I})^2 \rangle < 0$ which in turn can happen only if $P(\alpha)$ is negative. Thus any field which exhibits sub-Poissonian photon number statistics is a nonclassical state.

In order to quantify the amount of deviation from Poissonian distribution, the following quantity, called Mandel's Q-parameter has been introduced [35]:

$$Q = \frac{\langle \hat{n}^2 \rangle - \langle \hat{n} \rangle^2 - \langle \hat{n} \rangle}{\langle \hat{n} \rangle} \quad (1.50)$$

A value of $Q = 0$ means that the distribution is Poissonian ($\langle \hat{n}^2 \rangle - \langle \hat{n} \rangle^2 = \langle \hat{n} \rangle$). The Q-parameter vanishes when evaluated for a coherent state. A thermal state has $Q > 0$, and hence its distribution is larger than that of a Poissonian (super-Poissonian). If the Q-parameter takes negative values, then it is a signature of nonclassical nature and the width of the distribution is less than that of a Poissonian (sub-Poissonian).

The phenomenon of resonance fluorescence from a single atom, in addition to manifesting antibunching, also shows sub-Poissonian statistics. It was first observed by Short and Mandel [36]. This phenomenon has also been observed in a space-charge-limited Franck-Hertz setup by Teich and Saleh [37]. Constant-current-driven semiconductor laser [38] and light emitting diodes [39] have also shown sub-Poissonian statistics. In the process of parametric downconversion in a KD^*P crystal also sub-Poisson statistics is observed [40,41].

1.3 Squeezing

If we calculate the variance in the quadratures of the field in the vacuum or the coherent state, we find that the fluctuations in the two quadratures are equal and the Heisenberg uncertainty product between the quadrature operators is minimal. Thus,

$$\langle(\Delta\hat{X})^2\rangle_c = 1/4 = \langle(\Delta\hat{P})^2\rangle_c \quad (1.51)$$

States for which the uncertainty product is minimal:

$$\langle(\Delta\hat{X})^2\rangle_c \langle(\Delta\hat{P})^2\rangle_c = 1/16 \quad (1.52)$$

are called Minimum Uncertainty States (MUS). This minimal fluctuations in the quadratures is called the Standard Quantum Limit (SQL). These quantum fluctuations are randomly distributed in phase. However, there are states of the field for which the fluctuations in one quadrature are less than the SQL and correspondingly the other quadrature has increased fluctuations than the standard quantum limit. For these states the fluctuations are phase dependent. Such states are called *squeezed states*. The requirement for squeezing in the quadrature \hat{X} is then

$$\langle(\Delta\hat{X})^2\rangle_s < \langle(\Delta\hat{X})^2\rangle_c, \quad (1.53)$$

where the subscript V refers to the squeezed state average and the subscript 'c' refers to either coherent state or vacuum expectation values. Expressed in terms of normalised variance the squeezing condition (1.53) becomes

$$\langle:(\Delta\hat{X})^2: \rangle_s < 0. \quad (1.54)$$

Correspondingly, the fluctuations in the other quadrature, P, are larger than the SQL

$$\langle(\Delta\hat{P})^2\rangle_s > \langle(\Delta\hat{P})^2\rangle_c. \quad (1.55)$$

In terms of the operators a and a^\dagger , the variance in the quadrature X is

$$\begin{aligned} \langle(\Delta\hat{X})^2\rangle &= \langle(\hat{X} - \langle\hat{X}\rangle)^2\rangle \\ &= \langle[(\hat{a} - \langle\hat{a}\rangle) + (\hat{a}^\dagger - \langle\hat{a}^\dagger\rangle)]^2\rangle. \end{aligned} \quad (1.56)$$

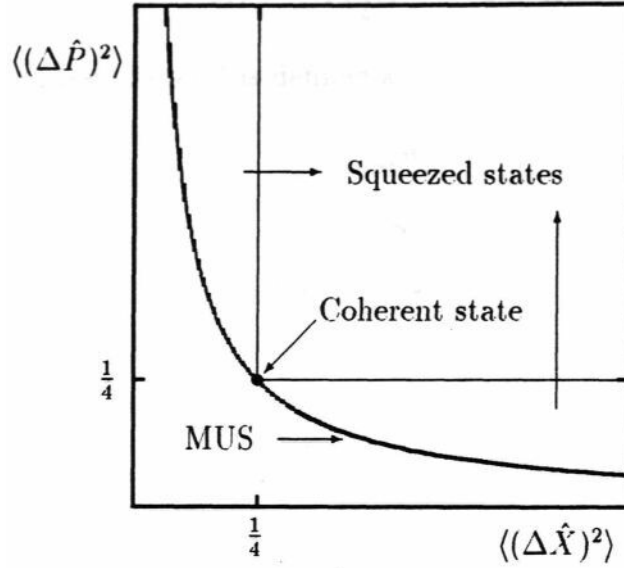


Figure 1.2: The family of minimum uncertainty states

Using the P-representation for the density operator, (1.56) can be written as

$$\langle(\Delta\hat{X})^2\rangle = \frac{1}{4} \left\{ 1 + \int d^2\alpha P(\alpha) \right\} \quad (1.57)$$

The condition (1.53) or (1.54) for squeezing of fluctuations in the X-quadrature, would then require that

$$\int d^2\alpha P(\alpha) [(\alpha + \alpha^*) - (\langle\alpha\rangle + \langle\alpha^*\rangle)]^2 < 0. \quad (1.58)$$

The quantity in the square brackets of the integrand cannot be negative, which only leaves the distribution $P(\alpha)$ to be negative. Thus squeezed states are nonclassical states, having no classical analogues.

If the squeezed states satisfy the condition (1.52) for minimum uncertainty, then such states are called *squeezed coherent states*. There exists a family of such squeezed coherent states (see Fig. 1.2). Coherent states are a special case of MUS for which the dispersions in both the quadratures are equal (phase independent).

Squeezed coherent states are generated by the action of a unitary squeezing operator

1.3 Squeezing

If we calculate the variance in the quadratures of the field in the vacuum or the coherent state, we find that the fluctuations in the two quadratures are equal and the Heisenberg uncertainty product between the quadrature operators is minimal. Thus,

$$\langle(\Delta\hat{X})^2\rangle_c = 1/4 = \langle(\Delta\hat{P})^2\rangle_c \quad (1.51)$$

States for which the uncertainty product is minimal:

$$\langle(\Delta\hat{X})^2\rangle_c \langle(\Delta\hat{P})^2\rangle_c = 1/16 \quad (1.52)$$

are called Minimum Uncertainty States (MUS). This minimal fluctuations in the quadratures is called the Standard Quantum Limit (SQL). These quantum fluctuations are randomly distributed in phase. However, there are states of the field for which the fluctuations in one quadrature are less than the SQL and correspondingly the other quadrature has increased fluctuations than the standard quantum limit. For these states the fluctuations are phase dependent. Such states are called *squeezed states*. The requirement for squeezing in the quadrature \hat{X} is then

$$\langle(\Delta\hat{X})^2\rangle_s < \langle(\Delta\hat{X})^2\rangle_c, \quad (1.53)$$

where the subscript V refers to the squeezed state average and the subscript 'c' refers to either coherent state or vacuum expectation values. Expressed in terms of normalised variance the squeezing condition (1.53) becomes

$$\langle(\Delta\hat{X})^2\rangle_s < 0. \quad (1.54)$$

Correspondingly, the fluctuations in the other quadrature, P, are larger than the SQL

$$\langle(\Delta\hat{P})^2\rangle_s > \langle(\Delta\hat{P})^2\rangle_c. \quad (1.55)$$

In terms of the operators a and a^\dagger , the variance in the quadrature X is

$$\begin{aligned} \langle(\Delta\hat{X})^2\rangle &= \langle(\hat{X} - \langle\hat{X}\rangle)^2\rangle \\ &= \langle[(\hat{a} - \langle\hat{a}\rangle) + (\hat{a}^\dagger - \langle\hat{a}^\dagger\rangle)]^2\rangle. \end{aligned} \quad (1.56)$$

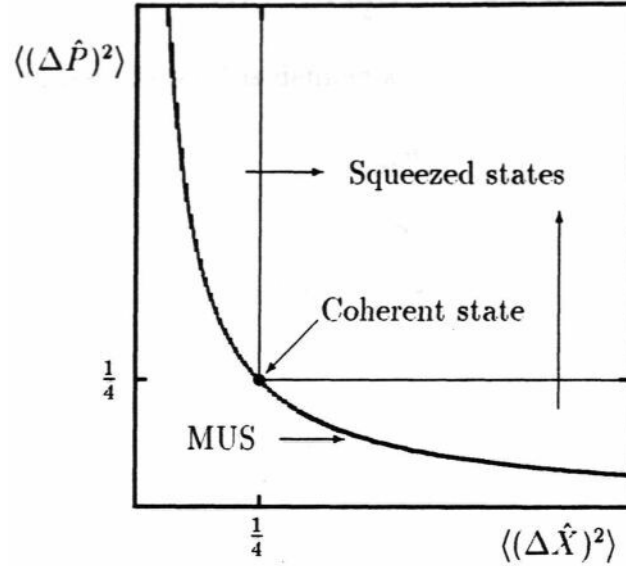


Figure 1.2: The family of minimum uncertainty states

Using the P-representation for the density operator, (1.56) can be written as

$$\langle(\Delta\hat{X})^2\rangle = \frac{1}{4} \left\{ 1 + \int d^2\alpha P(\alpha) \right\} \quad (1.57)$$

The condition (1.53) or (1.54) for squeezing of fluctuations in the X-quadrature, would then require that

$$\int d^2\alpha P(\alpha) [(\alpha + \alpha^*) - (\langle\alpha\rangle + \langle\alpha^*\rangle)]^2 < 0. \quad (1.58)$$

The quantity in the square brackets of the integrand cannot be negative, which only leaves the distribution $P(\alpha)$ to be negative. Thus squeezed states are nonclassical states, having no classical analogues.

If the squeezed states satisfy the condition (1.52) for minimum uncertainty, then such states are called *squeezed coherent states*. There exists a family of such squeezed coherent states (see Fig. 1.2). Coherent states are a special case of MUS for which the dispersions in both the quadratures are equal (phase independent).

Squeezed coherent states are generated by the action of a unitary squeezing operator

References

- [1] R. Hanbury Brown and R.Q. Twiss, *Nature* 177, 27 (1956).
- [2] E. Wolf, *Proceedings of the Symposium on Optical Masers*, (Polytechnic Press, Brooklyn, New York, 1963), p29.
- [3] L. Mandel and E. Wolf, *Rev. Mod. Phys.* 37, 231 (1965).
- [4] C.L. Mehta and E.C.G. Sudarshan, *Phys. Rev.* 138, B274 (1965).
- [5] R.J. Glauber, *Phys. Rev.* 130, 2529 (1963).
- [6] R.J. Glauber, *Phys. Rev.* 131, 2766 (1963).
- [7] R.J. Glauber, *Quantum Optics and Electronics*, edited by C. DeWitt, A. Blandin and C. Cohen-Tannoudji (Gordon and Breach, New York, 1965).
- [8] V.L. Man'ko, *Recent Developments in Quantum Optics*, Proceedings of the International Conference on Quantum Optics held at Hyderabad, edited Ramarao Inguva (Plenum, New York, 1993).
- [9] V.I. Man'ko, *Quantum Measurements in Optics*, edited by P. Tombesi and D.F. Walls, (Plenum, New York, 1992).
- [10] J.R. Klauder and Bo-Sture Skagerstam, *Coherent States: Applications in Physics and Mathematical Physics*, (World Scientific, Singapore, 1985).
- [11] M. Sargent, M.O. Scully and W.E. Lamb, *Laser Physics*, (Addison-Wesley, Massachusetts, 1974).
- [12] W.H. Louisell, *Quantum Statistical Properties of Radiation* (Wiley, New York, 1973).
- [13] C.W. Gardiner, *Quantum Noise* (Springer, Berlin, 1991).
- [14] E.C.G. Sudarshan, *Phys. Rev. Lett.* 10, 277 (1963).
- [15] J.R. Klauder and E.C.G. Sudarshan, *Fundamentals of Quantum Optics* (W.A. Benjamin, New York, 1968).
- [16] D.F. Walls, *Nature* 280, 451 (1979).

References

- [17] D.F. Walls, *Nature* 306, 111 (1983).
- [18] L. Mandel, *Physica Scripta* 112, 31 (1986).
- [19] Special issue of *J. Mod. Opt.* 34 (1987).
- [20] Special issue of *J. Opt. Soc. Am.* B4 (1987).
- [21] M.C. Teich and B.E.A. Saleh, *Progress in Optics*, Vol. 26, edited by E. Wolf, (North Holland, Amsterdam, 1988).
- [22] M.C. Teich and B.E.A. Saleh, *Quantum Optics* 1, 153 (1989).
- [23] *Squeezing and Nonclassical Light*, edited by P. Tombesi and E.R. Pike, (Plenum, New York, 1989).
- [24] K. Zaheer and M.S. Zubairy, *J. Mol. and Opt. Phys.* 28, 143 (1990).
- [25] Y. Yamamoto, S. Machida, S. Saito, N. Imoto, T. Yanagawa, M. Kitagawa and G. Bjork, *Progress in Optics*, v28, ed. E. Wolf (North-Holland, Amsterdam, 1990).
- [26] S. Reynaud, A. Heidmann, E. Giacobino and C. Fabre, *Progress in Optics*, Vol. 30, edited by E. Wolf, (North Holland, Amsterdam, 1992).
- [27] H.J. Carmichael and D.F. Walls, *J. Phys. B* 9, L43 (1976).
- [28] H.J. Kimble and L. Mandel, *Phys. Rev. A* 13, 2123 (1976).
- [29] H.J. Kimble, M. Dagenais, L. Mandel, *Phys. Rev. Lett.* 39, 691 (1977).
- [30] H.J. Kimble, M. Dagenais, L. Mandel, *Phys. Rev. A* 18, 201 (1978).
- [31] M. Dagenais and L. Mandel, *Phys. Rev. A* 18, 2217 (1978).
- [32] J.D. Cresser, J. Hagger, G. Leuchs, F.M. Rateike and H. Walther in *Dissipative Systems in Quantum Optics*, edited by R. Bonifacio, Springer 1982.
- [33] L. Mandel, *Proc. Phys. Soc. (London)* 72, 1037 (1958).
- [31] L. Mandel, *Proc. Phys. Soc. (London)* 74, 233 (1959).
- [35] L. Mandel, *Optics Lett.* 4, 205 (1979).
- [36] R. Short and L. Mandel, *Phys. Rev. Lett.* 51, 384 (1983).
- [37] M.C. Teich and B.E.A. Saleh, *J. Opt. Soc. Am.* B2, 275 (1985).
- [38] S. Machida, Y. Yamamoto and Y. Itaya, *Phys. Rev. Lett.* 58, 1000 (1987).

- [39] P.R. Tapster, J.G. Rarity and J.S. Satchell, *Europhys. Lett.* 4, 293 (1987).
- [40] J.G. Rarity, P.R. Tapster and E. Jakeman, *Opt. Commun.* 62, 201 (1987).
- [41] P.R. Tapster, J.G. Rarity and J.S. Satchell, *Phys. Rev. A* 37, 2963 (1988).
- [42] D. Stoler, *Phys. Rev. D* 1, 3217 (1970).
- [43] D. Stoler, *Phys. Rev. D* 4, 1925 (1971).
- [44] H.P. Yuen, *Phys. Rev. A* 13, 2226 (1976).
- [45] J.N. Hollenhorst, *Phys. Rev. D* 19, 1669 (1979).
- [46] C.M. Caves, *Phys. Rev. D* 23, 1693 (1981).
- [47] R.E. Slusher, L.W. Hollberg, B. Yurke, J.C. Mertz and J.F. Valley, *Phys. Rev. Lett.* 55, 2409 (1985).
- [48] R.M. Shelby, M.D. Levenson, S.H. Perlmutter, R.G. De Voe and D.F. Walls, *Phys. Rev. Lett.* 57, 691 (1986).
- [49] L.-A. Wu, H.J. Kimble, J.L. Hall and H. Wu, *Phys. Rev. Lett.* 57, 2520 (1986).
- [50] M.W. Maeda, P. Kumar and J.H. Shapiro, *Opt. Lett.* 12, 161 (1987).
- [51] M.G. Raizen, L.A. Orozco, M. Xiao, T.L. Boyd and H.J. Kimble, *Phys. Rev. Lett.* 59, 198 (1987).

Chapter 2

Generation of nonclassical states by time-dependent perturbations on oscillator

In this chapter¹, the generation and dynamics of nonclassical states in a quantum harmonic oscillator whose frequency is time dependent is studied. The interest in this problem arises from the fact that many physical systems, especially electromagnetic radiation, can be successfully modelled by harmonic oscillators and the results for this generic system can be Carried over to various specific systems. For example, as will be shown in the next chapter, the model can be applied to the motion of a trapped ion in a Paul trap.

The plan of this chapter is as follows. In section 2.1, some general results, which are independent of the explicit time dependence of the frequency are given. In section 2.2, a specific time dependence, namely a linear sweep of ω^2 is considered, and the Heisenberg equations of motion for the position and momentum of the quantum oscillator are solved *exactly*. In section 2.3 it is then shown that the fluctuations in the quadratures \hat{X} and X show squeezing and the photon number statistics is shown to display sub-Poissonian nature. Thus, the quantum harmonic oscillator with a time dependent frequency is shown to generate nonclassical states. Two limits, sudden and adiabatic, also manifest. It is shown that the nonclassical nature is maximal for sudden changes in the frequency, whereas for adiabatic changes it is minimal.

¹ Results of this chapter were presented at the International Conference on Quantum Optics, Hyderabad, January 5-10, 1991, the proceedings of which were published in *Recent Developments in Quantum Optics* edited by Ramarao Inguva, (Plenum, New York, 1993); published in Phys. Rev. Lett. 26. 3665 (1991) and presented at LAMP seminar at ICTP, Trieste, Italy in February 1992.

2.1 Exact analytical approach

Consider a harmonic oscillator Hamiltonian [1]

$$\hat{H} = \frac{\hat{p}^2}{2} + \frac{1}{2}(1 + \beta(t))\omega^2 \hat{x}^2 \quad (2.1)$$

where we have set $m = 1$. The operators x and p satisfy the commutation relation

$$[\hat{x}, \hat{p}] = i \quad (\hbar = 1). \quad (2.2)$$

The explicit time dependence of the frequency ω appears through the β -term in (2.1). In what follows, the exact form of the time dependence of the frequency is of no consequence. For convenience, let us define dimensionless quadrature operators X and P , as follows:

$$\begin{aligned} X &= \sqrt{\frac{\omega}{2}} \hat{x} \\ P &= \sqrt{\frac{1}{2\omega}} \hat{p} \end{aligned} \quad (2.3)$$

and they satisfy the commutation relation

$$[X, P] = \frac{i}{2}. \quad (2.4)$$

It is also convenient to work with a dimensionless time $\tau = \omega t$. Now, for a given form of the time dependence, let us assume that the solutions are known for the Heisenberg equations of motion for the quadratures \hat{X} and \hat{P} , the equations of motion being:

$$\begin{aligned} \frac{d\hat{X}}{d\tau} &= P \\ \frac{d\hat{P}}{d\tau} &= -(1 + \beta(\tau))X. \end{aligned} \quad (2.5)$$

Let $U(\tau)$ and $V(\tau)$ be two functions which are the independent solutions of (2.5) or equivalently of the second order differential equation

$$\frac{d^2\phi}{d\tau^2} = -(1 + \beta(\tau))\phi. \quad (2.6)$$

Times U and V form the fundamental system of solutions. Then, the general solution of this homogeneous system (2.5) can be written as

$$\begin{pmatrix} \hat{X}(\tau) \\ P(\tau) \end{pmatrix} = \begin{pmatrix} U(\tau) & V(\tau) \\ \dot{U}(\tau) & \dot{V}(\tau) \end{pmatrix} \begin{pmatrix} X(0) \\ \hat{P}(0) \end{pmatrix} \quad (2.7)$$

From (2.7) it is natural to choose the initial conditions for the functions U and V as

$$\begin{aligned} U(0) &= V(0) = 1, \\ U'(0) &= V'(0) = 0. \end{aligned} \quad (2.8)$$

Let us now consider a matrix Y defined for the functions U , V and their derivatives

$$Y = \begin{pmatrix} U & V \\ \dot{U} & \dot{V} \end{pmatrix} \quad (2.9)$$

The determinant of this matrix is called the Wronskian of the functions U and V . A sufficient condition for the two functions U and V to be linearly independent is that the Wronskian be non-vanishing. Since U and V are independent, the Wronskian will have a non-zero value.

To show that the value of the Wronskian is invariant, we consider the following matrix differential equation

$$\frac{dY}{d\tau} = A(\tau)Y \quad (2.10)$$

where, the co-efficient matrix is given by (2.5)

$$A(\tau) = \begin{pmatrix} 0 & 1 \\ -(1 + \beta(\tau)) & 0 \end{pmatrix}. \quad (2.11)$$

Using Abel's identity for the Wronskian from the theory of differential equations [2,3], we have

$$\det Y(\tau) = \det Y(0) \exp \int_0^\tau \text{Trace} A(\tau_1) d\tau_1. \quad (2.12)$$

Since $\text{Trace} A(\tau) = 0$,

$$\det Y(\tau) = \det Y(0). \quad (2.13)$$

Thus, the Wronskian remains invariant. This implies that

$$UV - UV = I \quad (2.14)$$

holds true for all times.

We now define lowering and raising operators as

$$\begin{aligned} a &= X + iP \\ a^\dagger &= X - iP \end{aligned} \quad (2.15)$$

which at $t = 0$ satisfy the Bosonic commutation relation

$$[a, a^\dagger] = 1. \quad (2.16)$$

Using the definition (2.15) and the solution (2.7), $a(t)$ and $a^\dagger(\tau)$ become:

$$\begin{aligned} a(\tau) &= u(\tau)a(0) + v(\tau)a^\dagger(0) \\ a^\dagger(\tau) &= v^*(\tau)a(0) + u^*(\tau)a^\dagger(0) \end{aligned} \quad (2.17)$$

where, $u(t)$ and $v(t)$ are given in terms of the solution (2.7) as

$$\begin{aligned} u(\tau) &= \frac{1}{2} [(U + V) + i(\dot{U} - \dot{V})] \\ v(\tau) &= \frac{1}{2} [(U - \dot{V}) + i(U + \dot{V})]. \end{aligned} \quad (2.18)$$

It then follows from the invariance of the Wronskian (condition (2.14)), that

$$|u|^2 - |v|^2 = 1 \quad (2.19)$$

for all times. Condition (2.19) also follows from requiring that the Bosonic commutation relation (2.16) holds true for the transformed operators $a(\tau)$ and $a^\dagger(\tau)$, i.e.,

$$[a(\tau), a^\dagger(\tau)] = 1. \quad (2.20)$$

This implies that the transformation (2.17) is a canonical transformation. Thus, we have a Bogoliubov transformation of the lowering and raising operators as a result of the time dependent frequency and the *co-efficients of the transformation depend explicitly on time*.

Every canonical transformation can be represented as an unitary transformation [4], and hence we have

$$a(r) = S^{-1}(r)a(0)S(r). \quad (2.21)$$

The explicit form of the time evolution operator $S(r)$ can be obtained as follows. One can rewrite (2.17) as

$$\hat{a}(\tau) = e^{i\theta_u} \left[|u(\tau)|\hat{a} + |v(\tau)|e^{i(\theta_v - \theta_u)}\hat{a}^\dagger \right]. \quad (2.22)$$

The term in the square brackets can be obtained by the action of a "squeeze" operator [5-9]. Thus if $T = \exp(\frac{1}{2}(z\hat{a}^{\dagger 2} - h.c.))$, where $z = |z|e^{i\theta}$, then

$$T^{-1}\hat{a}T = \cosh |z|\hat{a} + e^{i\theta} \sinh |z|\hat{a}^\dagger \quad (2.23)$$

where, the operator identity ([10], p136)

$$e^{\xi\hat{A}}\hat{B}e^{-\xi\hat{A}} = \hat{B} + \frac{\xi}{1!}[\hat{A}, \hat{B}] + \frac{\xi^2}{2!}[\hat{A}, [\hat{A}, \hat{B}]] + \dots \quad (2.24)$$

has been used. If one identifies

$$|z| = \cosh^{-1} |u| \text{ and } \theta = \theta_v - \theta_u, \quad (2.25)$$

then (2.23) yields,

$$T^{-1}\hat{a}T = |u|\hat{a} + |v|e^{i(\theta_v - \theta_u)}\hat{a}^\dagger. \quad (2.26)$$

Again using the identity (2.24), we can show that

$$\exp(-i\theta_u\hat{a}^\dagger\hat{a})\hat{a}\exp(i\theta_u\hat{a}^\dagger\hat{a}) = \hat{a}e^{i\theta_u}. \quad (2.27)$$

Hence we have,

$$\begin{aligned} \hat{a}(\tau) &= u(\tau)\hat{a} + v(\tau)\hat{a}^\dagger \\ &= e^{i\theta_u} \left[|u(\tau)|\hat{a} + |v(\tau)|e^{i(\theta_v - \theta_u)}\hat{a}^\dagger \right] \\ &= \tilde{S}^{-1}\hat{a}\tilde{S} \end{aligned} \quad (2.28)$$

where $S(\tau)$ is

$$S(\tau) = \exp(i\theta_u \hat{a}^\dagger \hat{a}) \exp\left(\frac{1}{2}\left[e^{i(\theta_v - \theta_u)} \cosh^{-1} |u| \hat{a}^{\dagger 2} - h.c.\right]\right). \quad (2.29)$$

As a result of the time dependent frequency, one expects transition to occur between the levels of the oscillator. The probability of finding the oscillator in the state $|n\rangle$ at time τ given that at $\tau = 0$ it was in the state $|m\rangle$ is

$$p_{nm}(\tau) = |\langle n | \tilde{S}(\tau) | m \rangle|^2 \quad (2.30)$$

The evaluation of these matrix elements can be done if one expresses \tilde{S} in a normally ordered form. This is done using the disentangling theorem for the $SU(1,1)$ group [11-13]. The transition probability then becomes

$$p_{nm} = \left(\frac{1}{|u|^{2m-3}}\right) \frac{1}{n!m!} |\langle 0 | (\hat{a} + \frac{v}{u} \hat{a}^\dagger)^n (\hat{a}^\dagger - \frac{v^*}{u^*} \hat{a})^m | 0 \rangle|^2. \quad (2.31)$$

The actual steps involved obtaining (2.31) are provided in the Appendix 2A. As an example, let $m = 0$ and $n = 2$. Then

$$\begin{aligned} |\langle 2 | \tilde{S}(\tau) | 0 \rangle|^2 &= \frac{|u|^3}{2} |\langle 0 | (\hat{a} + \frac{v}{u} \hat{a}^\dagger)^2 | 0 \rangle|^2 \\ &= \frac{|u||v|^2}{2}. \end{aligned} \quad (2.32)$$

Quasiprobability distributions (a resume is given in chapter 6), like the Glauber-Sudarshan P -function, Q -function and Wigner function are very useful in gaining insight into the quantum statistical aspects of a problem. Many states which are highly nonclassical have simple and rather well behaved representations in terms of the Wigner function. The Wigner function is defined as the Fourier transform of the quantum characteristic function X_w : [10] and [14] (section 4.4)

$$\Phi(\alpha) = \frac{1}{\pi^2} \int d^2\xi \exp(\xi^* \alpha - \xi \alpha^*) \chi_w(\xi, \xi^*), \quad (2.33)$$

where

$$\chi_w(\xi, \xi^*) = \text{Tr}\{\hat{\rho} \exp[\xi \hat{a}^\dagger - \xi^* \hat{a}]\} \quad (2.34)$$

and $\Phi(\alpha)$ satisfies the normalisation condition $\int d^2\alpha \Phi(\alpha) = 1$.

What is the effect of the transformation that arises due to the time dependent frequency on the Wigner function? To see that, we substitute the transformation (2.17) into (2.33) and we have,

$$\Phi(\alpha, \alpha^*, \tau) = \frac{1}{\pi^2} \int d^2\xi \exp(\xi^* \alpha - \xi \alpha^*) \text{Tr}\{\hat{\rho} \exp[\xi(u^* \hat{a}^\dagger + v^* \hat{a}) - h.c.]\}. \quad (2.35)$$

On changing the integration variable ξ to $\lambda = (\xi u^* - \xi^* v)$, and noting that the Jacobian of the transformation is unity, we have

$$\Phi(\alpha, \alpha^*, \tau) = \frac{1}{\pi^2} \int d^2\lambda \exp\{\lambda^*(u^* \alpha - v \alpha^*) - \lambda(u \alpha^* - v^* \alpha)\} \text{Tr}\{\hat{\rho} \exp(\lambda \hat{a}^\dagger - \lambda^* \hat{a})\}. \quad (2.36)$$

Comparing the equation (2.36) and (2.33) we can express the Wigner function at time τ , in terms of the function at $t = 0$ [1]:

$$\Phi(\alpha, \alpha^*, \tau) = \Phi([u^*(\tau)\alpha - v(\tau)\alpha^*], [u(\tau)\alpha^* - v^*(\tau)\alpha], 0). \quad (2.37)$$

The Wigner function thus evolves along the classical trajectories. This is expected as the Hamiltonian is quadratic in \hat{X} and \hat{P} . The time evolution is especially simple if the Wigner function associated with the initial state is a Gaussian [15]. According to the moment theorem for Gaussian processes [16], all moments of order higher than two are expressible in terms of those of order one and two. Thus, the Gaussian nature of the Wigner function simplifies the calculation of higher order moments. The Wigner function for a very large class of harmonic oscillator states has the following general Gaussian structure, [15]

$$\Phi(\alpha) = \frac{1}{\pi \sqrt{(\gamma^2 - 4|\mu|^2)}} \exp\left(-\frac{\mu(\alpha - \alpha_0)^2 + \mu^*(\alpha^* - \alpha_0^*)^2 + \gamma|\alpha - \alpha_0|^2}{\gamma^2 - 4|\mu|^2}\right) \quad (2.38,$$

where the parameters in (2.38) have the following meaning in terms of the mean values and variances

$$\langle \hat{a} \rangle = \alpha_0$$

$$\langle \hat{a}^2 \rangle - \langle \hat{a} \rangle^2 = -2\mu^* \quad (2.40)$$

$$\langle \frac{1}{\alpha} (\hat{a}^\dagger \hat{a} + \hat{a} \hat{a}^\dagger) \rangle - \langle \hat{a}^\dagger \rangle \langle \hat{a} \rangle = 7. \quad (2.41)$$

The function (2.38) corresponds to the Wigner function for (a) coherent states when $\mu = 0$ and $\gamma = 5$; (b) squeezed states when $\mu \neq 0$, $\alpha_0 \neq 0$ and $\gamma^2 - 4|\mu|^2 = \frac{1}{4}$; (c) thermal states when $\mu = 0$, $\alpha_0 = 0$ and $\gamma > 1/2$ and (d) also to mixtures of thermal and coherent states.

As an example of the use of the Gaussian nature of Wigner function, let us evaluate the Mandel's Q-parameter, which involves the evaluation of second moments. The Mandel's Q-parameter as defined in chapter 1 gives a quantitative measure of how much the photon number distribution deviates from a Poissonian distribution. In order to determine Q, we need to evaluate $\langle \hat{n}^2 \rangle = \langle (\hat{a}^\dagger \hat{a})^2 \rangle$ and $\langle \hat{n} \rangle = \langle \hat{a}^\dagger \hat{a} \rangle$. The mean value of $(\hat{a}^\dagger \hat{a})^2$ in terms of the Wigner function is

$$\langle \hat{a}^\dagger \hat{a} \hat{a}^\dagger \hat{a} \rangle = \int \Phi(\alpha) (|\alpha|^4 - |\alpha|^2) d^2\alpha. \quad (2.42)$$

According to the moment theorem for Gaussian processes [16], all higher order moments (> 2) can be expressed in terms of the second and first moments. In particular, if the first moment is zero, then all odd order moments are zero and the even order moments are given by

$$\langle X_i X_j X \dots \rangle = \frac{(2N)!}{N! 2^N} \{ \sigma_{ij} \sigma_{kl} \sigma_{mn} \dots \}_{\text{sym}}, \quad (2.43)$$

where the subscript 'sym' means symmetric form of the product of the variance matrices σ and $2N$ is the order of the moment. Since, in (2.42), $\langle \hat{a} \rangle = \alpha_0 \neq 0$, in general, we can define $\bar{\alpha} = \alpha - \alpha_0$, so that we can apply the result (2.43) for the barred variables. Then (2.42) becomes,

$$\langle \hat{a}^\dagger \hat{a} \hat{a}^\dagger \hat{a} \rangle = \int \Phi(\alpha) (|\bar{\alpha} + \alpha_0|^4 - |\bar{\alpha} + \alpha_0|^2) d^2\alpha, \quad (2.44)$$

$$= \langle |\bar{\alpha} + \alpha_0|^4 \rangle - \langle |\bar{\alpha} + \alpha_0|^2 \rangle. \quad (2.45)$$

Expanding the quantities $|\bar{\alpha} + \alpha_0|^4$ and $|\bar{\alpha} + \alpha_0|^2$ and noting that for the barred variables

$$\langle |\bar{\alpha}|^4 \rangle = 2\langle |\bar{\alpha}|^2 \rangle^2 + \langle \bar{\alpha}^2 \rangle \langle \bar{\alpha}^{*2} \rangle, \quad (2.46)$$

$$\langle \bar{\alpha}^3 \rangle = \langle \bar{\alpha} \rangle = 0, \quad (2.47)$$

we have

$$\langle (\hat{a}^\dagger \hat{a})^2 \rangle = 2\langle |\bar{\alpha}|^2 \rangle^2 + |\alpha_0|^4 + 4|\alpha_0|^2 \langle |\bar{\alpha}|^2 \rangle - |\alpha_0|^2 - \langle |\bar{\alpha}|^2 \rangle + \langle \bar{\alpha}^2 \rangle \alpha_0^{*2} + \langle \bar{\alpha}^{*2} \rangle \alpha_0^2 + \langle \bar{\alpha}^2 \rangle \langle \bar{\alpha}^{*2} \rangle. \quad (2.48)$$

Using the definitions (2.39) to (2.41), we have

$$\langle (\hat{a}^\dagger \hat{a})^2 \rangle = 2\gamma^2 + |\alpha_0|^4 - |\alpha_0|^2 - 7 - 2\mu^* \alpha_0^{*2} - 2\mu \alpha_0^2 + 4|\mu|^2 + 4|\alpha_0|^2 \gamma \quad (2.49)$$

and $\langle \hat{a}^\dagger \hat{a} \rangle$ is given by

$$\langle \hat{a}^\dagger \hat{a} \rangle = \gamma - \frac{1}{\alpha} + |\alpha_0|^2. \quad (2.50)$$

Combining (2.49) and (2.50), we have the final expression for Mandel's Q-parameter

$$Q = \frac{\langle \hat{n}^2 \rangle - \langle \hat{n} \rangle^2 - \langle \hat{n} \rangle}{\langle \hat{n} \rangle}, \quad (2.51)$$

$$\sim \left(\frac{\gamma^2 + 2|\alpha_0|^2 \gamma - 1 - 2(\alpha_0^*)^2 \mu^* - 2\alpha_0^2 \mu + 4|\mu|^2}{7 + |\alpha_0|^2 - \frac{1}{2}} \right) - 1. \quad (2.52)$$

It is clear from (2.37) and (2.38) that the Wigner function will remain Gaussian with time dependent parameters α_0, γ and $1/z$:

$$\alpha_0(\tau) = u(\tau)\alpha_0 + v(\tau)\alpha_0^* \quad (2.53)$$

$$\mu(\tau) = u^{*2} + v^{*2}\mu^* - u^*v^*\gamma \quad (2.54)$$

$$\gamma(\tau) = (u^*u + v^*v)\gamma - 2\mu u^*v - 2\mu^*uv^*, \quad (2.55)$$

where $u(\tau)$ and $v(\tau)$ are the time dependent co-efficients of the Bogoliubov transformation (2.17). Thus, if the initial Wigner function of a state was Gaussian, as a result of the Bogoliubov transformation (2.17) the Gaussian nature remains intact after the transformation, but for a redefinition of the parameters.

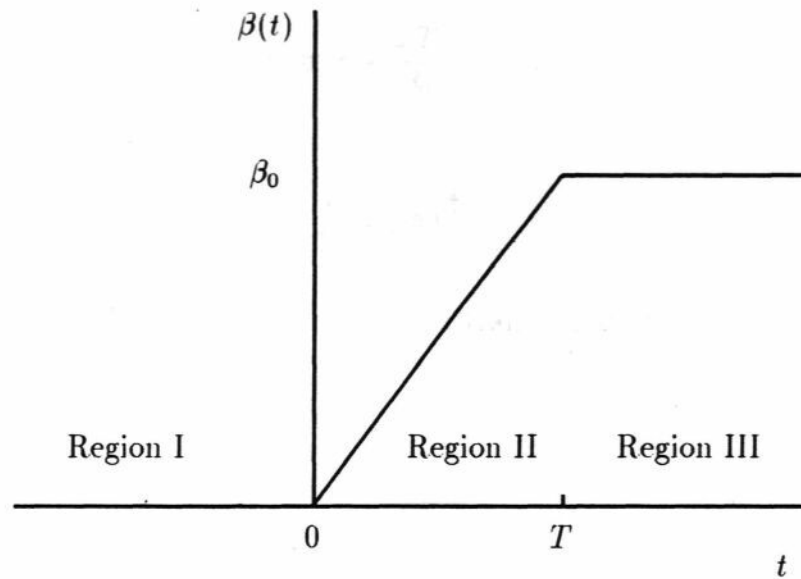


Figure 2.1: Form of the function $\beta(t)$. The sudden limit corresponds to $\lim_{T \rightarrow 0}$ and the adiabatic limit to $\lim_{T \rightarrow \infty}$.

2.2 Linear sweep of ω^2 , a specific case

In this section, we consider as an example, a specific form of the time dependent frequency.

Let $\beta(t)$ in (2.1) be of the following form (see Fig.2.1):

$$\beta(t) = \begin{cases} 0 & \text{for } -\infty < t < 0 & \text{(Region I)} \\ \beta_0 \frac{t}{T} & \text{for } 0 < t < T & \text{(Region II)} \\ \beta_0 & \text{for } T < t < \infty. & \text{(Region III)} \end{cases} \quad (2.55)$$

With this form of the time dependence one *has* to solve the Heisenberg equations of motion (2.5) for the dimensionless operators X and P . In region I, we have just an oscillatory solution at the oscillation frequency ' ω ':

$$\hat{X}^{(I)}(\tau) = X(0) \cos(\tau) + P(0) \sin(\tau) \quad (2.56)$$

$$\hat{P}^{(I)}(\tau) = -X(0) \sin(\tau) + P(0) \cos(\tau). \quad (2.57)$$

To find the solution in the region II, we make the following transformation for the dimensionless time variable, $T \rightarrow \tau'$,

$$\tau' = r + \frac{\omega T}{\beta_0} \quad (2.58)$$

and we define a new variable, z

$$z \equiv \frac{2}{3} \left(\frac{\beta_0}{\omega T} \tau'^3 \right)^{\frac{1}{2}}. \quad (2.59)$$

Then, the Heisenberg equations of motion (2.5) get transformed to

$$\begin{aligned} \frac{d\hat{X}}{d\tau'} &= \hat{P} \\ \frac{d\hat{P}}{d\tau'} &= -(\beta_0 \frac{\tau'}{\omega T}) \hat{X} \end{aligned} \quad (2.60)$$

or equivalently, \hat{X} and \hat{P} are solutions of the second-order differential equation

$$\frac{d^2\phi}{d\tau'^2} + \left(\frac{\beta_0}{\omega T} \right) \tau' \phi = 0. \quad (2.61)$$

The exact solution for the Heisenberg equation of motion for the operators X and P in the region II can be written in terms of Bessel functions of order $\frac{1}{3}$: [17]

$$\hat{X}^{(II)}(\tau') = C_1 \sqrt{\tau'} J_{\frac{1}{3}}(z) + C_2 \sqrt{\tau'} Y_{\frac{1}{3}}(z) \quad (2.62)$$

$$\hat{P}^{(II)}(\tau') = C_3 \sqrt{\tau'} J_{\frac{1}{3}}(z) + C_4 \sqrt{\tau'} Y_{\frac{1}{3}}(z). \quad (2.63)$$

The co-efficients C_1 to C_4 are fixed by requiring $X^{(II)}(\tau') \rightarrow \bar{X}^{(I)}(\tau = 0) = X(0)$ and $\bar{P}^{(II)}(\tau') \rightarrow \bar{P}^{(I)}(\tau = 0) = P(0)$. In region III, the solution is again oscillatory, but with a frequency of oscillation $\sqrt{1 + \beta_0 \omega}$. Thus,

$$\hat{X}^{(III)}(\tau) = C_5 \cos(\sqrt{1 + \beta_0 \omega} \tau) + C_6 \sin(\sqrt{1 + \beta_0 \omega} \tau) \quad (2.64)$$

$$\hat{P}^{(III)}(\tau) = C_7 \cos(\sqrt{1 + \beta_0 \omega} \tau) + C_8 \sin(\sqrt{1 + \beta_0 \omega} \tau). \quad (2.65)$$

As before the constants C_5 to C_8 are determined by requiring the continuity of X and P at $r = T$. Thus the entire solution is obtained. The variances in the quadratures can then be calculated in a straight forward manner.

Following our results [1] various authors have extended the results obtained by us². Other forms of specific time dependences can also be considered. For example, in the case of quantised motion of an ion in a Paul trap, the time dependence is sinusoidal. This case is discussed in detail in the next chapter.

2.3 Numerical approach

In the previous two sections, the exact analytical solution for the Heisenberg equations of motion (2.5) was considered. The previous section described a specific example where an analytical solution is possible. But there are problems where such an analytical solution is not possible. To handle such situations, in this section a numerical approach to the problem is given.

We rewrite (2.5) in terms of the mean values of the operators X and P : [21]

$$\begin{aligned}\varphi_1 &= \varphi_2 \\ \varphi_2 &= -(1 + \text{flr}))^\wedge\end{aligned}\quad (2.66)$$

where

$$\begin{aligned}\varphi_1 &\approx (X) \\ \varphi_2 &= (P).\end{aligned}\quad (2.67)$$

Also, let

$$\begin{aligned}\Psi_1 &= \langle \tilde{X}^2 \rangle \\ \Psi_2 &\equiv \langle \hat{X} \hat{P} + \hat{P} \hat{X} \rangle \\ \Psi_3 &\equiv \langle \hat{P}^2 \rangle.\end{aligned}\quad (2.68)$$

²Janszky et al [18,19], based on [1] have shown that a series of well-timed frequency jumps leads to more pronounced squeezing. In a later publication [20], Aliaga et al have obtained our results by a completely equivalent method using a maximum entropy principle procedure.

Then, we have,

$$\begin{aligned}\Psi_1 &= 2\Psi_2 \\ \Psi_2 &= -(1 + \beta(\tau))\Psi_1 + \Psi_3 \\ \Psi_3 &= -2(1 + \beta(\tau))\Psi_2.\end{aligned}\tag{2.69}$$

The initial conditions for (2.66) and (2.69) are determined from (2.67) and (2.68) evaluated at $\tau = 0$ for a given initial state. Systems (2.66) and (2.69) are numerically integrated using standard Runge-Kutta algorithm and the fluctuations in the quadratures A'' and P at time τ are directly obtained as

$$\begin{aligned}\langle (\Delta \tilde{X})^2 \rangle &= \Psi_1 - \varphi_1^2 \\ \langle (\Delta \tilde{P})^2 \rangle &= \Psi_3 - \varphi_2^2.\end{aligned}\tag{2.70}$$

The time dependence of the Mandel's Q-parameter is obtained directly from (2.51) substituting for the time dependent parameters given by (2.52) to (2.54).

2.4 Demonstration of nonclassical properties

In this section, a discussion of the results for the case of $\beta(\tau)$, given by (2.55) in section 2.2, is given to demonstrate nonclassical effects like, squeezing of fluctuations and sub-Poissonian statistics. One could use either the exact analytical approach of section 2.2 or the numerical approach of section 2.3. We use the exact solutions for the regions II and III (see Fig.2.1) with proper boundary conditions. One can then use this solution to evaluate \hat{A}^- , \hat{P} and $\hat{X}\hat{P} + \hat{P}\hat{X}$ and evaluate the expectation values for various initial states. Alternatively, one could determine these quantities by a direct numerical integration of the equations of motion for the expectation values [21].

We next present the numerical results for the non-classical properties like, squeezing and sub-Poissonian statistics of the oscillator. In Fig.2.2 we show the squeezing in the component \tilde{X} when initially the oscillator is in the ground state. We observe that a linear sweep produces a *significant amount of squeezing*. The squeezing properties are

much more *pronounced* for the case of a *sudden jump* [22]. As expected the adiabatic changes [23] do not produce any noticeable squeezing. From the calculation of the phases θ_u and θ_v , we also find that the two quadratures \hat{X} and \hat{P} are in general correlated for most of the time (see Fig.2.3). Note that for fast sweeping, the variance exhibits periodic behaviour. For the parameters of the Fig.2.2 this period is found to be π which follows from (2.6) and (2.55) as $1 + \beta_0 \rightarrow 2$. In Fig.2.4, we show the squeezing characteristics if initially the oscillator state is squeezed in the quadrature P . The quadrature X exhibits quite a significant amount of squeezing which in turn depends on the rate of the frequency sweep. For the initial vacuum state the Wigner function is Gaussian (2.38) with equal noise in the two quadratures ($\mu = 0$ and $\gamma = \frac{1}{2}$). In Fig.2.5, we show the time evolution of the Wigner function (2.38). We show the behaviour at a time when the system shows maximum amount of squeezing in the X quadrature.

Finally, in Fig.2.6, we show the generation of sub-Poissonian statistics when initially the state is a coherent state. The time dependent behaviour of the Q parameter was calculated from (2.51) using (2.52) to (2.54). It is similar to that shown in Fig.2.2. In general this is not expected, except when the mean value of the field is so large, that a linearisation around the mean value can be done. For Fig.2.2, the mean value is zero, but this is not so for Fig.2.6. The linear sweep of the restoring force can produce *large amounts of sub-Poissonian statistics*. Several possibilities for realising the present model exist; for example, one can use a cavity with a material whose dielectric constant is varied with time.

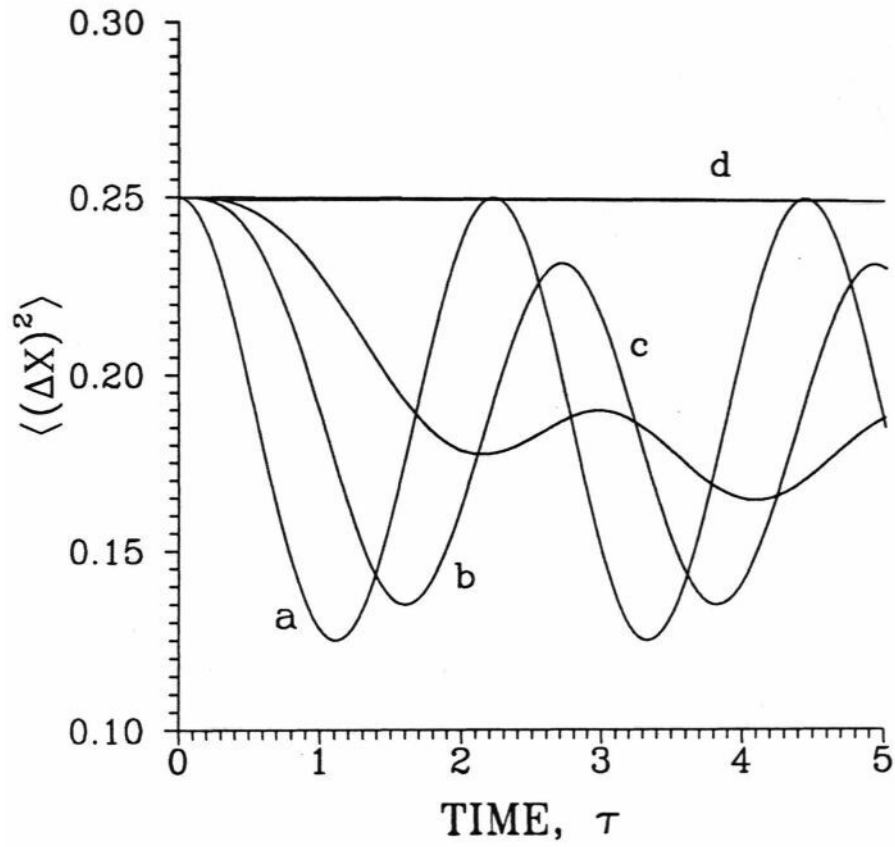


Figure 2.2: The variance of the quadrature X versus time, τ for an oscillator initially in the ground state. The parameters are: $\beta_0 = 1$ and $\omega T = (a)10^{-3}$, (b)1, (c)3 and (d) 10^3 . The cases (a) and (d) correspond, respectively, to sudden and adiabatic limits.

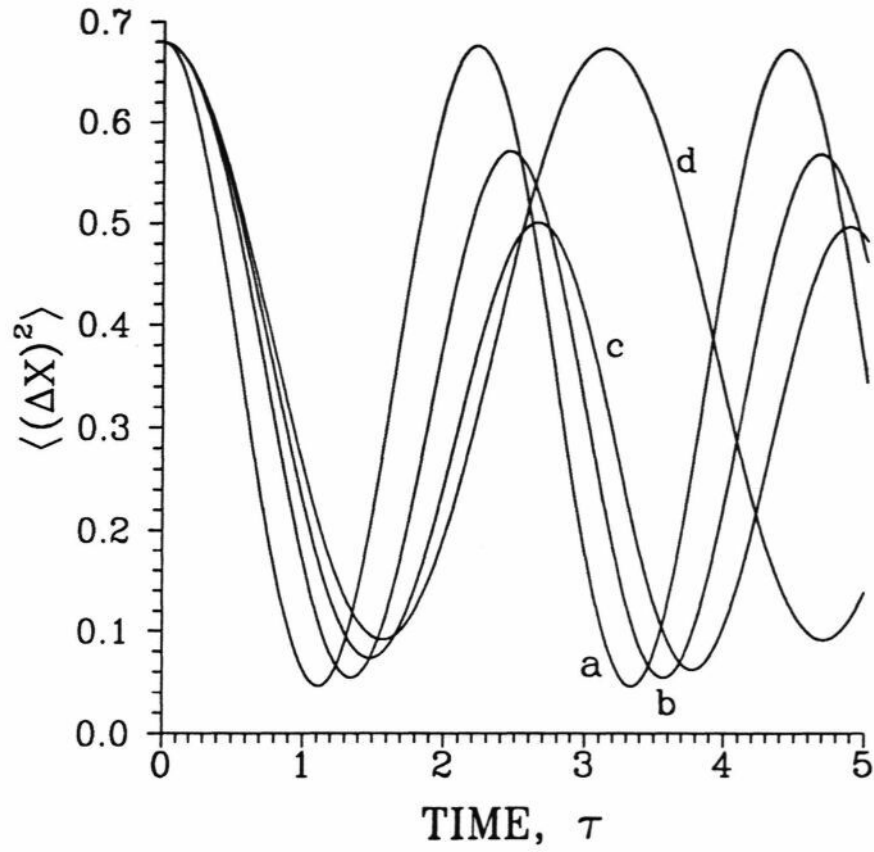


Figure 2.3: Same as Fig.2.2, but with the oscillator initially in a squeezed coherent state $|\alpha, \zeta\rangle$ with $a = 1$ and $\zeta = 0.5e^{-i\pi}$.

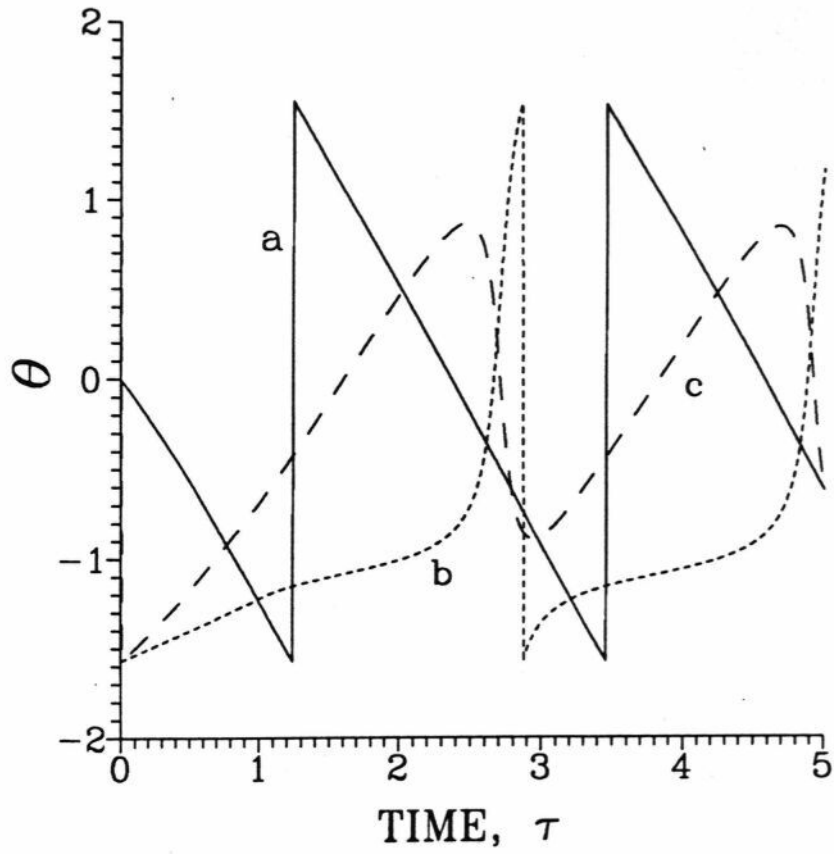


Figure 2.4: The phases of u (curve (a)), v (curve (b)) and μ (curve (c)) versus time, τ corresponding curve (b) of Fig.2.2. As the phases are non-zero for most of the time, the quadratures X and P are correlated most of the time.

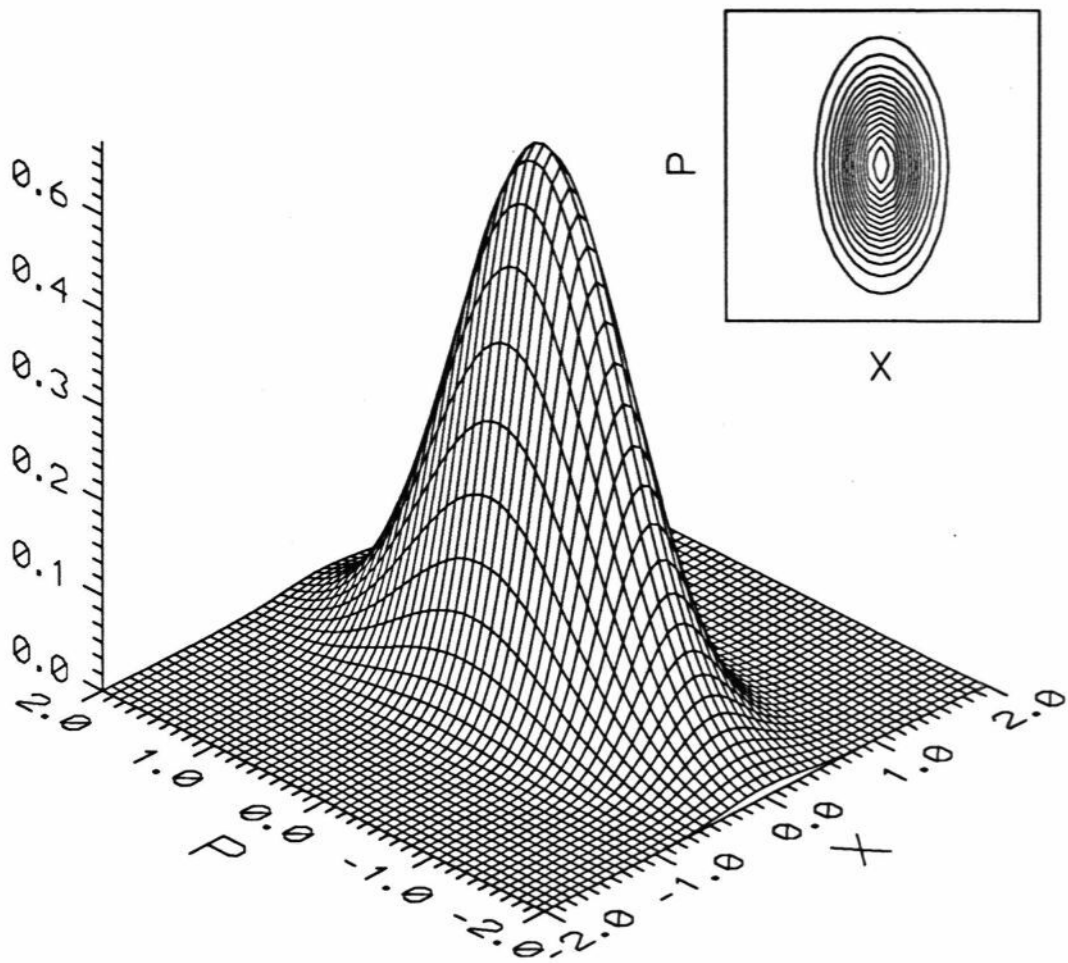


Figure 2.5: Wigner function $\Phi(\alpha, \alpha^*, \tau)$ with $\alpha = (X) + i\langle P \rangle$ for the system initially in vacuum state for $\omega T = 10^{-3}$, $\beta_0 = 1$ and $\tau = 1.1$ which corresponds to the minimum in Fig.2.2. Squeezing in the quadrature X can be seen in the inset which shows contours of constant values of the Wigner function.

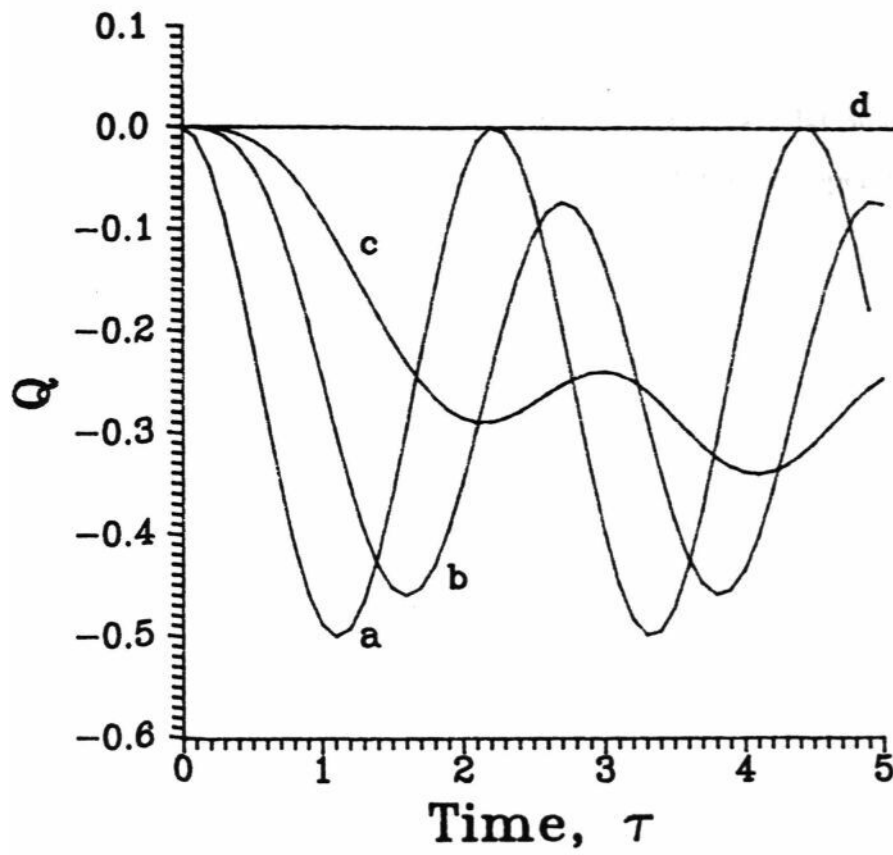


Figure 2.6: Mandel's Q -parameter as a function of τ for the case of an oscillator initially in a coherent state $|\alpha\rangle$, $\alpha = 1$. The parameter ωT has been chosen as (a) 10^{-3} , (b) 1, (c) 3 and (d) 10^3 .

Appendix 2A

Calculation of the matrix element $\langle n|S|m\rangle$

In this appendix we give the intermediary steps involved in the calculation of the matrix element in (2.30). In calculating such matrix elements the following operator identities are useful [12,13]:

$$e^{\lambda \hat{A}} \hat{B}^m e^{-\lambda \hat{A}} = \left[\sum_{n=0}^{\infty} \frac{\lambda^n}{n!} \{\hat{A}^n, \hat{B}\} \right], \quad (2A.1)$$

$$e^{\lambda \hat{A}} e^{\hat{B}} e^{-\lambda \hat{A}} = \exp \left(\sum_{n=0}^{\infty} \frac{\lambda^n}{n!} \{\hat{A}^n, \hat{B}\} \right), \quad (2A.2)$$

$$e^{\hat{A}+\hat{B}} = e^{\hat{A}} e^{\hat{B}} e^{C_2^*} e^{C_3^*} \dots, \quad (2A.3)$$

where

$$\{\hat{A}^0, \hat{B}\} = \hat{B} \quad (2A.4)$$

$$\{\hat{A}^{n+1}, \hat{B}\} = [\hat{A}, \{\hat{A}^n, \hat{B}\}]. \quad (2A.5)$$

Equation (2A.3) is called Zassenhaus formula and is a dual of the BCH formula (Baker-Campbell-Hausdorff formula). The quantities C_n^* are

$$C_2^* = -\frac{1}{2}[\hat{A}, \hat{B}] \quad (2A.6)$$

$$C_3^* = \frac{1}{3}[\hat{B}, [\hat{A}, \hat{B}]] + \frac{1}{6}[\hat{A}, [\hat{A}, [\hat{A}, \hat{B}]]] \quad (2A.7)$$

and so on. If C_2^* commutes with \hat{A} and \hat{B} , then all higher terms vanish. Equation (2.29) can be written as:

$$S = e^{i(\hat{a}^\dagger \hat{a})} \exp \left(\frac{|\zeta|}{2} e^{i\theta} \hat{a}^\dagger{}^2 - \frac{|\zeta|}{2} e^{-i\theta} \hat{a}^2 \right), \quad (2A.8)$$

where

$$X = i\theta_u \quad (2A.9)$$

$$O = \theta_v - \theta_u \quad (2A.10)$$

$$|\zeta| = \cosh^{-1}|u|. \quad (2A.11)$$

Recalling that the state $|n\rangle$ can be obtained from the **vacuum** by the action of \hat{a}^\dagger (see 1.10), we have

$$\langle n|S|m\rangle = \frac{1}{n!m!} \langle 0|\hat{a}^n e^{X(\hat{a}^\dagger\hat{a})} \exp\left(\frac{|\zeta|}{\gamma} e^{i\theta} \hat{a}^{\dagger 2} - \frac{|\zeta|}{\gamma} e^{-i\theta} \hat{a}^2\right) \hat{a}^{\dagger m} |0\rangle. \quad (2A.12)$$

The second exponential **operator** in (2A.12) can then be disentangled using the disentangling theorem for the $SU(1,1)$ group. The $SU(1,1)$ group generators, A'_-, A'_+ and K_3 satisfy the following commutation relations

$$[K_-, K_+] = 2K_3 \quad (2A.13)$$

and

$$[K_3, K_\pm] = \pm K_\pm, \quad (2A.14)$$

where the generators are

$$K_+ = \frac{\hat{a}^{\dagger 2}}{2} \quad (2A.15)$$

$$A'_- = \frac{\hat{a}}{2} \quad (2A.16)$$

$$K_3 = \frac{1}{2} \left(\hat{a}^\dagger \hat{a} + \frac{1}{2} \right). \quad (2A.14)$$

According to the disentangling theorem [11]

$$\exp(\gamma_+ K_+ + \gamma_- A'_- + \gamma_3 K_3) = \exp(\Gamma_+ K_+) \exp(\ln(\Gamma_3) K_3) \exp(\Gamma_- K_-), \quad (2A.18)$$

where

$$\phi^2 = \frac{1}{4} \gamma_3^2 - \gamma_+ \gamma_- \quad (2A.19)$$

$$\Gamma_\pm = \frac{2\gamma_\pm \sinh(\phi)}{2\phi \cosh(\phi) - \gamma_3 \sinh(\phi)} \quad (2A.20)$$

$$\Gamma_3 = (\cosh(\phi) - \frac{\gamma_3}{2\phi} \sinh(\phi))^2. \quad (2A.21)$$

Thus we get,

$$\langle n|S|m\rangle = \frac{1}{\sqrt{n!m!}} \langle 0|\hat{a}^n e^{\lambda(\hat{a}^\dagger \hat{a})} e^{\xi \hat{a}^\dagger \hat{a}} e^{\Lambda \hat{a}^\dagger \hat{a}} e^{-\xi^* \hat{a}^2} \hat{a}^\dagger{}^m |0\rangle, \quad (2A.22)$$

where

$$\xi = \frac{v}{2u} \quad (2A.23)$$

$$\Lambda = -\ln(|u|). \quad (2A.24)$$

Using the operator identities (2A.1) and (2A.2) we can reorder these terms. After re-ordering, we get

$$\langle n|S|m\rangle = \frac{e^{n\lambda+(m-2)\Lambda}}{\sqrt{|u|n!m!}} \langle 0|(\hat{a} + 2\xi \hat{a}^\dagger)^n (\hat{a}^\dagger - 2\xi^* \hat{a})^m |0\rangle. \quad (2A.25)$$

Substituting the definitions (2A.9) to (2A.11) and (2A.23) and (2A.24), we have

$$\langle n|S|m\rangle = \left(\frac{e^{in\theta_u}}{|u|^{m-2}\sqrt{|u|}} \right) \frac{1}{\sqrt{n!m!}} \langle 0|(\hat{a} + \frac{v}{u} \hat{a}^\dagger)^n (\hat{a}^\dagger - \frac{v^*}{u^*} \hat{a})^m |0\rangle, \quad (2A.26)$$

and hence

$$p_{nm} = \left(\frac{1}{|u|^{2m-3}} \right) \frac{1}{n!m!} |\langle 0|(\hat{a} + \frac{v}{u} \hat{a}^\dagger)^n (\hat{a}^\dagger - \frac{v^*}{u^*} \hat{a})^m |0\rangle|^2. \quad (2A.27)$$

References

- [1] G.S. Agarwal and S. Arun Kumar, Phys. Rev. Lett. 67, 3665 (1991).
- [2] E.L. Ince, *Ordinary Differential Equations* (Dover, New York, 1956), p. 119.
- [3] A.D. Myskis, *Advanced Mathematics for Engineers* (Mir Publishers, Moscow, 1975), p. 609.
- [4] J. von Neumann, Math. Ann. 104, 570 (1931).
- [5] D. Stoler, Phys. Rev. D 1, 3217 (1970).
- [6] D. Stoler, Phys. Rev. D 4, 1925 (1971).
- [7] H.P. Yuen, Phys. Rev. A 13, 2226 (1976).
- [8] J.N. Hollenhorst, Phys. Rev. D 19, 1669 (1977).
- [9] R. London and P.L. Knight, J. Mod. Opt. 34, 709 (1987).
- [10] W.H. Louisell, *Quantum Statistical Properties of Radiation* (Wiley, New York, 1973).
- [11] K. Wodkiewicz and J.H. Eberly, J. Opt. Soc. Am. B 2, 458 (1985).
- [12] R.M. Wilcox, J. Math. Phys. 8, 962 (1967).
- [13] W. Witschel, J. Phys. B.: Atom. Molec. Phys. 6, 527 (1973).
- [14] C.W. Gardiner, *Quantum Noise* (Springer, Berlin, 1991).
- [15] G.S. Agarwal, J. Mod. Opt. 34, 909 (1987).
- [16] C.W. Gardiner, *A Handbook of Stochastic Methods*, (Springer, Berlin, 1983).
- [17] E. Kamke, *Differentialgleichungen: Lösungsmethoden und Lösungen*, Leipzig, 1959, §2.162, Eq(17).
- [18] J. Janszky and P. Adam, Phys. Rev. A 46, 6091 (1992).
- [19] T. Kiss, J. Janszky and P. Adam, Phys. Rev. A 49, 4935 (1994).
- [20] J. Aliaga, G. Crespo and A.N. Proto, Phys. Rev. Lett. 70, 434 (1993).

- (21] S. Arun Kumar, Recent *Developments in Quantum Optics* Proceedings of the International Conference on Quantum Optics held at Hyderabad, edited by Ramarao Inguva (Plenum, New York, 1993).
- [22] J. Janszky and Y.Y. Yushin, Opt. Commun. 59,151 (1986).
- [23] R. Graham, J. Mod. Opt. 34, 873 (1987).

Chapter 3

Quantised motion of an ion in a Paul trap

In the recent years, rapid progress has been made in the field of high-resolution spectroscopy. One of the main concerns of high-resolution spectroscopy is to minimise the energy of atomic motion and to confine atoms in a very small volume of phase space so that line broadening due to the motion of the emitting atoms is reduced considerably. Although one can have good Doppler-free spectroscopy done, say, by detecting the light emitted by atoms in a direction perpendicular to the motion of the particles, due to second-order (or transverse) Doppler effect one still has transit-time broadening (proportional to u^2). Therefore one has to resort to "cooling", which involves reduction of velocities as well as suppression of spread in the distribution of velocities. In addition to cooling, one is interested in the trapping of a single atom, ion or a charged particle in a localised position for a long time so that very accurate measurements can be done. Thus for example, the g-factor of an electron has been measured in a Penning trap to an accuracy of ± 2 parts in 10^{12} [1]. There are also various other reasons for the interest in trapping — (a) improvement of precision in atomic clocks due to the possibility of long measurement times and hence less uncertainty in energy measurements [2], (b) obtaining unique states of condensed matter, (c) possibility of the observation of Bose condensation, (d) traps form an ideal testing ground for testing quantum mechanics, for example, experiments have been made to test the predictions made by certain theories of nonlinear quantum mechanics [3], to observe quantum Zeno effect [4], for direct observation of quantum jumps [5-7] and a host of other possibilities.

In this chapter¹, the generic model studied in the previous chapter is applied to a material oscillator, namely a single ion trapped in a Paul trap. A Paul trap is a device which is used to trap ions and charged particles in a quadrupole confining potential. To describe the motion of the trapped ion one has to solve the equations of motion of the trapped particle. Eventhough the solution to the equations of motion can be obtained classically, if the energy of motion of the ion has to be minimised, one has to resort to a quantum mechanical treatment. That a fully quantum mechanical treatment is necessary was demonstrated by Diedrich et al. [8] who placed a single ion in the ground state of its motion. In section 3.1 of this chapter, following a short description of a Paul trap, the solution to the equation of motion of the trapped particle in the classical context is considered. A description of the secular approximation, first introduced by Kapitza [9], for the time-dependent potential is given. In section 3.2 and the subsequent sections the motion is described in a fully quantum mechanical description. Time evolution of the position and momentum operators for the quantum oscillator are obtained. Explicit forms of the non-stationary wave functions in the Schrodinger picture for various oscillator states and the time evolution of the Wigner distribution are obtained in section 3.3. In the later part of the section numerical results are presented. A plot showing the uncertainties in the position of the ion are shown to be squeezed. A plot of the Wigner distribution is also provided. In section 3.4, a utility of this approach to understand the occurence and to calculate the strength of sidebands in the flourescence spectrum of an ion in a Paul trap is demonstrated.

3.1 Paul trap

A Paul trap is a device used to confine ions and charged particles into a small region of space inside a potential well formed due to a combination of **rf** and static fields. Due to Earnsliaw's theorem [10-12] it is impossible to have a stable confinement of charged

¹ Results of this chapter were presented at the National Laser Symposium held at the IIT, Madras, February 17-19, 1993 and at a workshop titled Coherent States: New Developments and Perspectives held at the University of Hyderabad, Hyderabad, October 29-31, 1993.

particles in an entirely electrostatic assembly. Hence, the problem is circumvented by creating a dynamic potential well by the application of a rapidly oscillating and a static field.

In Fig.3.1, the essential features of a Paul trap are shown [13,14]. It consists of two electrodes — a ring electrode, the radius of which is given by r_0 , two endcap electrodes separated by a distance of $2z_0$ from each other. The typical dimensions of the trap are between 1 and 40 mm. The potential is quadratic in each of the three rectangular coordinates of the ion. Thus,

$$\phi(x, y, z) = \frac{\phi_{dc} + \phi_{ac} \cos(\Omega t)}{r_0^2 + 2z_0^2} (x^2 + y^2 - 2z^2), \quad (3.1)$$

where ϕ_{dc} and ϕ_{ac} are the dc and ac components of the potential and Ω is the frequency of the rf potential. The equation of motion of a charge e of mass m is then given by three uncoupled equations. So, without loss of generality, let us consider motion in one dimension only. The equation of motion is then

$$m \frac{d^2 x}{dt^2} + \frac{2e}{r_0^2 + 2z_0^2} (\phi_{dc} + \phi_{ac} \cos(\Omega t)) x = 0. \quad (3.2)$$

Equation (3.2) can be rewritten in the form

$$\frac{d^2 x}{d\tau^2} + [2q \cos(2\tau)] x = 0, \quad (3.3)$$

where,

$$\tau = \frac{\Omega t}{2}, \quad (3.4)$$

$$a = \frac{8e\phi_{dc}}{m\Omega^2 (r_0^2 + 2z_0^2)}, \text{ and} \quad (3.5)$$

$$q = \frac{4e\phi_{ac}}{m\Omega^2 (r_0^2 + 2z_0^2)}. \quad (3.6)$$

The classical equation (3.3) is just the canonical form of the Mathieu equation whose solution has been studied in detail [15-19].

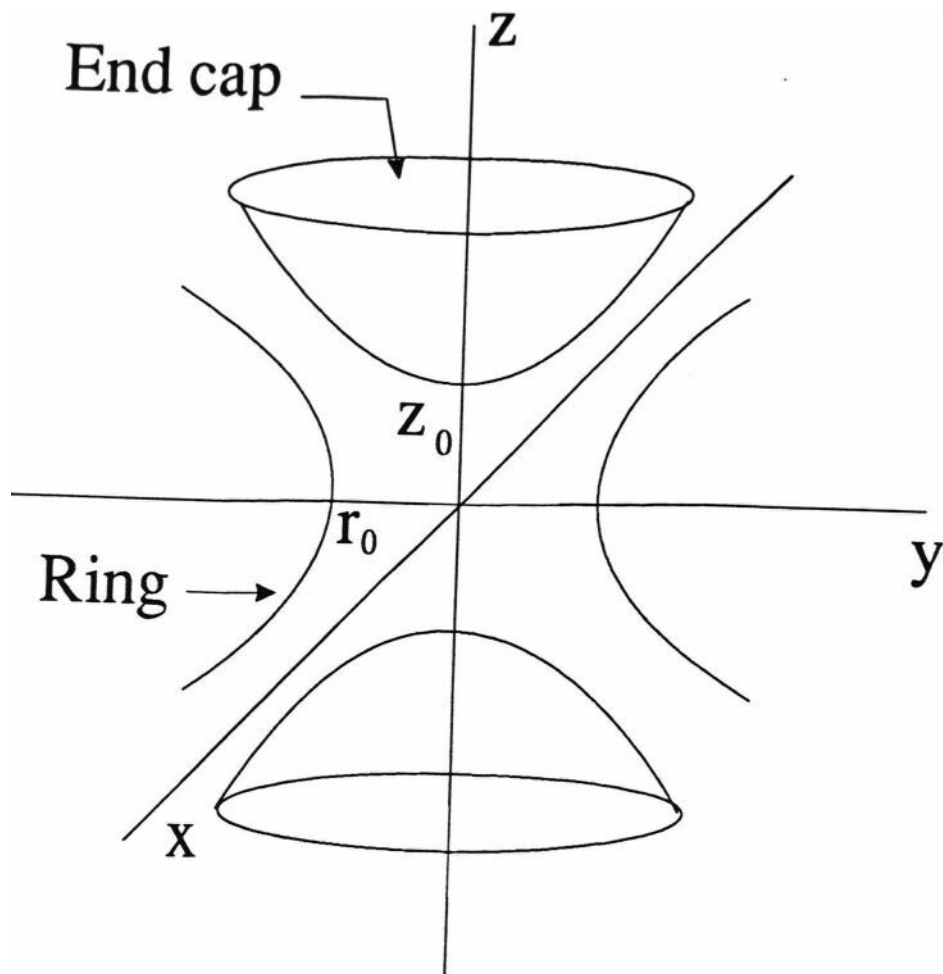


Figure 3.1: A schematic of a Paul trap.

3.1.1 Secular approximation

Let us study an approximation to the solution of the equation of motion of a particle under the influence of a high frequency force, first introduced by Kapitza [9,20-23]. Consider the motion in one dimension of a particle under the influence of a time independent potential $G(x)$ and an oscillatory force of high frequency $f(x, t) = \frac{\partial v(x)}{\partial x} \cos(\Omega t)$. The frequency Ω is large with respect to the frequency of motion due to the potential $G(x)$. The equation of motion of the particle is

$$m \frac{d^2 x}{dt^2} = -\frac{dG}{dx} + \left(\frac{\partial v}{\partial x} \right) \cos(\Omega t). \quad (3.7)$$

An approximate solution to (3.7) consists in resolving the function $x(t)$ into a slowly varying part, $X(t)$ and a rapidly varying part, $\xi(t)$ oscillating at the same frequency as the applied force. Thus,

$$x(t) = X(t) + \xi(t). \quad (3.8)$$

It is assumed that the amplitude of ξ is much smaller than X and its time average over a period τ vanishes.

Substituting (3.8) in (3.7) and expanding in powers of ξ to first order, we have

$$m \frac{d^2 X}{dt^2} + m \frac{d^2 \xi}{dt^2} = -\frac{dG}{dx} - \xi \frac{d^2 G}{dx^2} + f(X, t) + \xi \frac{\partial f}{\partial X}.$$

Equating the rapidly varying parts separately, we have

$$m \frac{d^2 \xi}{dt^2} = f(X, t), \quad (3.10)$$

integrating which, we get

$$\xi = -\frac{f}{m\Omega^2}. \quad (3.11)$$

If we take the time average of (3.9), using (3.11) and the fact that average of $\cos^2(\Omega t) = \frac{1}{2}$, we get

$$m \frac{d^2 X}{dt^2} = -\frac{dG}{dX} - \frac{(\frac{\partial v}{\partial x})^2}{4m\Omega^2}. \quad (3.12)$$

Thus, the time averaged motion of the particle is under the influence of An effective time independent potential, given by

$$\dot{v} = G(x) + \frac{(\frac{\partial v}{\partial x})^2}{4m\Omega^2}. \quad (3.13)$$

For the case of an ion in a Paul trap, the oscillatory force is $\frac{\partial v(x)}{\partial x} \cos(\Omega t)$ where, $v(x)$ is

$$v(x) \equiv \frac{2e\phi_{ac}x^2}{r_0^2 + 2z_0^2}. \quad (3.14)$$

Thus, the time averaged or the secular motion of the ion is given by

$$\frac{d^2x}{d\tau^2} + \frac{\Omega^2}{4}(a + \frac{1}{2}q^2)x = 0, \quad (3.15)$$

which is a harmonic motion with frequency, ω_s , given by

$$\omega_s = \frac{\Omega}{2}\sqrt{a + \frac{1}{2}q^2}. \quad (3.16)$$

This analysis holds in the limit of small a and q (large Ω). Fig.3.2 shows the stability regions for the Mathieu equation (3.3) in the (a, q) plane. The motion of the ion is stable and thus confinable only for certain ranges of a and q values [16]. The regions marked I and II in Fig.3.2 represent the stable regions. For most of the experimental arrangements the a and q values lie in the first stable region (I) near the origin of the coordinates a and q . The higher stable regions are difficult to maintain experimentally as they correspond to few orders of magnitude larger values for the dc and **rf potentials**. Moreover, the above approximation cannot be done and perturbative approaches are no longer valid in these regions.

3.1.2 Floquet solution

According to Floquet's theorem, the solutions to (3.3) are of the form

$$x(\tau) = Q(\tau)P(\tau), \quad (3.17)$$

where $Q(\tau) = e^{i\nu\tau}$ represents the slow motion or secular motion and $P(\tau)$ is a π -periodic function representing the micromotion. Any solution which satisfies the condition

$$x(\tau + k\pi) = C^k x(\tau) \quad (3.18)$$

where

$$C = e^{i\nu\pi} \quad (3.19)$$

is called a Floquet solution. The quantity ν is called the characteristic exponent. For the unstable regions the characteristic exponent, ν takes on complex values with a negative imaginary part, thereby leading to unstable motion of the ion. For real values of the exponent, the motion is quasiperiodic and therefore stable.

Let $U(\tau)$ and $V(\tau)$ be the two linearly independent solutions to (3.3) satisfying the initial conditions

$$U(0) = V(0) = 1 \quad \text{and} \quad (3.20)$$

$$\dot{U}(0) = \dot{V}(0) = 0. \quad (3.21)$$

Since for stable trapping of ions in a Paul trap, the characteristic exponent should be real, we have the following general solution to (3.3) ([18], pp 64)

$$x(\tau) = A \sum_{k=-\infty}^{\infty} c_{2k} \cos((2k + \nu)\tau) + B \sum_{k=-\infty}^{\infty} c_{2k} \sin((2k + \nu)\tau). \quad (3.22)$$

Thus we can identify the solutions U and V as

$$U(\tau) = \sum_{k=-\infty}^{\infty} c_{2k} \cos((2k + \nu)\tau) \quad (3.23)$$

$$V(\tau) = \frac{1}{\sum_{k=-\infty}^{\infty} c_{2k}^2 (2k + \nu)^2} \sum_{k=-\infty}^{\infty} c_{2k} \sin((2k + \nu)\tau), \quad (3.24)$$

where the co-efficients c_{2k} are normalised such that $\sum_{k=-\infty}^{\infty} c_{2k}^2 = 1$ so that the initial conditions (3.20) and (3.21) are satisfied by U and V . The approximate value of the characteristic exponent ν is determined from the conditions

$$\cos(\pi\nu) - U(\pi) = 0 \quad (3.25)$$

or

$$\cos(\pi\nu) - 1 = 2U(\pi/2)V(\pi/2) = 0 \quad (3.26)$$

by direct integration of (3.3). More accurate value of ν is obtained as follows. Substituting (3.22) in (3.3), we get the following recursion relation

$$\nu_{2k}c_{2k} = (c_{2k-2} + c_{2k+2}), \quad (3.27)$$

where

$$\nu_{2k} = \frac{a - (2k + \nu)^2}{q} \quad -\infty < k < \infty. \quad (3.28)$$

Rearranging (3.27), we have

$$\nu_{2k} = \frac{c_{2k-2}}{c_{2k}} + \frac{c_{2k+2}}{c_{2k}}. \quad (3.29)$$

Defining the ratios,

$$G_m = \frac{c_m}{c_{m-2}}, \quad (3.30)$$

we have from (3.29)

$$G_m = \nu_m \frac{1}{\nu_{m+2} - \dots} \quad (3.31)$$

Similarly, by defining the ratios

$$H_{-m} = \frac{c_{-m-2}}{c_{-m}}, \quad (3.32)$$

we have

$$H_{-m} = \bar{\nu}_{-m-2} \frac{1}{\bar{\nu}_{-m-4} - \dots}. \quad (3.33)$$

Using continued fractions, the ratios G_m and H_{-m} can be obtained for some large m . Once G_m and H_{-m} are determined, then the rest of the terms from G_{m-2} to G_0 and H_{-m+2} to H_0 are obtained as

$$G_{l-2} = \frac{1}{\nu_{l-2} - G_l}, \quad m > l > 2 \quad (3.34)$$

and

$$H_{-l+2} = \bar{\nu}_{-l} - H_{-l}, \quad m \geq l \geq 2. \quad (3.35)$$

If the characteristic exponent is correct, then the quantities G_0 and H_0 should verify the identity

$$G_0 H_0 = 1. \quad (3.36)$$

The exact characteristic exponential is then obtained from (3.28), Thus

$$\nu_0 = \frac{a - \nu^2}{9}, \quad (3.37)$$

or

$$\nu = \sqrt{a - \nu_0 q}, \quad (3.38)$$

where ν_0 is obtained from (3.29) using the previously determined ratios G_2 and H_0 . The definitions (3.30) and (3.32) can then be used to obtain the co-efficients c_{2k} 's in terms c_0 . The term C_0 can then be fixed by requiring that $\sum_{k=-\infty}^{\infty} c_{2k} = 1$, as demanded by the initial condition $U(0) = 1$.

3.2 Quantum dynamics

The motion described by (3.3) corresponds to the quantum Hamiltonian

$$H = \frac{\hat{p}^2}{2m} + \frac{1}{2}m\omega^2(t)\hat{x}^2, \quad (3.39)$$

where

$$\omega^2(t) = \ddot{\tau}[a - 2q \cos(\Omega t)]. \quad (3.40)$$

Thus, the motion of the ion is that of an oscillator whose frequency is time dependent in a sinusoidal manner. The equations of motion for the position and momentum are given by

$$\begin{aligned} \frac{d\hat{x}}{dt} &= \frac{p}{m} \\ \frac{d\hat{p}}{dt} &= -m\omega^2(t)\hat{x}. \end{aligned} \quad (3.41)$$

The Schrodinger equation now involves a potential periodic in time. For large periodicity one can do a time average to obtain the secular motion.

In what follows we consider the quantum case. And the general solution of the Heisenberg equation (3.41). We will also find the time evolution of the wave function of the system or equivalently, we will obtain the time dependent density matrix *without using the approximations* used in arriving at (3.16). We will further show that the state corresponding to the centre of mass motion is a nonclassical state.

We redefine the variables \mathbf{x} and \mathbf{p} so that

$$\hat{X} = \sqrt{\frac{m\omega_0}{2\hbar}}\hat{x}, \text{ and } \hat{P} = \sqrt{\frac{1}{2m\hbar\omega_0}}\hat{p}, \quad (3.42)$$

where ω_0 is the intrinsic frequency of the time independent oscillator given by setting $q = 0$ in (3.3). We thus get

$$\omega_0^2 = \frac{\Omega^2 a}{4}. \quad (3.43)$$

Once the parameter a and the frequency Ω are chosen, the natural frequency ω_0 gets fixed. Thus varying the ratio $\frac{\omega_0}{\Omega}$ for a fixed a value corresponds to sweeping of the frequency of the oscillator. The new position and momentum operators satisfy the commutation relation

$$[\hat{X}, \hat{P}] = \frac{i}{\Omega}. \quad (3.44)$$

In the Heisenberg picture, the equations of motion for the operators \hat{X} and \hat{P} are

$$\frac{d\hat{X}}{dt} = \omega_0 \hat{P}, \quad \frac{d\hat{P}}{dt} = -\frac{\Omega^2}{4}(a - 2q \cos(\Omega t))\hat{X} \quad (3.45)$$

or, in terms of the scaled time $\tau = \frac{t}{2}$, we have,

$$\begin{aligned} \frac{d\hat{X}}{d\tau} &= \frac{2\omega_0}{\Omega} \hat{P}, \\ \frac{d\hat{P}}{d\tau} &= -\frac{\Omega}{2\omega_0}(a - 2q \cos(\tau))\hat{X}. \end{aligned} \quad (3.46)$$

We can also define the lowering and raising operators a and a^\dagger by the relations

$$a = \hat{X} + i\hat{P}, \quad (3.47)$$

$$a^\dagger = \hat{X} - i\hat{P} \quad (3.48)$$

with

$$[\hat{a}, \hat{a}^\dagger] = 1. \quad (3.49)$$

The solution of (3.46) can be expressed as

$$\begin{aligned} X(\tau) &= U(\tau)X(0) + \left(\frac{2\omega_0}{\Omega}\right)V(\tau)\hat{P}(0) \\ P(\tau) &= \dot{U}(\tau)\left(\frac{2\omega_0}{\Omega}\right)^{-1}\hat{X}(0) + V(\tau)P(0) \end{aligned} \quad (3.50)$$

where $U(\tau)$ and $V(\tau)$ are given by (3.23) and (3.24). Note that the solutions $U(\tau)$ and $V(\tau)$ satisfy the property

$$U(\tau)\dot{V}(\tau) - V(\tau)\dot{U}(\tau) = 1, \quad (3.51)$$

so that equal time Heisenberg commutation relations hold, viz.,

$$[X(\tau), P(\tau)] = \frac{i}{\hbar} \quad (3.52)$$

The time dependent variances of the operators X and P can be obtained from (3.50) for various oscillator initial states.

Using (3.50) we obtain the time dependence of the lowering and raising operators as

$$\hat{a}(\tau) \equiv u(\tau)\hat{a}(0) + v(\tau)\hat{a}^\dagger(0), \quad (3.53)$$

$$\hat{a}^\dagger(\tau) = v^*(\tau)\hat{a}(0) + u^*(\tau)\hat{a}^\dagger(0), \quad (3.54)$$

where the co-efficients $u(\tau)$ and $v(\tau)$ are given in terms of the solutions of (3.3) as

$$u(\tau) = \frac{1}{2} \left((U + \dot{V}) + i \left(\frac{\Omega \dot{U}}{2\omega_0} - \left(\frac{2\omega_0 V}{\Omega} \right) \right) \right), \quad (3.56)$$

$$v(\tau) = \frac{1}{2} \left((U - V) + i \left(\frac{\Omega U}{2\omega_0} + \left(\frac{2\omega_0 V}{\Omega} \right) \right) \right). \quad (3.56)$$

We have thus a Bogoliubov transformation of operators with time dependent coefficients.

As was done in chapter 2 the equation (3.53) can be expressed as a unitary transformation. We rewrite (3.53) as

$$\hat{a}(\tau) = \exp(i\theta_u \hat{a}^\dagger \hat{a}) (|u|\hat{a}(0) + |v|\exp(i[\theta_v - \theta_u])\hat{a}(0)). \quad (3.57)$$

and therefore,

$$\hat{a}(\tau) = \tilde{S}^{-1}(\tau) \hat{a} \tilde{S}(\tau), \quad (3.58)$$

where

$$\tilde{S}(\tau) = \exp(i \text{fata}) \exp \left(\frac{1}{2} \epsilon^{i(\theta_v - \theta_u)} \cosh(|u|) \hat{a}^\dagger - h.c. \right). \quad (3.59)$$

The equation (3.58) relates the Heisenberg operator at time r to the operator at time $\tau = 0$. It should be borne in mind that all the parameters $\theta_u, \theta_v, |u|$ and $|v|$ depend on time τ . The Fourier series decomposition of the functions $u(\tau)$ and $v(\tau)$ can be obtained by using the definition of the functions U and V from (3.23) and (3.24). We thus have

$$\begin{aligned} u(t) = & \frac{1}{2} \left[\sum_{k=-\infty}^{\infty} c_{2k} \cos\left((k + \frac{\nu}{2})\Omega t\right) + \frac{1}{\omega_0 D} \sum_{k=-\infty}^{\infty} c_{2k} \left(k + \frac{\nu}{2}\right) \cos\left((k + \frac{\nu}{2})\Omega t\right) \right] \\ & - \frac{i}{2} \left[\left(\frac{\Omega}{\omega_0}\right) \sum_{k=-\infty}^{\infty} c_{2k} \left(k + \frac{\nu}{2}\right) \sin\left((k + \frac{\nu}{2})\Omega t\right) + \right. \\ & \left. \frac{1}{D} \sum_{k=-\infty}^{\infty} c_{2k} \sin\left((k + \frac{\nu}{2})\Omega t\right) \right], \end{aligned} \quad (3.60)$$

$$\begin{aligned} v(t) = & \frac{1}{2} \left[\sum_{k=-\infty}^{\infty} c_{2k} \cos\left((k + \frac{\nu}{2})\Omega t\right) - \frac{\Omega}{\omega_0 D} \sum_{k=-\infty}^{\infty} c_{2k} \left(k + \frac{\nu}{2}\right) \cos\left((k + \frac{\nu}{2})\Omega t\right) \right] \\ & - \frac{i}{2} \left[\left(\frac{\Omega}{\omega_0}\right) \sum_{k=-\infty}^{\infty} c_{2k} \left(k + \frac{\nu}{2}\right) \sin\left((k + \frac{\nu}{2})\Omega t\right) - \right. \\ & \left. \frac{1}{D} \sum_{k=-\infty}^{\infty} c_{2k} \sin\left((k + \frac{\nu}{2})\Omega t\right) \right], \end{aligned} \quad (3.61)$$

where D is given by

$$D = 2 \sum_{k=-\infty}^{\infty} c_{2k} \left(k + \frac{\nu}{2}\right). \quad (3.62)$$

3.3 Dynamics in the Schrodinger picture

Explicit wave functions corresponding to different states of the time dependent oscillator can be obtained by going into the Schrodinger picture. The time evolution of the density matrix can be obtained from the evolution operator, $S(\tau)$

$$\hat{\rho}(\tau) = \tilde{S}(\tau) \hat{\rho}(0) \tilde{S}^{-1}(\tau). \quad (3.63)$$

Therefore, if $|\psi(0)\rangle$ is the initial state, then the state of the oscillator at time r will be

$$|\psi(\tau)\rangle = \hat{S}(\tau)|\psi(0)\rangle. \quad (3.64)$$

Let the initial state be the ground state, $|\psi_0\rangle$, of the oscillator. Thus,

$$\hat{a}|\psi_0\rangle = 0. \quad (3.65)$$

In the Schrodinger picture, after a time r , the ground state evolves to $|\psi_0(\tau)\rangle$. Since the evolution operator, S , is unitary,

$$\tilde{S}^{-1}\tilde{S} = \tilde{S}\tilde{S}^{-1} = 1, \quad (3.66)$$

introducing $S^{-1}S$ between a and $|\psi_0\rangle$ in (3.65) and multiplying by S from the left, we are left with

$$\tilde{S}\hat{a}\tilde{S}^{-1}\tilde{S}|\psi_0\rangle = 0. \quad (3.67)$$

But,

$$S|\psi_0(0)\rangle = |\psi_0(\tau)\rangle \quad (3.68)$$

and

$$\tilde{S}\hat{a}\tilde{S}^{-1} = u^*(\tau)\hat{a}(0) - v(\tau)\hat{a}^\dagger(0) = \text{fc}(r). \quad (3.69)$$

This state $|\psi_0(\tau)\rangle$ would then be the ground state with respect to the transformed operator $b(\tau)$:

$$[u^*(\tau)\hat{a}(0) - v(\tau)\hat{a}^\dagger(0)]|\psi_0(\tau)\rangle = 0. \quad (3.70)$$

Let us now determine the coordinate representation of this ground state. So we have to determine the quantity

$$\langle x|S|\psi_0\rangle. \quad (3.71)$$

Using the definition of the unitary evolution operator \hat{S} and the disentangling theorem for the $SU(1,1)$ group (cf. Appendix 2A) we arrive at the following expression

$$\langle x|\hat{S}|\psi_0\rangle = \sqrt{\frac{m\omega}{\pi\hbar}} \frac{1}{\sqrt{|u|}} \sum_{n=0}^{\infty} \frac{(2n-1)!!}{2^n(2n)!} \left(\frac{|v|}{|u|}\right)^n e^{i(\theta_u+\theta_v)} H_{2n}\left(\frac{m\omega}{\hbar}x\right) \exp\left(-\left[\frac{m\omega}{2\hbar}\right]x^2\right). \quad (3.72)$$

The above infinite series can be summed by considering arguments concerning scaling of Gaussians (see Appendix 3A) and thus determining the wave function with correct phase factor and the result is

$$\langle x|S|\psi_0\rangle = \sqrt{\frac{m\omega}{\pi\hbar}} \frac{1}{\sqrt{u^* - v}} \exp\left(-\left(\frac{x^*}{u^* - v}\right)^2 \left(\frac{m\omega}{2\hbar}\right)x^2\right). \quad (3.73)$$

At time $t = 0$, (3.73) is just the wave function for a simple harmonic oscillator, as expected.

The transformation (3.53) and (3.54) can be used to investigate the time evolution of the Wigner function which is defined by

$$\Phi(\alpha, \alpha^*) = \frac{1}{\pi^2} \int d^2\beta \text{Tr}\left(\hat{\rho} \exp(\beta \hat{a}^\dagger - \beta^* \hat{a})\right) \exp(-\beta \alpha^* + \beta^* \alpha). \quad (3.74)$$

We showed in the previous chapter ((2.33) to (2.55)) that whatever be the time dependence of the frequency of the oscillator, a Gaussian Wigner function retains its Gaussian nature and that the Wigner function evolves along the classical orbits.

For numerical purposes, in order to obtain the variances in \hat{X} and \hat{P} , the Floquet solutions were determined as described in section 3.1.2. First by a direct numerical integration of (3.3), the characteristic exponent was obtained. Then using continued fractions the co-efficients c_{2k} 's were obtained. The variances were then directly obtained for specific initial states of the oscillator. Alternatively, one could also calculate the variances by a direct integration of the equations for the meanvalues as given in the previous chapter. In Fig.3.3 the uncertainty in the position the ion for various values of ω_0/Ω is plotted against time. We see that there is strong squeezing in the position uncertainty. Similar results were also reported in [24-28]. In Fig.3.4 we plot the Wigner function at a time when the variance in the position goes to a minimum. It is a Gaussian with the width along A'' squeezed.

3.4 External perturbations and the transitions caused by the electromagnetic field

Consider a two-level optical transition in an electromagnetic field. The total Hamiltonian describing a particle in a trap in the presence of electromagnetic field is

$$H = \hbar\omega_a \hat{S}^z + \left(\frac{\hat{p}^2}{2m} + \frac{1}{2} m \omega^2(t) \hat{x}^2 \right) - \frac{(\vec{d} \cdot \vec{E})}{\hbar} (\hat{S}^+ \exp(ik\hat{x} - i\omega_l t) + h.c.) \quad (3.75)$$

where the internal degrees of freedom are described by the spin operators. The centre of mass motion in the trap is described by the time dependent oscillator. Both ground and excited electronic states have a periodic potential associated with them. The ions' initial state is $|-, 0\rangle$, where $|-\rangle$ labels the ground state of the electronic state and $|0\rangle$ labels the ground state of the motion of the centre of mass of the ion. The final state is $|-, 1\rangle$ i.e., we are basically considering Raman transitions in which the centre of mass motion is excited to the state $|1\rangle$. In the interaction picture (3.75) becomes

$$H_1(t) = -\left(\frac{\vec{d} \cdot \vec{E}}{\hbar}\right) (\hat{S}^+ \exp[i(\omega_a - \omega_l)t + ik\hat{x}(t)] + h.c.) \quad (3.76)$$

where $\hat{x}(t)$ denotes the quantised motion of the centre of mass. Let us first calculate the excitation probability i.e., we calculate the probability of finding the ion in the state $|+\rangle$ and we sum over all states associated with the centre of mass motion. Using (3.76) the state at time t is

$$|\Psi(t)\rangle = |\Psi(0)\rangle - \frac{i}{\hbar} \int_0^t H_1(t_1) dt_1 |\Psi(0)\rangle \quad (3.77)$$

and hence the probability of finding the ion in the excited state $|+\rangle$ is

$$\begin{aligned} P &= \frac{1}{\hbar^2} \text{Tr}_{\text{cm}} \int_0^t \int_0^t \langle + | H_1(\tau_1) | \Psi(0) \rangle \langle \Psi(0) | H_1(\tau_2) | + \rangle d\tau_1 d\tau_2 \\ &= \left| \frac{(\vec{d} \cdot \vec{E})}{\hbar} \right|^2 \int_0^t d\tau_1 \int_0^t d\tau_2 \langle 0 | \exp(-i(\omega_a - \omega_l)\tau_1 - ik\hat{x}(\tau_1)) \\ &\quad \exp(+i(\omega_a - \omega_l)\tau_2 + ik\hat{x}(\tau_2)) | 0 \rangle, \end{aligned} \quad (3.78)$$

where $|0\rangle$ is the ground state of the centre of motion of the ion. The transition rate is then

$$R = \lim_{t \rightarrow \infty} \frac{\partial P}{\partial t} = \left| \frac{(\vec{d} \cdot \vec{E})}{\hbar} \right|^2 \lim_{t \rightarrow \infty} \frac{\partial}{\partial t} \int_0^t d\tau_1 \int_0^t d\tau_2 \langle 0 | \exp(-i(\omega_a - \omega_l)\tau_1 - ik\hat{x}(\tau_1))$$

$$\exp(+i(\omega_a - \omega_l)\tau_2 + ik\hat{x}(\tau_2)) |O\rangle. \quad (3.79)$$

$$\begin{aligned} & \left| \frac{(\vec{d} \cdot \vec{E})}{\hbar} \right|^2 k^2 \lim_{\Omega \rightarrow \infty} \int_0^t d\tau' \{ (1 + A(t)A^*(\tau')) \exp(-i(\omega_a - \omega_l)(t - \tau')) \\ & \quad + \text{c.c.} \}. \end{aligned} \quad (3.80)$$

Note that the operator \hat{x} can be written as

$$\hat{x}(t) = A(t)\hat{a}(0) + A(t)\hat{a}^\dagger(0) \quad (3.81)$$

where the amplitude $A(t)$ is given by

$$A(t) = \alpha \sum_{k=-\infty}^{\infty} c_{2k} e^{i(\nu+2k)\frac{\Omega t}{2}} + \beta \sum_{k=-\infty}^{\infty} c_{2k} e^{-i(\nu+2k)\frac{\Omega t}{2}}, \quad (3.82)$$

with α and β as given by

$$\alpha = \sqrt{\frac{\hbar}{8m\omega_0}} \left(1 - \frac{2\omega_0}{D\Omega}\right) \quad (3.83)$$

$$\beta = \sqrt{\frac{\hbar}{8m\omega_0}} \left(1 + \frac{2\omega_0}{D\Omega}\right), \quad (3.84)$$

and D as defined in (3.62). On substituting (3.82) in (3.80) and retaining only the time independent contributions, we get

$$\begin{aligned} R = & 2\pi \left| \frac{(\vec{d} \cdot \vec{E})}{\hbar} \right|^2 \delta(\omega_a - \omega_l) + 2\pi \alpha^2 k^2 \left| \frac{(\vec{d} \cdot \vec{E})}{\hbar} \right|^2 \sum_n |c_{2n}|^2 \\ & \delta\left(\omega_a - \omega_l - \frac{\nu\Omega}{2} - n\Omega\right) \end{aligned} \quad (3.85)$$

$$+ 2\pi \beta^2 k^2 \left| \frac{(\vec{d} \cdot \vec{E})}{\hbar} \right|^2 \sum_n |c_{2n}|^2 \delta\left(\omega_a - \omega_l + \frac{\nu\Omega}{2} + n\Omega\right). \quad (3.86)$$

Here the quantity αk is roughly the ratio of the ion's excursion to optical wavelength. Thus, the excitation probability shows resonances at

$$\omega_l = \omega_a \quad \omega_l = \omega_a \pm \frac{\nu\Omega}{2} - n\Omega. \quad (3.87)$$

For $n = 0$, we get the familiar side bands obtained from the secular motion of the ion. The strength of these side bands is proportional to $|c_0|^2$. The following is a table of the co-efficients $|c_{2n}|^2$ obtained with $a = 0.04$ and $q = 0.2$ corresponding to the Ref. [31]

Chapter 3. Quantised motion of an ion in a Paul trap

| $2n$ | $ c_{2n} ^2$ |
|------|------------------------|
| -4 | 7.214×10^{-7} |
| -2 | 3.556×10^{-3} |
| 0 | 0.816 |
| 2 | 1.300×10^{-3} |
| 4 | 1.606×10^{-7} |

In conclusion, in this chapter, we have considered a material oscillator (quantised motion of the centre of mass of the ion) and applied the results of the previous chapter to show that an even more restriction of the motion of the ion in the confined environment of a Paul trap is possible. We have obtained explicit form of the ground state wave function in coordinate space. Further, by considerations of transitions induced by the interaction between the ion and external electromagnetic fields, we have also studied the occurrence and strength of the side-bands in the fluorescence spectrum of the ion in a Paul trap.

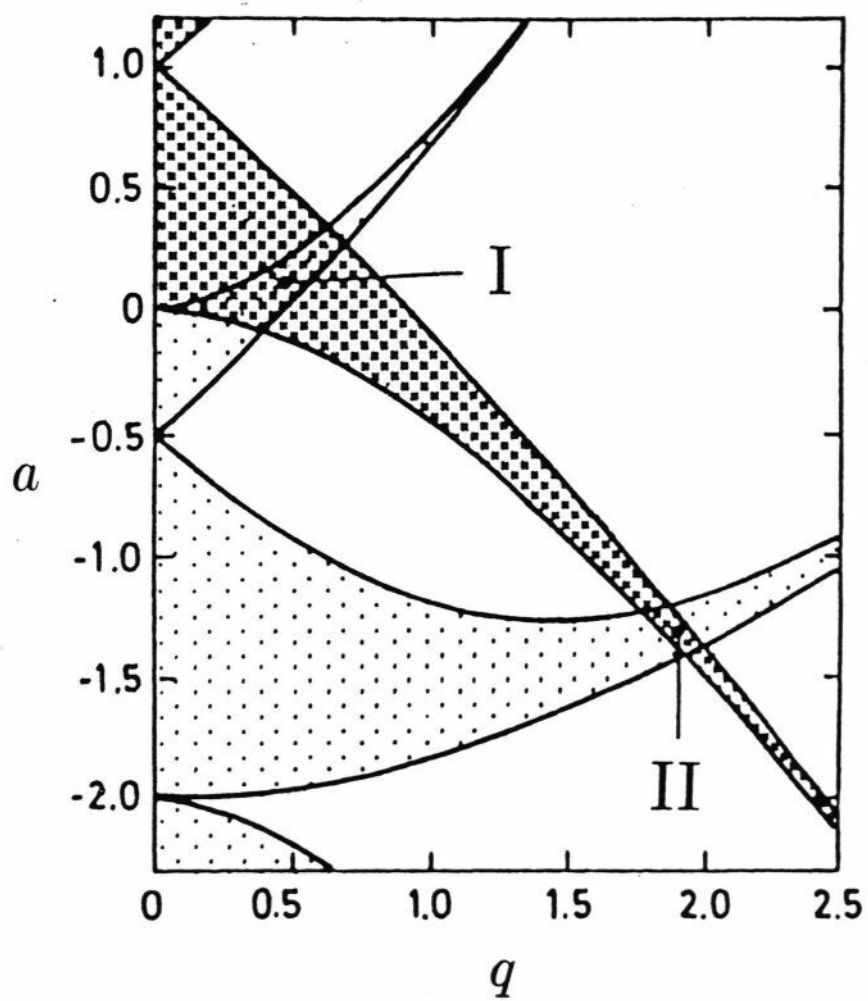


Figure 3.2: Stability regions for the Mathieu equation.

Chapter 3. Quantified motion of an ion in a Paul trap

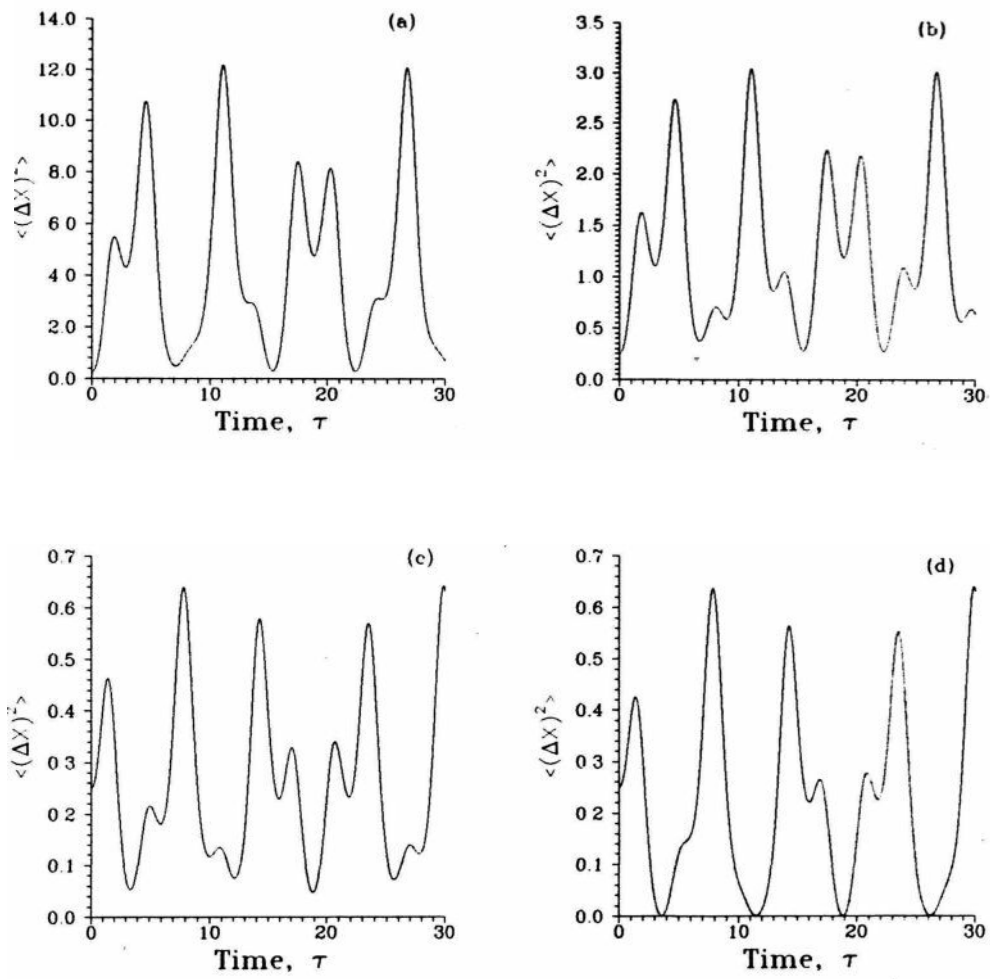


Figure 3.3: The uncertainty in the position of the ion as a function of time. The corresponding parameters are $a = 0.04, q = 0.2$ and $\frac{\omega_0}{\omega} =$ (a) 1, (b) 0.5, (c) 0.1, (d) 0.01. The initial state is the vacuum.

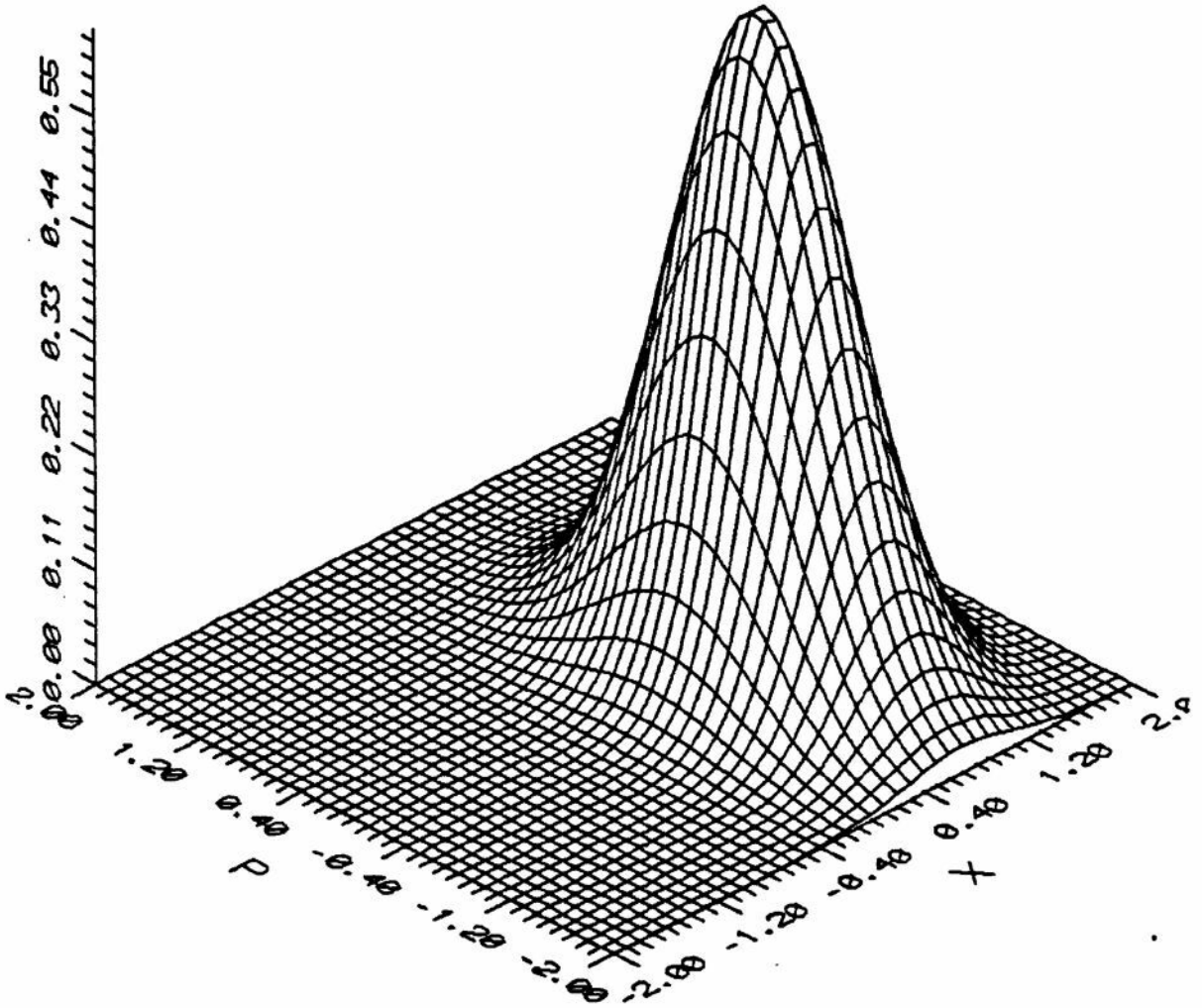


Figure 3.4: Wigner function at a later time when the initial state (at $t = 0$) is a coherent state with $\alpha = 1$, $a = 0.04$, $q = 0.2$ and $\omega_0/\Omega = 0.1$.

Appendix 3A

Scaling of Gaussians

In this appendix, the steps involved in obtaining (3.73) from (3.72) are given. We notice that in obtaining (3.73) from (3.72), there is a scale transformation involved in changing the Gaussian $e^{-\rho^2}$ to $e^{-\epsilon\rho^2}$, where $p = (\frac{m\omega_0}{2\hbar}x)$ and ϵ , in general, is complex. So, we are interested in expanding a scaled Gaussian in terms of unsealed functions. First, we note the fact that the scaled exponential that we are interested in is an even function and hence we infer that the expansion should not contain any odd valued terms. Moreover, (3.72) already has only even terms in it. Let

$$\exp(-\epsilon\rho^2) = \sum_{k=0}^{\infty} d_{2k} H_{2k}(\rho) \epsilon^{-\rho^2} \quad (3A.1)$$

where $\epsilon \in \mathbb{C}$. We will show that if the co-efficients d_{2k} are determined, then essentially we would have determined the scaled Gaussian in terms of unsealed functions and thereby also sum the infinite series (3.72). Multiplying by $H_{2n}(\rho)$ from both the sides of (3A.1) and integrating over the whole real line, we have

$$\int_{-\infty}^{\infty} \exp(-\epsilon\rho^2) H_{2n}(\rho) d\rho = \sum_{k=0}^{\infty} d_{2k} \int_{-\infty}^{\infty} H_{2k}(\rho) H_{2n}(\rho) \exp(-\rho^2) d\rho. \quad (3A.2)$$

Using the orthogonality relation for Hermite polynomials $\int_{-\infty}^{\infty} H_k(\rho) H_n(\rho) d\rho = 2^n(n!) \sqrt{\pi} \delta_{kn}$, we have

$$d_{2n} = \frac{2}{2^{2n}(2n)! \sqrt{\pi}} \int_0^{\infty} e^{-\rho^2} H_{2n}(\rho) d\rho. \quad (3A.3)$$

Now one has to determine the integral in the above equation to determine J_{2n} . From [32] (§7.376, Eqn(2), p838) we have the following relation

$$\int_{x=0}^{x=\infty} e^{-2\alpha x^2} x^\nu H_{2n}(x) dx = (-1)^n 2^{2n-\frac{1}{2}-\frac{\nu}{2}} \frac{\Gamma(\frac{\nu+1}{2}) \Gamma(n+\frac{1}{2})}{\sqrt{\pi} \alpha^{\frac{(\nu+1)}{2}}} F(-n, \frac{\nu+1}{2}, \frac{1}{2}, \frac{1}{2\alpha}) \quad (3A.4)$$

with $\text{Re}(\alpha) > 0$ and $\text{Re}(\nu) > -1$. In the integral in (3A.3), $\text{Re}(\epsilon) > 0$ and $\text{Re}(\nu) = 0$. Therefore,

$$\int_{\rho=0}^{\rho=\infty} e^{-\epsilon \rho^2} H_{2n}(\rho) d\rho = (-1)^n 2^{2n-\frac{1}{2}} \frac{1}{\sqrt{\pi \frac{\epsilon}{2}}} \Gamma\left(\frac{1}{2}\right) \Gamma\left(n + \frac{1}{2}\right) F\left(-n, \frac{1}{2}; \frac{1}{2}, \frac{1}{\epsilon}\right). \quad (3A.5)$$

Noting that ([32], §9.121(1), p1040)

$$F(-n, \beta; \beta, -z) = (1+z)^n \quad (3A.6)$$

and

$$\Gamma\left(n + \frac{1}{2}\right) = \frac{(2n-1)!!}{2^n} \sqrt{\pi} \quad (3A.7)$$

for arbitrary values of n and substituting (3A.7) and (3A.6) into (3A.5), we have

$$d_{2n} = (-1)^n \frac{1}{2^n} \frac{(2n-1)!!}{(2n)!} \frac{1}{\sqrt{\epsilon}} \left(1 - \frac{1}{\epsilon}\right)^n H_{2n}(\rho) e^{-\rho^2}.$$

Thus, (3A.5) can be written as (3A.8)

$$\exp(-\epsilon \rho^2) = \sum_{n=0}^{\infty} (-1)^n \frac{(2n-1)!!}{2^n (2n)!} \frac{1}{\sqrt{\epsilon}} \left(1 - \frac{1}{\epsilon}\right)^n H_{2n}(\rho) e^{-\rho^2}. \quad (3A.9)$$

Now, let

$$\epsilon = \eta + 1, \quad (3A.10)$$

with

$$-\left(\frac{\eta}{\eta+1}\right) = \left(\frac{|v|}{|u|}\right) e^{i(\theta_u + \theta_v)}. \quad (3A.11)$$

Then (3A.9) can be written as

$$\sqrt{\eta+1} \exp(-(\eta+1)\rho^2) = \sum_{n=0}^{\infty} (-1)^n \frac{(2n-1)!!}{2^n (2n)!} \left(\frac{\eta}{\eta+1}\right)^n H_{2n}(\rho) e^{-\rho^2}. \quad (3A.12)$$

On comparing the corresponding terms in (3.72) and (3A.12), we finally have

$$\langle x | \hat{S} | 0 \rangle = \sqrt{\frac{m\omega}{\pi \hbar}} \frac{1}{\sqrt{|u|}} \sqrt{\eta+1} \exp(-(\eta+1)\rho^2). \quad (3A.13)$$

Substituting the value for η in the above equation yields the desired **result**:

$$\langle x | \hat{S} | 0 \rangle = \sqrt{\frac{m\omega}{\pi \hbar}} \frac{1}{\sqrt{|u|}} \sqrt{\frac{u^*}{u^* - v}} \exp\left(-\left(\frac{|u^*}{u^* - v}\right) \left(\frac{m\omega}{2\hbar}\right) x^2\right). \quad (3A.14)$$

References

- [1] R.S. Van Dyck Jr., P.B. Schwinberg and H.G. Dehmelt, Phys. Rev. Lett. 59, 26 (1987).
- [2] W. Neuhauser, M. Hohenstatt and P.E. Toschek, Phys. Rev. A 22,1137 (1980).
- [3] J.J. Bellinger, D.J. Heinzen, W.M. Itano, S.L. Gilbert and D.J. Wineland, Phys. Rev. Lett. 63, 1031 (1989).
- [4] W.M. Itano, D.J. Heinzen, J.J. Bellinger and D.J. Wineland, Phys. Rev. A 41, 2295 (1990).
- [5] W. Nagourney, J. Sandberg and H.G. Dehmelt, Phys. Rev. Lett. 56, 2797 (1986).
- [6] T. Sauter, W. Neuhauser, R. Blatt and P.E. Toschek, Phys. Rev. Lett. 57, 1696 (1986).
- [7] J.C. Bergquist, R.C. Hulet, W.M. Itano and D.J. Wineland, Phys. Rev. Lett. 57, 1699 (1986).
- [8] F. Diedrich, J.C. Bergquist, W.M. Itano and D.J. Wineland, Phys. Rev. Lett. 62, 403 (1989).
- [9] P.L. Kapitza, Zh. Eksp. Teor. Fiz. 21, 588 (1951).
- [10] J.C. Maxwell, *Treatise on Electricity and Magnetism* (Dover, New York, 1962), pp 174-176.
- [11] J.A. Stratton, *Electromagnetic Theory* (McGraw-Hill, New York, 1941), p.116.
- [12] However, in a recent letter Chiao et.al (Raymond Y. Chiao and Jack Boyce, Phys. Rev. Lett. 73, 3383 (1994)) consider a situation where there is an apparent violation of this theorem.
- [13] W. Paul and M. Raether, Z. Phys. 140, 262 (1955).
- [14] R.F. Wuerker, H.M. Goldenberg and R.V. Langmuir, J. Appl. Phys. 30, 441 (1959).
- [15] E. Fischer, Z. Phys. 156, 1 (1959).
- [16] R. Blumel, C. Kappler, W. Quint and H. Walther, Phys. Rev. A 40, 808 (1989).

- [17] E.T. Whittaker and C.N. Watson, *Modem Analysis*, (Cambridge University Press, Cambridge, 1927).
- [18] N.W. McLachlan, *Theory and Application of Mathieu Functions*, (Dover, New York, 1964).
- [19] M. Abramowitz and I. Stegun, *Handbook of Mathematical Functions*, (Dover, New York, 1965).
- [20] L.D. Landau and E.M. Lifshitz, *Mechanics*, (Pergamon, Oxford, 1976), pp. 93-95.
- [21] R.J. Cook, D.G. Shankland and A.L. Wells, Phys. Rev. A 31, 564 (1985).
- [22] S. Stenholm, Rev. Mod. Phys. 58, 699 (1986).
- [23] D.J. Wineland, W.M. Itano, Van Dyck, Adv. atom, molec, Phys. **19**, 135 (1984).
- [24] M. Combescure, Ann. Inst. Henri Poincare 44, 293 (1986).
- [25] L.S. Brown, Phys. Rev. Lett. 66, 527 (1991).
- [26] R.J. Glauber, *Recent Developments in Quantum Optics*, Proceedings of the International Conference on Quantum Optics held at Hyderabad, edited by Ramarao Inguva (Plenum, New York, 1993), pp. 1-13.
- [27] R.J. Glauber, *Quantum Measurements*, (Plenum, New York, 1992).
- [28] Fu li Li, Phys. Lett. A 168, 400 (1992).
- [29] G.S. Agarwal and S. Arun Kumar, Phys. Rev. Lett. 67, 3665 (1991).
- [30] G.S. Agarwal, J. Mod. Opt. **34**, 909 (1987).
- [31] V. Enders, Ph. Courteille, W. Neuhauser and R. Blatt, J. Mod. Optics **39**, 325 (1992).
- [32] I.S. Gradshteyn and I.M. Ryzhik, *Table of Inregrals, Series and Products*, (Academic Press, New York,. 1965).

Chapter 4

Nonclassical light generation in a cavity of variable length

In this chapter¹, a simple model consisting of a cavity with a movable mirror in one dimension is considered. This problem has received considerable attention in the recent past in the context of particle creation [1-5]. The radiation that is produced due to the mirror motion is a purely quantum mechanical effect having no classical analogues. Hence we expect nonclassical features to manifest in the fields so produced. This radiation arises due to the interaction of the mirror with the vacuum fluctuations of a quantised field. The mirror need not be a physical one but a sudden change in the refractive index of medium can also produce real photons from an initial vacuum state [6-8]. In this chapter, we study the quantum statistical properties of the field so produced due to accelerated mirror motion and study the nonclassical nature of the field. We restrict to only one dimension. In four dimensions the problem was studied by Candela et al [9]. The problem of a spherical mirror expanding with uniform acceleration was considered by Frolov et al [10]. By making a conformal transformation, the nonstationary problem is mapped onto that of a stationary one and the field solution inside the cavity is obtained. Then by the application of a canonical quantisation procedure [1,3,11], a quantised version of the solution is derived. It then follows that the "in-out" mirror motion corresponds to a Bogolubov transformation of the annihilation and creation operators. Then, by a calculation of the variances in the field quadratures, it is shown that initially, the

¹ Results of this chapter were presented as invited talk at the "Discussion Meeting on Non-classical Aspects of Radiation", held at the Indian Institute of Science, Bangalore, 10-12 January, 1994 and at the "National Workshop on Recent Advances in Quantum Optics", held at the Centre for Advanced Technology, Indore, 7-10, March, 1994.

state of the field is vacuum or a coherent state, then, the motion of the mirror produces squeezing of fluctuations in the field quadratures. It is also shown that the various modes of the cavity get correlated as a result of the mirror motion.

4.1 The model

Consider a scalar electromagnetic field within a region bounded by two mirrors, one of which executes an "in-out" motion. The requirement that the motion $q(ct)$ of the mirror starts at some finite past and stops at some finite future, at least asymptotically, is what is classified as an "in-out" motion (see Fig.4.1). We restrict the mirror motion to only one dimension.

Let us consider the wave equation for an electromagnetic field in the region bounded by the two mirrors

$$\frac{\partial^2 \phi(x, ct)}{\partial x^2} = \frac{\partial^2 \phi(x, ct)}{\partial (ct)^2}, \quad (4.1)$$

where, $\phi(x, ct)$ is the scalar electromagnetic field and c is the velocity of light in vacuum. The usual boundary conditions demand that the field vanishes at the boundaries $x = 0$ and $x = q(ct)$. So we have the boundary condition,

$$\phi(x = 0, ct) = \phi(x = q(ct), ct) = 0 \quad \forall ct. \quad (4.2)$$

The solution of (4.1) with boundary condition (4.2) is simple for the case of stationary mirrors:

$$u_n \sim \sin\left(\frac{n\pi x}{L}\right) \exp\left(-i\frac{n\pi ct}{L}\right), \quad (4.3)$$

when the mirrors are located at $x = 0$ and $x = L$. The basic idea in solving the non-stationary problem is to do a conformal transformation [1,3,11], such that it, reduces to that of a stationary problem in the transformed coordinates.

To that end we make the following transformation [1,11]

$$\begin{aligned} w + s &= R(ct + x) \\ w - s &= R(ct - x) \end{aligned} \quad (4.4)$$

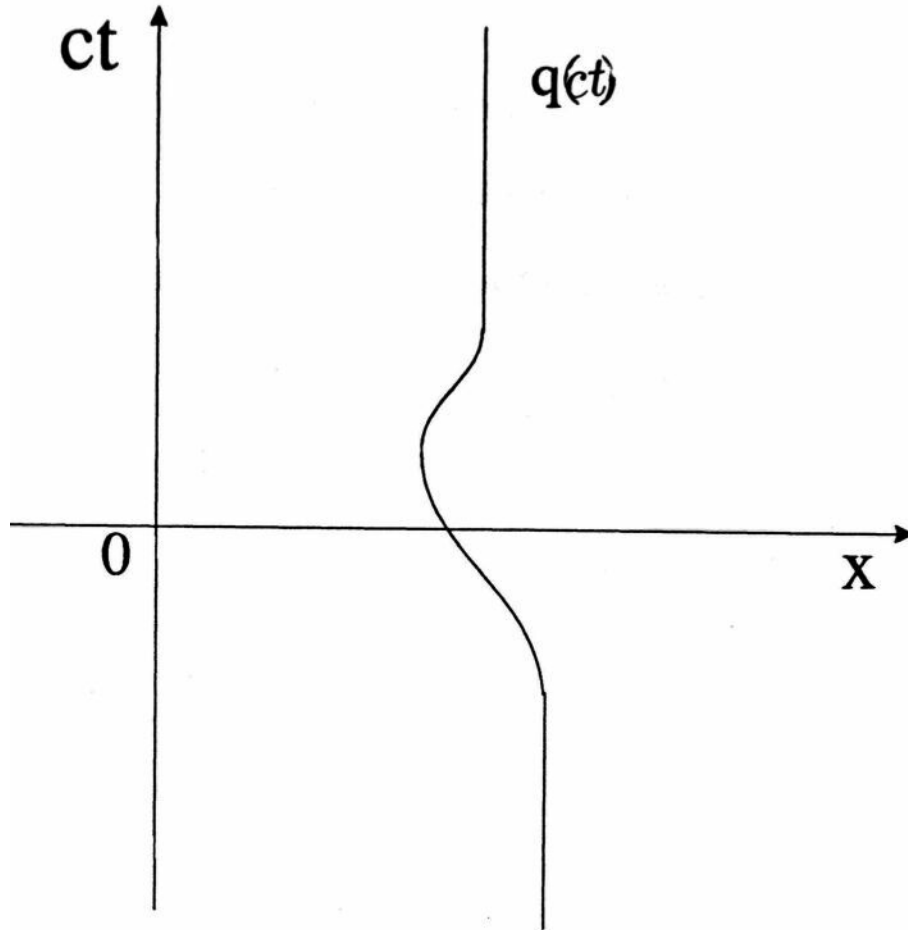


Figure 4.1: An "in-out" motion.

where R is a function that has to be determined. The function R can be determined by requiring that the transformation (4.4), map the boundary at $x = 0$ to $s = 0$ and $x = q(ct)$ to $s = 1$. Thus from the transformation (4.4) it immediately follows that, R must satisfy

$$R(ct + q(ct)) - R(ct - q(ct)) = 2. \quad (4.5)$$

Furthermore, there is another condition on the function R arising due to a physical restriction on the mirror motion — that its velocity should be strictly less than that of

light:

$$|\dot{q}(ct)| < 1. \quad (4.6)$$

Differentiating (4.5) with respect to time, we have,

$$R'(\zeta)(1+q) = R'(\zeta)(1 - q) \quad (4.7)$$

where $\xi = ct + q(ct)$ and $\xi = ct - q(ct)$. Solving for $\dot{q}(ct)$, we have

$$\dot{q}(ct) = \frac{R'(ct - q(ct)) - R'(ct + q(ct))}{R'(ct - q(ct)) + R'(ct + q(ct))}. \quad (4.8)$$

On comparing (4.6) and (4.8), we find that

$$|R'(ct - q(ct)) - R'(ct + q(ct))| < |R'(ct - q(ct)) + R'(ct + q(ct))|. \quad (4.9)$$

It thus follows that, R should be such that R' should not change its sign if condition (4.6) is to be satisfied.

As a result of the transformation (4.4), the wave equation gets transplanted to

$$R'(R^{-1}(w + s))R'(R^{-1}(w - s)) \left(\frac{\partial^2 \phi(s, w)}{\partial w^2} - \frac{\partial^2 \phi(s, w)}{\partial s^2} \right) = 0, \quad (4.9)$$

and the boundary condition becomes

$$\phi(s = 0, w) = \phi(s = 1, w) = 0 \quad \forall w. \quad (4.11)$$

The solution for (4.10) with initial conditions (4.11) is, in the transformed (s, w) coordinate system

$$\begin{aligned} u_n &\sim N e^{-in\pi w} \sin(n\pi s) \\ &\sim N \frac{e^{-in\pi(w-s)} - e^{-in\pi(w+s)}}{2i}, \end{aligned} \quad (4.12)$$

where N is a normalisation constant.

The basis of solutions $\{u_n, u_n^*\}$ is orthogonal in the inner product defined as

$$\langle u_n, u_k \rangle \equiv i \int_0^1 [u_k \frac{\partial u_n^*}{\partial w} - u_n^* \frac{\partial u_k}{\partial w}] ds. \quad (4.13)$$

Since $(u_n, u_n) = -n\pi$ the normalisation constant is $\sqrt{n\pi}$. The inner product has the following properties:

$$\begin{aligned}\langle u_n, u_k \rangle &= -\delta_{n,k} \\ \langle u_n, u_k^* \rangle &= 0 \\ \langle u_n^*, u_k^* \rangle &= \delta_{n,k}.\end{aligned}\tag{4.14}$$

Thus,

$$u_n(s, w) = \frac{1}{2i\sqrt{n\pi}} [e^{-in\pi(w-s)} - e^{-in\pi(w+s)}].\tag{4.15}$$

To get the solution in the original (x, ct) co-ordinate system, we use the transformation (4.4) in (4.15):

$$u_n(x, ct) = \frac{1}{2i\sqrt{n\pi}} [e^{-in\pi R(ct-x)} - e^{-in\pi R(ct+x)}]\tag{4.16}$$

Thus, for a given trajectory, $q(ct)$ of the mirror, the solution to the wave function (4.1) with boundary condition (4.2) is obtained when the function R is determined. Alternatively, one could specify the function R subject to the condition (4.9), so that $q(ct)$ satisfies (4.6). Solving (4.5) the trajectory corresponding to the function R can be obtained.

Let us now quantise the field inside the resonator [1,11]. The field inside the cavity is now an operator. Consider a time in the remote past, when the movable mirror was stationary at $q(ct) = D$. The field inside the cavity can then be written in terms of the complete set $\{u_n, u_n^*\}$ of solutions as

$$\phi(x, ct) = \sum_n u_n(x, ct) \hat{a}_n + u_n^*(x, ct) \hat{a}_n^\dagger.\tag{4.17}$$

The lowering and raising operators \hat{a}_n and \hat{a}_n^\dagger satisfy the bosonic commutation relation

$$[\hat{a}_n, \hat{a}_j^\dagger] = \delta_{nj}, [\hat{a}_n, \hat{a}_j] = [\hat{a}_n^\dagger, \hat{a}_j^\dagger] = 0.\tag{4.18}$$

After the mirror starts moving, the field inside the cavity is

$$\hat{\phi}(x, ct) = \sum_k v_k(x, ct) \hat{a}_k + v_k^*(x, ct) \hat{a}_k^\dagger\tag{4.19}$$

Chapter 4. Nonclassical *light generation in a cavity of variable length*

where, $\{u_k, u_k^*\}$ are the solutions (4.15) and \hat{b}_k and \hat{b}_k^\dagger are the raising and lowering operators for the non-stationary problem. Since the set $\{v_k, v_k^*\}$ forms an orthonormal basis, we can express (u_n, v_n^*) in terms of (u_k, u_k^*)

$$u_n(x, ct) = \sum_k \alpha_{nk} v_k(x, ct) + \beta_{nk} v_k^*(x, ct), \quad (4.20)$$

where the expansion coefficients α_{nk} and β_{nk} are determined from the definition of the inner product (4.13)

$$\begin{aligned} \alpha_{nk} &= -\langle u_n, v_k \rangle, \\ \beta_{nk} &= \langle u_n, v_k^* \rangle. \end{aligned} \quad (4.21)$$

Substituting (4.20) in (4.17), we have

$$\phi(x, ct) = \sum_n \left(\sum_k \alpha_{nk} v_k(x, ct) + \beta_{nk} v_k^*(x, ct) \right) \hat{a}_n + \left(\sum_k \alpha_{nk}^* v_k(x, ct) + \beta_{nk}^* v_k^*(x, ct) \right) \hat{a}_n^\dagger. \quad (4.22)$$

Rearranging the order of summation,

$$\hat{\phi}(x, ct) = \sum_k v_k(x, ct) \hat{b}_k + v_k^*(x, ct) \hat{b}_k^\dagger, \quad (4.23)$$

where

$$\begin{aligned} \hat{b}_k &= \sum_n \alpha_{nk} \hat{a}_n + \beta_{nk}^* \hat{a}_n^\dagger, \\ \hat{b}_k^\dagger &= \sum_n \alpha_{nk}^* \hat{a}_n^\dagger + \beta_{nk} \hat{a}_n \end{aligned} \quad (4.24)$$

and the operators \hat{b}_k and \hat{b}_k^\dagger satisfy the commutation relations

$$[\hat{b}_k, \hat{b}_j^\dagger] = \delta_{kj}, [\hat{b}_k, \hat{b}_j] = [\hat{b}_k^\dagger, \hat{b}_j^\dagger] = 0. \quad (4.25)$$

Thus the mirror motion corresponds to a Bogoliubov transformation of the annihilation and creation operators.

Let us now assume that before the mirror motion starts, the state of the field inside the cavity was the vacuum field. Thus, to begin with there are no photons in any of the modes of the cavity

$$a_k |0_k; in\rangle = 0, \quad (4.26)$$

where Ok in $|0_k; in\rangle$ refers to the vacuum of the k -th mode and 'in' refers to the remote past. After the mirror starts moving, the operators a_k and a_k^\dagger get transformed to new operators b_k and b_k^\dagger . With respect to these new operators, the state $|0_k; in\rangle$ will no longer be a vacuum state, but will be a squeezed vacuum state. **Similarly**, if the **initial** state was a coherent state, with respect to the new operators, it will no longer be coherent state, but will be a squeezed state.

4.2 Specific case: demonstration of squeezing

Let us consider a specific example. There are two approaches: (1) either one can specify a specific trajectory $q(ct)$ of the mirror and from that determine the function R ? or (2) one can specify a function R and then work out a trajectory corresponding to it. Here we choose the second approach. In [11], it was shown that the criterion for particle (photon) creation in the infinite future, due to the mirror motion is that if $R_{in}(\xi)$ satisfies

$$R_{in}(\xi) \xrightarrow{\xi \rightarrow -\infty} 4 + \text{constant}, \quad (4.27)$$

then, $R_{in}(\xi)$ should not satisfy,

$$R_{in}(\xi) \xrightarrow{\xi \rightarrow +\infty} \frac{\xi}{d} + \text{constant}' \quad (4.28)$$

On the contrary, if it satisfies (4.28), then there is no particle creation and the states $|0_k; in\rangle$ are the same as $|0_k; out\rangle$. So, based on this criterion, consider the function R of the following form [11] (see Fig.4.2):

$$\begin{cases} \frac{\xi}{D} & \text{if } \xi \leq 0 \\ \xi + \frac{\lambda}{\pi} \sin(\frac{\pi\xi}{d}) & \text{if } \xi > 0. \end{cases} \quad (4.29)$$

where

$$A = \frac{d}{D} - 1. \quad (4.30)$$

The requirement demanded by the condition (4.6) or (4.9) is guaranteed by

$$|\lambda| < 1. \quad (4.31)$$

For this functional form of R ,

$$\begin{aligned} \alpha_{nk} &= \sqrt{\frac{2}{n}} J_{n-k}(-n\lambda) \\ f_{nk} &= -\sqrt{\frac{2}{n}} J_{n+k}(-n\lambda), \end{aligned} \quad (4.32)$$

where J_n is a Bessel function of order n . The steps involved in the evaluation of α_{nk} and f_{nk} are provided in the Appendix 4A.

Now, the number of photons created in the mode 'k' which had no photons to begin with (i.e., the mode is in the state $|0_k; in\rangle$), as a result of the mirror motion is [5]

$$\langle 0; in | \hat{b}_k^\dagger \hat{b}_k | 0; in \rangle = \sum_{n=1}^{\infty} |\beta_{nk}|^2, \quad (4.33)$$

where, β_{nk} is given by (4.21) and (4.32) corresponding to R given in (4.29). In Fig.4.3 we plot the number of photons created in each mode of the cavity. It shows that only low frequency modes get any excitation as $q(ct)$ has only low frequency components in it. Since the frequency ω is given by

$$\omega = \frac{n\pi c}{L}, \quad (4.34)$$

where L is the cavity dimension, the frequency of light corresponding to the low-order modes (n) would then correspond to optical frequencies ($\omega \sim 10^{15}$) if L is of the order of a micrometer. Thus, in a micron-sized cavity, one can hope to detect photons in the optical domain.

We can now calculate the variance $S(\theta)$ in the field quadrature defined as

$$S(\theta) = \langle \bar{X}_n^2(\theta) \rangle - \langle \bar{X}_n(\theta) \rangle^2, \quad (4.35)$$

where

$$X_n(\theta) = e^{-i\theta} \hat{b}_n + e^{i\theta} \hat{b}_n^\dagger. \quad (4.36)$$

To determine if there is squeezing, we differentiate $S(q)$ with respect to θ to obtain S_{\min} . If $S_{\min} < 1$ for a particular mode, then it implies that the state of the radiation in that mode is squeezed. In Fig.4.4 we plot S_{\min} versus A for various modes of the cavity. Curves 4.4(a) through (d) correspond to the modes $k = 1, 5, 10$ and 20 respectively. We see that there is considerable amount of squeezing of fluctuations in all the modes of the cavity.

From (4.24), if we calculate the expectation value of $\hat{b}_m^\dagger \hat{b}_n$ taken with respect to the initial vacuum state, we have

$$(0; in | \hat{b}_m^\dagger \hat{b}_n | 0; in) = \sum_k \beta_{km} \beta_{kn}^*. \quad (4.37)$$

We thus see that the correlation between the n th and the m th mode is nonzero

$$\langle \hat{b}_m^\dagger \hat{b}_n \rangle - \langle \hat{b}_m^\dagger \rangle \langle \hat{b}_n \rangle \neq 0 \quad . \quad (4.38)$$

as $\langle \hat{b}_n \rangle = 0$ for initial vacuum state. Thus, in addition to squeezing, the mirror motion also introduces correlations between the various modes of the cavity.

In this chapter, we have shown that an "in-out" motion of a mirror satisfying conditions for particle creation, i.e., satisfying (4.27) and *not* (4.28), in a one dimensional cavity creates particles (photons) and that the state of this field is nonclassical as it manifests squeezing of fluctuations in one of its quadratures. We have also shown that the mirror motion also introduces correlations between the various modes of the cavity.

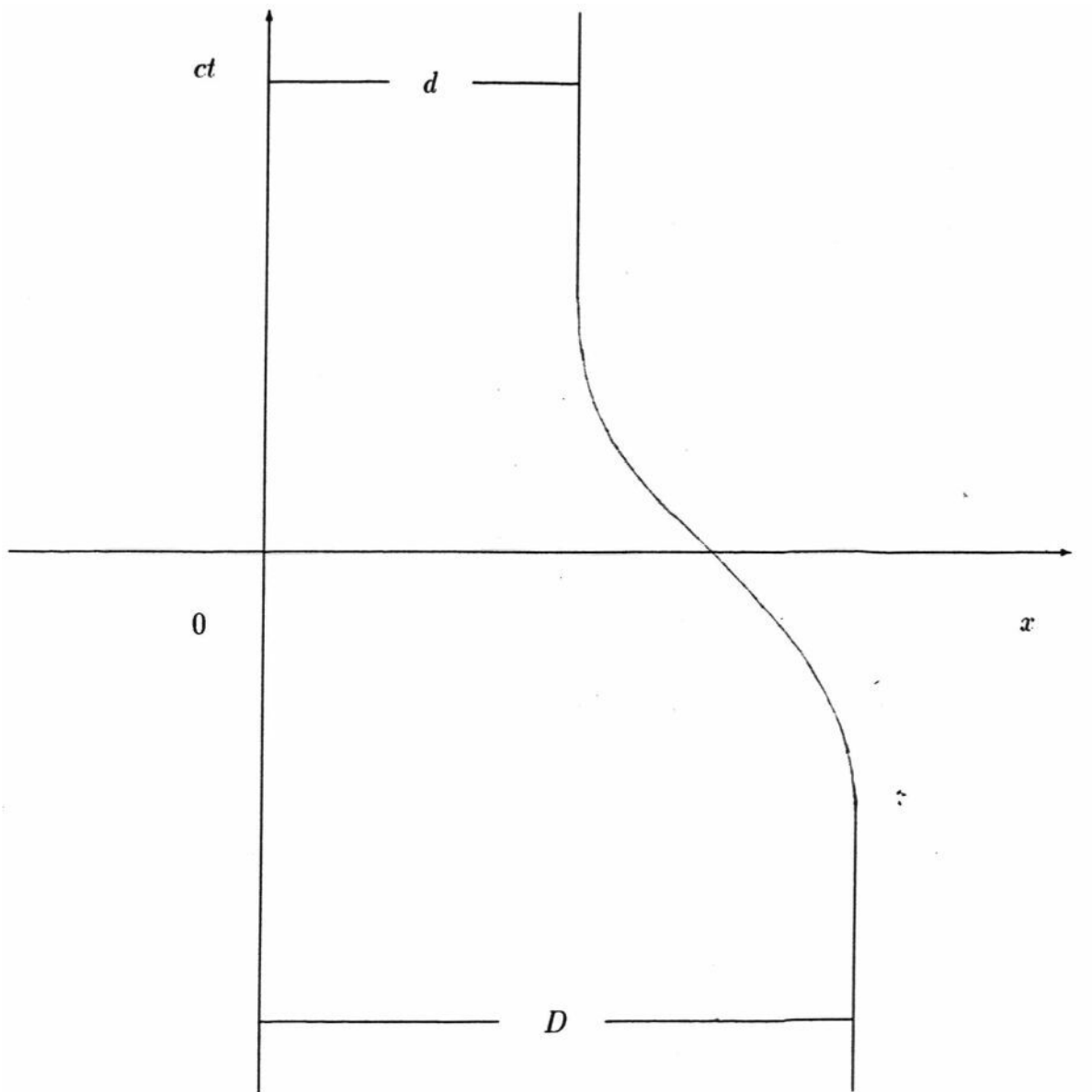


Figure 4.2: Trajectory of the mirror corresponding to $R_{\text{in}}(\xi)$ given by (4.29).

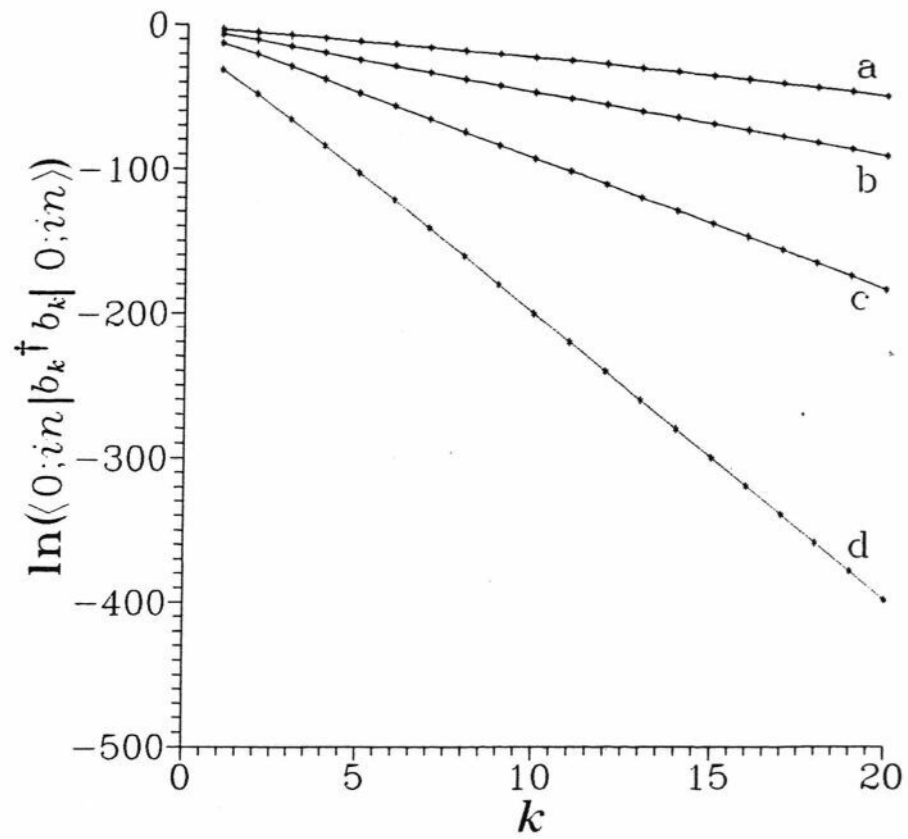


Figure 4.3: Spectrum of photons created due to the mirror motion.

Chapter 4. *Nonclassical light generation in a cavity of variable length*

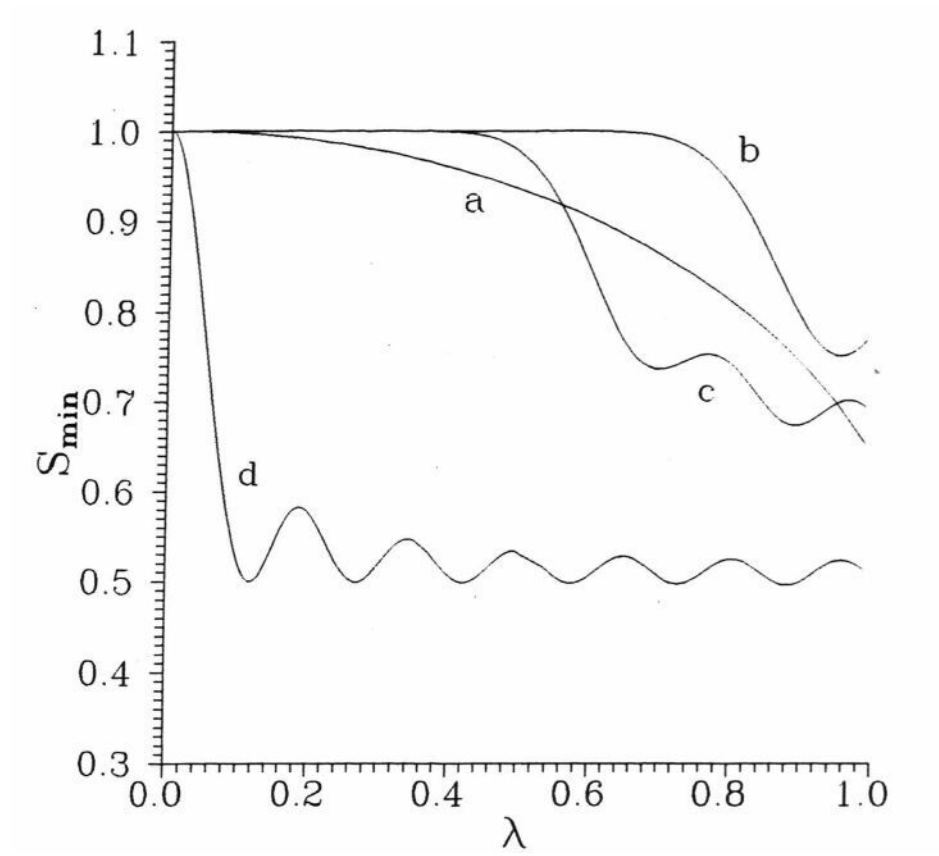


Figure 4.4: Demonstration of squeezing in the cavity.

Appendix 4A

Derivation of α_{nk} and β_{nk}

In this appendix the quantities a_{nk} and b_{nk} corresponding to the function R_{in} given by (4.29) are derived. From (4.21), α_{nk} and β_{nk} are defined as

$$\begin{aligned}\alpha_{nk} &= -\langle u_n, v_k \rangle, \\ \beta_{nk} &= \langle u_n, v_k^* \rangle.\end{aligned}\quad (4A.1)$$

Let us consider the evaluation of β_{nk} . We need to evaluate

$$\begin{aligned}\beta_{nk} &= \langle u_n, v_k^* \rangle, \\ &= i \int_0^{t_0} dx \left[v_k^* \frac{\partial u_n}{\partial t} - u_n^* \frac{\partial v_k}{\partial t} \right].\end{aligned}\quad (4A.2)$$

Since the inner product (4.13) is independent of time [11], let us choose $t = 2d$. Then,

$$\beta_{nk} = -\frac{1}{2\pi\sqrt{nk}} \int_0^d dx \sin\left(\frac{k\pi x}{d}\right) \left[i n \pi \left(\frac{1}{d} + \frac{\lambda}{d} \cos\left(\frac{\pi x}{d}\right) \right) \right] \quad (4A.4)$$

On substituting the functional form of $R_{in}(\xi)$, we have

$$\beta_{nk} = \frac{-1}{2\pi\sqrt{nk}} \int_0^d dx \sin\left(\frac{k\pi x}{d}\right) \left[i(n-k)\pi + \frac{i n \pi \lambda}{d} \cos\left(\frac{\pi x}{d}\right) - 2i \right] \sin\left(\frac{n\pi x}{d} + n\lambda \sin\left(\frac{\pi x}{d}\right)\right). \quad (4A.5)$$

Upon redefining $\frac{\pi x}{d}$ as x , we have

$$\beta_{nk} = \frac{-1}{\pi\sqrt{nk}} \int_0^\pi dx \sin(kx) \left[(n-k) + n\lambda \cos(x) \right] \sin\left(nx + n\lambda \sin(x)\right). \quad (4A.6)$$

Using the properties of trigonometric identities, we then obtain

$$\beta_{nk} = -\frac{1}{\pi\sqrt{nk}} \int_0^\pi dx \frac{1}{2} \left[(n-k) + n\lambda \cos(x) \right] \left\{ \cos\left[(n-k)x + n\lambda \sin(x)\right] - \cos\left[(n+k)x + n\lambda \sin(x)\right] \right\}$$

$$= -\frac{1}{2\pi\sqrt{nk}} \int_0^\pi dx \{ (n-k + n\lambda \cos(x)) \cos((n-k)x + n\lambda \sin(x)) - (n+k + n\lambda \cos(x)) \cos((n+k)x + n\lambda \sin(x)) + 2k \cos((n+k)x + n\lambda \sin(x)) \}. \quad (4A.7)$$

$$= -\frac{1}{2\pi\sqrt{nk}} \int_0^\pi dx \{ (n-k + n\lambda \cos(x)) \cos((n-k)x + n\lambda \sin(x)) - (n+k + n\lambda \cos(x)) \cos((n+k)x + n\lambda \sin(x)) + 2k \cos((n+k)x + n\lambda \sin(x)) \}. \quad (4A.8)$$

Defining $\delta = (n-k)x + n\lambda \sin(x)$ and $\phi = (n+k)x + n\lambda \sin(x)$

$$\beta_{nk} = -\frac{1}{\pi\sqrt{nk}} \int_0^\pi dx \cos[(n+k)x + n\lambda \sin(x)] - \frac{1}{2\pi\sqrt{nk}} \left[\int_0^{(-1)^{n-k}} d\delta \cos(\delta) - \int_0^{(-1)^{n+k}} d\phi \cos(\phi) \right] \quad (4A.9)$$

$$= -\frac{1}{\pi\sqrt{nk}} \int_0^\pi dx [\cos((n+k)x + n\lambda \sin(x))]. \quad (4A.10)$$

Using the integral representation of Bessel functions ([13], §8.411, Eqn (1), p 952), we thus have

$$\beta_{nk} = -\sqrt{\frac{k}{n}} J_{n+k}(-n\lambda), \quad (4A.11)$$

where J_ν is Bessel function of the first kind of order ν . Along similar lines, we obtain for

α_{nk}

$$\alpha_{nk} = \sqrt{\frac{k}{n}} J_{n-k}(-n\lambda). \quad (4A.12)$$

References

- [1] G.T. Moore, J. Math. Phys. **11**, 2679 (1970).
- [2] W.G. Unruh, Phys. Rev. D 14, 870 (1976).
- [3] S.A. Fulling and P.C.W. Davies, Proc. R. Soc. London A 348, 393 (1976).
- [4] P.C. Davies and S.A. Fulling, Proc. R. Soc. London, A 356. 237 (1977).
- [5] N. Birrell and P.C. Davies, *Quantum Fields in curved Space* (Cambridge University, Cambridge, 1982).
- [6] E. Yablonovitch, Phys. Rev. Lett. 62, 1742 (1989).
- [7] V.V. Hizhnyakov, Quantum Optics 4, 345 (1992).
- [8] C.K. Law, Phys. Rev. A 49, 433 (1994).
- [9] P. Candelas and D. Deutsch, Proc. R. Soc. London A 354, 79 (1977).
- [10] V.P. Frolov and E.M. Serebriany, J. Phys. A 12, 2415 (1979).
- [11] M. Castagnino and R. Ferraro, Ann. of Phys. 154, pp. 1-23 (1984).
- [12] Sarben Sarkar, Quantum Optics 4, 345 (1992).
- [13] I.S. Gradshteyu and I.M. Ryzhik, *Table of Integrals, Series and Products*, (Academic Press, New York, 1965).

Chapter 5

Intensity-Intensity Correlations for Micromaser

In this and the next chapter, the nonclassical properties of the field generated in a micromaser are discussed. A micromaser is a device which is a practical realisation of the Jaynes-Cummings Model (JCM) [1] in Quantum Optics. The JCM consists of a single two-level atom in interaction with a single mode of a quantised radiation field.

The intensity-intensity correlation functions of light beams have occupied a prominent place in physics since the discovery of the Hanbury Brown-Twiss effect [2,3]. Such correlations not only provide information on the photon statistical aspects but also provide lot of information on the dynamical processes leading to the production of light beams. The intensity-intensity correlations of thermal light beams, a single mode laser oscillating near threshold [4,5], radiation produced by a coherently driven atom [6,7], optical parametric oscillators [9,10] have been extensively studied. In some cases such as resonance fluorescence these type of correlations exhibit strong non-classical properties, like antibunching and squeezing [6-8]. In this chapter¹, results on a study of the intensity-intensity correlations, which is a higher-order correlation effect, of the field produced by a micromaser are given.

Micromaser is known to exhibit very unusual non-classical properties [11,12]. The field generated in a micromaser has many features which are markedly different from the fields generated in conventional masers and lasers [13,14]. In conventional lasers, because of the random Poissonian pumping process, whatever nonclassical effects that could have been there, get masked and we get a purely Poissonian photocount. On the other hand

¹ Results of this chapter are published in Phys. Rev. A 50, 680 (1994).

in a micromaser, essentially there is a single atom interacting with the cavity field and its nonclassical effects are not lost as in usual lasers. But in a micromaser, since the frequency of the field is in the microwave region and since there are no sensitive photon detectors in the microwave region, one is forced to infer about the field only through a study of the emerging atomic beam. For example, the sub-Poissonian character of the field in the micromaser has been established by studies involving the statistics of the atoms leaving the cavity [11,12]. Calculations have been done to measure the field amplitude correlation functions and thus obtain the spectrum of the field [15-20]. In this chapter, we calculate the two-photon intensity-intensity correlations for the micromaser field and study its spectral properties [21].

The outline of this chapter is as follows: In Sec. 5.1 the construction of a micromaser is described and a discussion of the salient features of the micromaser field are given. In Sec. 5.2 the procedure for the calculation of different types of two-photon correlations is outlined. These two-time correlations are calculated using the master equation for the micromaser field. Detailed results on the behaviour of the eigenvalues of the Liouville operator for a range of excitation conditions and cavity parameters are presented. From the intensity-intensity correlations the antibunching property and the multiple-exponential decay of the micromaser field are demonstrated. In Sec. 5.3 results of a detailed numerical study pertaining to these correlation functions are given. In Sec. 5.4 proposals as to how these two-photon correlations for the micromaser field can be probed in experimental setups are presented.

5.1 Micromaser

The most fundamental problem in Quantum Optics is the problem of describing radiation-matter interaction between a two-level atom and a single-mode of quantised electromagnetic radiation. This is the famous Jaynes-Cummings Model after it was first studied by Jaynes and Cummings [1]. Lot of subsequent work has been done on this problem, like the discovery of collapse [22] and revival phenomena [23]. Initially, this was just a

toy model as it was very difficult to detect and isolate a single atom and the atom-field coupling co-efficient was extremely small to be measured. But with the recent studies on the Rydberg atoms, it is now possible to excite atoms to very high principal quantum number states (Rydberg states). The Rydberg states are very strongly coupled to the fields in the microwave region of the electromagnetic spectrum. Since microwaves have wavelengths of the order of millimeter, it is possible to construct cavities which are resonant, to very low order modes. These states have an additional advantage that they have very long life-times (from 10^{-3} to 1 second). In any cavity used to contain radiation, there is an unavoidable loss of radiation due to leakage from the cavity. A quantitative measure of how good a cavity can hold radiation without much losses is given by its quality factor or Q-value, a low-value corresponding to a leaky cavity and a high one to a good cavity. The micromaser device consists of a high-Q microwave cavity made of superconducting Niobium and cooled to sub-Kelvin temperatures. Q-values as high as 10^{10} have been achieved in such cavities. These tecnological advances have made possible the development of the micromaser [24,25].

A typical micromaser setup consists of the following. A low-velocity beam of atoms prepared by an atomic beam oven and velocity selected by a Fizeau velocity selector is made to enter the high-Q maser cavity (see figure 5.1). Prior to their entry into the cavity they are excited to the maser transition by a properly tuned laser. They are injected into the cavity at such a low rate that at most only one atom is present inside the cavity at any given time. Moreover, the velocity of the atoms in the beam is such that the interaction time τ of the atom with the cavity field is much smaller than the cavity field damping time γ^{-1} . Thus, while an atom is inside the cavity, neglecting the cavity field damping rate, the coupled atom-field system is described by the Jaynes-Cummings Hamiltonian

$$H_{JCM} = \frac{\hbar\omega_0}{2}\hat{S}_z + faah + \frac{\gamma}{2}(\hat{S}^+\hat{a} + \hat{S}^-\hat{a}^\dagger) \quad (5.1)$$

where $\hbar\omega_0$ is the atomic level separation, ω is the frequency of the cavity mode, g is the dipole coupling constant and \hat{S}_z, \hat{S}^\pm are the atomic spin operators. If initially the density operator of the cavity field is $\hat{\rho}_f(t_i)$, the moment an atom enters the cavity the density

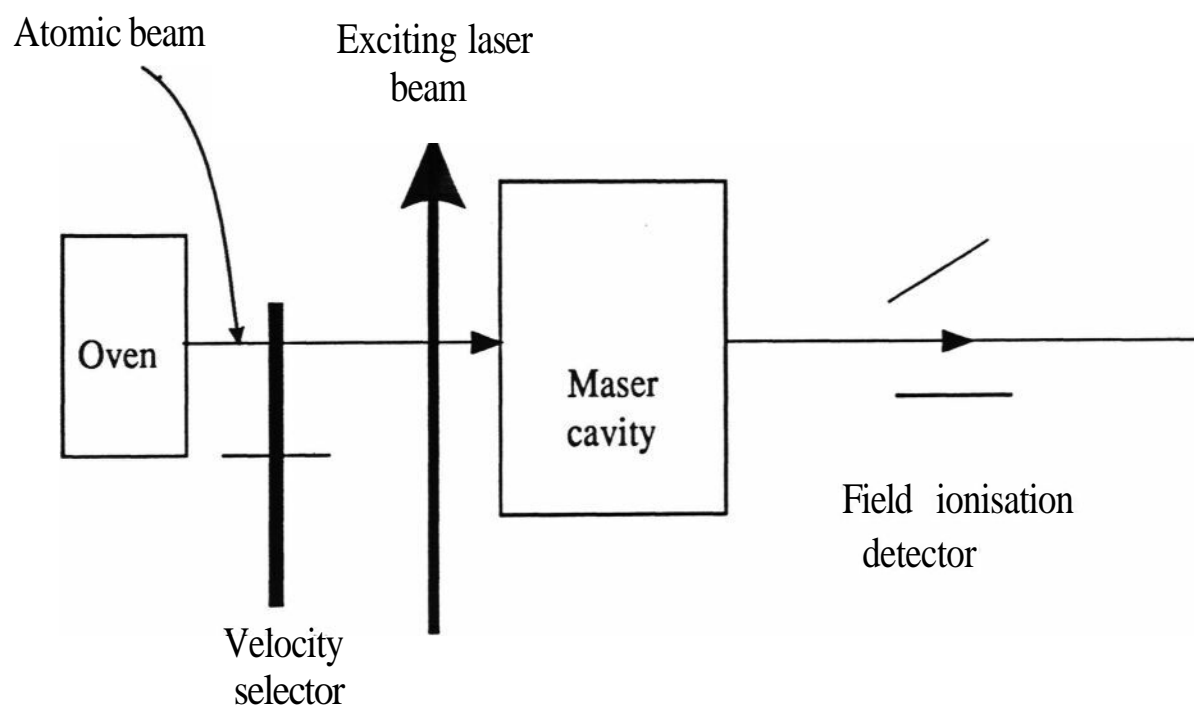


Figure 5.1: A typical micromaser setup.

operator $\hat{\rho}(t_i)$ of the combined atom-field system is given by

$$\hat{\rho}(t_i) = \hat{\rho}_f(t_i) \otimes \hat{\rho}_a(t_i). \quad (5.2)$$

After the JC interaction, the field density matrix is given by

$$\begin{aligned} \hat{\rho}_f(t_{i+1}) &= \text{Tr}_{\text{atom}} \left(\hat{U}(\tau) \hat{\rho}(t_i) \hat{U}^\dagger(\tau) \right), \\ &= F(\tau) \hat{\rho}_f(t_i). \end{aligned} \quad (5.3)$$

where $U(\tau)$ is the time-evolution operator corresponding to the Jaynes-Cummings Hamiltonian,

$$U(\tau) = \exp \left(-i \hat{H}_{JCM} \tau \right). \quad (5.4)$$

Between the time the i th atom exits the cavity and the $(i+1)$ th one enters, the evolution of the field is governed by the master equation of an harmonic oscillator interacting with a thermal bath

$$\begin{aligned} \dot{\rho}_f &= \frac{1}{2}(n_b + 1)(2\hat{a}\hat{\rho}_f\hat{a}^\dagger - \hat{a}^\dagger\hat{a}\hat{\rho}_f - \hat{\rho}_f\hat{a}^\dagger\hat{a}) + \frac{1}{n_b}(2\hat{a}^\dagger\hat{\rho}_f\hat{a} - \hat{a}\hat{a}^\dagger\hat{\rho}_f - \hat{\rho}_f\hat{a}\hat{a}^\dagger), \\ &= L\hat{\rho}_f. \end{aligned} \quad (5.5)$$

where n_b is the mean thermal photon number in the cavity, L is the Liouvillian operator describing the coupling between an oscillator and the thermal bath. Thus, the field density matrix at time t_{i+1} is given by

$$\hat{\rho}_f(t_{i+1}) = \exp(Lt_p)F(\tau)\hat{\rho}_f(t_i), \quad (5.6)$$

where $t_p (= t_{i+1} - t_i - \tau \simeq t_{i+1} - t_i)$ is the time interval between the i th atom leaving the cavity and the $(i+1)$ th one entering it. After many interactions with successive atoms injected into the cavity, the field density operator reaches a steady state. Thus, at steady state

$$\hat{\rho}_f(t_{i+1}) = \hat{\rho}_f(t_i) = \rho_{\text{st}}. \quad (5.7)$$

Now, we rewrite (5.6) as follows

$$\hat{\rho}_f(t_{i+1}) = (1 + [\exp(\hat{L}t_p) - 1])(1 + [F(\tau) - 1])\hat{\rho}_f(t_i), \quad (5.8)$$

Since the cavity decay time is very large, the decrease in photon number in time interval t_p is very small. Thus, we can make the approximation

$$\sqrt{\gamma t_p} \simeq \epsilon \quad (5.9)$$

where ϵ is a smallness parameter. We can further approximate that

$$g\tau \sim \epsilon \quad (5.10)$$

since the interaction time T is very small compared to the cavity damping time. This implies that there is only a very small amount of Rabi oscillation during the time interval τ . Therefore, in these limits we can make the following approximations

$$\exp(\hat{L}t_p) - 1 \sim \gamma t_p, \quad (5.11)$$

$$F(r) - 1 \sim (g\tau)^2. \quad (5.12)$$

We thus have, from (5.6)

$$\hat{\rho}(t_{i+1}) \sim \{1 + L t_p + (F(\tau) - 1)\} \hat{\rho}(t_i) \quad (5.13)$$

Using the steady state condition (5.7), we have

$$(1 - \hat{L}t_p)\hat{\rho}_{st} = F(\tau)\hat{\rho}_{st}. \quad (5.14)$$

Thus before this steady state is reached, the change in field density operator in the time interval between the injection of the i th atom and the $(i + 1)$ th atom is

$$\frac{\hat{\rho}(t_{i+1}) - \hat{\rho}(t_i)}{t_p} = \hat{L}(t_i) + r[F(r) - 1]\hat{\rho}(t_i), \quad (5.15)$$

where $r = t_p^{-1}$ is the injection rate of the atoms into the cavity. This equation gives the "coarse-grained" rate of change of the density operator. Replacing the left hand side by the derivative $\dot{\rho}$ and in the photon number representation, we have the master equation for the micromaser field

$$\dot{\rho}_{n,m} = -r \left\{ 1 - \left[\cos(g\sqrt{n+1}\tau) \right] \left[\cos(g\sqrt{m+1}\tau) \right] \right\} \rho_{n,m}$$

$$\begin{aligned}
 & +r \left[\sin(g\sqrt{n}\tau) \right] \left[\sin(g\sqrt{m}\tau) \right] \rho_{n-1,m-1} \\
 & -\frac{1}{2}(n_b + 1) \left[(n+m)\rho_{n,m} - 2\sqrt{(n+1)(m+1)}\rho_{n+1,m+1} \right] \\
 & -\frac{\gamma}{2}n_b \left[(n+1+m+1)\rho_{n,m} - 2\sqrt{nm}\rho_{n-1,m-1} \right].
 \end{aligned} \tag{5.16}$$

Due to the nonavailability of good detectors in the microwave regime, one is forced to infer about the micromaser field only by probing the atoms which exit from the cavity after interacting with the cavity field. At some distance from the exit point of the cavity, field ionisation detectors detect the excited Rydberg atoms. If the atoms are detected to be in the excited state, it implies that energy was not transferred to the cavity field. But on the other hand, if they are not in the excited state, then it implies that an energy transfer has taken place inside the cavity (assuming no energy loss in-between the exit point and the detectors).

5.2 Two-photon intensity-intensity correlations for the micromaser field

We now start from the standard master equation describing the dynamical evolution of the micromaser field. Let $\rho_n^{(k)}(t)$ be the off-diagonal element of the density matrix of the radiation field

$$\rho_n^{(k)}(t) = \langle n | \hat{\rho}(t) | n+k \rangle. \tag{5.17}$$

The dynamics for the field is given by [13,14]

$$\dot{\rho}_n^{(k)}(t) = \mathcal{A}_n^{(k)} \rho_{n-1}^{(k)} + \mathcal{B}_n^{(k)} \rho_n^{(k)} + \mathcal{C}_n^{(k)} \rho_{n+1}^{(k)}, \tag{5.18}$$

where

$$\mathcal{A}_n^{(k)} = r \sin(g\tau\sqrt{n}) \sin(g\tau\sqrt{n+k}) + \gamma n_b \sqrt{n(n+k)}, \tag{5.19}$$

$$\begin{aligned}
 \mathcal{B}_n^{(k)} = & -r[1 - \cos(g\tau\sqrt{n+1}) \cos(g\tau\sqrt{n+1+k})] \\
 & -\gamma(n_b + 1) \left(n + \frac{k}{2} \right) - \gamma n_b \left(n + 1 + \frac{k}{2} \right),
 \end{aligned} \tag{5.20}$$

$$\mathcal{C}_n^{(k)} = \gamma(n_b + 1) \sqrt{(n+1)(n+1+k)}. \tag{5.21}$$

It is to be noticed that in the dynamics of the micromaser field, the *index k is consented*. The steady state solution of Eq. (5.18) is

$$\rho_n^{(k)}(t) = \delta_{k0} p_n; \\ = p_0 \prod_{j=1}^n \left(\frac{n_b}{n_b + 1} + \frac{N \sin^2(g\tau\sqrt{j})}{j(n_b + 1)} \right).$$

Here p_0 is determined from normalisation and $N (= r/\gamma)$ is equal to the number of Atoms passing through the cavity in time interval γ^{-1} . The properties of the distribution (5.22) are well documented [13,14].

We now examine the following steady state two-photon correlations of the micromaser field

$$\mathcal{G}(t) = \lim_{t_0 \rightarrow \infty} \langle \hat{a}^{\dagger 2}(t_0 + t) \hat{a}^2(t_0) \rangle; \quad (5.23)$$

$$I(t) = \lim_{t_0 \rightarrow \infty} \langle \hat{a}^{\dagger}(t_0) \hat{a}^{\dagger}(t_0 + t) \hat{a}(t_0 + t) \hat{a}(t_0) \rangle. \quad (5.24)$$

Note that

$$\lim_{t \rightarrow \infty} I(t) = \langle \hat{a}^{\dagger} \hat{a} \rangle^2 \quad (5.25)$$

and

$$\mathcal{I}(0) = G(0). \quad (5.26)$$

The above correlations carry useful information on the field and both can be probed by suitable methods as discussed in Sec. 5.4. We will compute these correlations from the solution of Eq. (5.18) and the quantum regression theorem.

5.2.1 Calculation of \mathcal{G}

We write $\langle \hat{a}^{\dagger 2}(t_0 + t) \rangle$ in terms of the mean values at time $t = t_0$ as follows:

$$\begin{aligned} \langle \hat{a}^{\dagger 2}(t_0 + t) \rangle &= \sum_n \sqrt{(n+1)(n+2)} \rho_n^{(2)}(t_0 + t) \\ &= \sum_{n,m} \sqrt{(n+1)(n+2)} G_{nm}^{(2)}(t) \rho_m^{(2)}(t_0) \\ &= \sum_{n,m} \sqrt{(n+1)(n+2)} G_{nm}^{(2)}(t) (|m+2\rangle \langle m|), \end{aligned} \quad (5.27)$$

where we have defined the Green's function $G_{nm}^{(2)}$ from the time dependent solution of Eq. (5.18)

$$\rho_n^{(k)}(t_0 + t) = \sum_m G_{nm}^{(k)}(t) \rho_m^{(k)}(t_0). \quad (5.28)$$

Using the quantum regression theorem, we get from Eq. (5.27)

$$\begin{aligned} \langle \hat{a}^{\dagger 2}(t_0 + t) \hat{a}^2(t_0) \rangle &= \sum_{n,m} \sqrt{(n+1)(n+2)} G_{nm}^{(2)}(t) \langle m+2 | \hat{a}^2 \rangle \\ &= \sum_{n,m} \sqrt{(n+1)(n+2)(m+1)(m+2)} G_{nm}^{(2)}(t) \\ &\quad \rho_{m+2,m+2}(t_0) \end{aligned} \quad (5.29)$$

and hence in the steady state

$$\mathcal{G}(t) = \sum_{n,m} \sqrt{(n+1)(n+2)(m+1)(m+2)} G_{nm}^{(2)}(t) \rho_{m+2} \quad (5.30)$$

Note that

$$G_{nm}^{(2)}(0) = \delta_{nm}. \quad (5.31)$$

For certain applications one needs the Fourier transform of $\mathcal{G}(t)$

$$\int_{-\infty}^{+\infty} \mathcal{G}(t) e^{-i(\omega - \omega_c)t} dt, \quad (5.32)$$

which can be expressed as

$$\mathcal{G}(\omega - \omega_c) = 2\text{Re} \int_0^{\infty} \mathcal{G}(t) e^{-i(\omega - \omega_c)t} dt \quad (5.33)$$

$$= 2\text{Re} \mathcal{G}(s = +i(\omega - \omega_c)). \quad (5.34)$$

Here $\mathcal{G}(s)$ is the Laplace transform of $\mathcal{G}(t)$.

There are two approaches to solving for the spectrum — (a) an eigenvalue approach and (b) Green's function approach. In the eigenvalue method we note that for a fixed k , $\rho_n^{(k)}$'s form an infinite dimensional column vector and Eq. (5.18) can be solved by finding the eigenvalues $\lambda_\alpha^{(k)}$ and the eigenfunctions $\Phi_\alpha^{(k)}$ of the corresponding matrix defined by the right hand side of Eq. (5.18). Then $G_{nm}^{(2)}(t)$ can be expressed as

$$G_{nm}^{(2)}(t) = \sum_\alpha e^{-\lambda_\alpha^{(2)} t} g_{nm\alpha}. \quad (5.35)$$

In Appendix 5A, the details regarding the eigenvalue method are given.

In the Green's function approach we note that the Laplace transform of the Green's function obeys the equation

$$sG_{nm}^{(2)} - \delta_{nm} = \mathcal{A}_n^{(2)} G_{n-1,m}^{(2)} + \text{fl}^{\wedge} G_g + \mathcal{C}_n^{(2)} G_{n+1,m}^{(2)}. \quad (5.36)$$

The $G_{nm}^{(2)}$ can be computed by using the standard continued fraction methods [26,27]. The steps involved in solving (5.36) are provided in Appendix 5B.

5.2.2 Calculation of J

Using the same procedure which led to Eq. (5.30) we can show that

$$\mathcal{I}(t) = \sum_{n,m} G_{nm}^{(0)}(t) n(m+1) p_{m+1}. \quad (5.37)$$

In view of the property Eq. (5.25) it is expected that

$$G_{nm}^{(0)}(t) \xrightarrow{t \rightarrow \infty} p_n. \quad (5.38)$$

Clearly the matrix in Eq. (5.18) for $k = 0$ must have a zero eigenvalue and thus we can consider the fluctuation from the mean value

$$I = \mathcal{I}(t) - \langle \hat{a}^\dagger \hat{a} \rangle^2 = \sum_{n,m} \tilde{G}_{nm}^{(0)}(t) n(m+1) p_{m+1}, \quad (5.39)$$

where $\tilde{G}_{nm}^{(0)}(t)$ is obtained from $G_{nm}^{(0)}(t)$ by dropping the term corresponding to the zero eigenvalue.

5.3 Numerical results for different types of two-photon correlations

We first present results for the correlation function $\mathcal{G}(t)$ and its Fourier transform (5.32). The normalised spectrum is shown in Fig. 5.2 for different values of the transit times. This has been calculated using the continued fraction method [26,27]. For small transit times the spectrum is very narrow. The spectrum broadens with increase in the transit

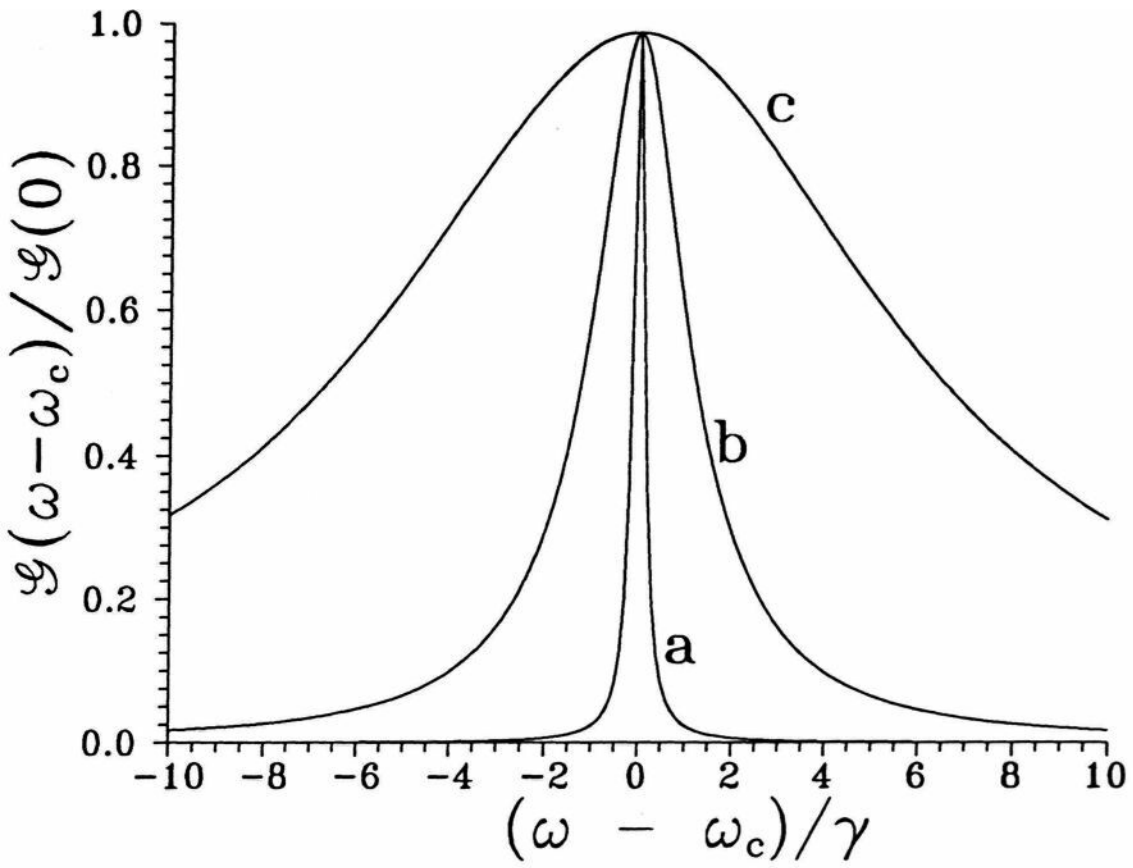


Figure 5.2: Normalised spectrum $\mathcal{G}(\omega - \omega_c)/\mathcal{G}(0)$ as a function of $(\omega - \omega_c)/\gamma$ for $N = 20$, $n_b = 1$ and for (a) $g\tau = 0.3$, (b) $g\tau = 1$ and (c) $g\tau = 3$.

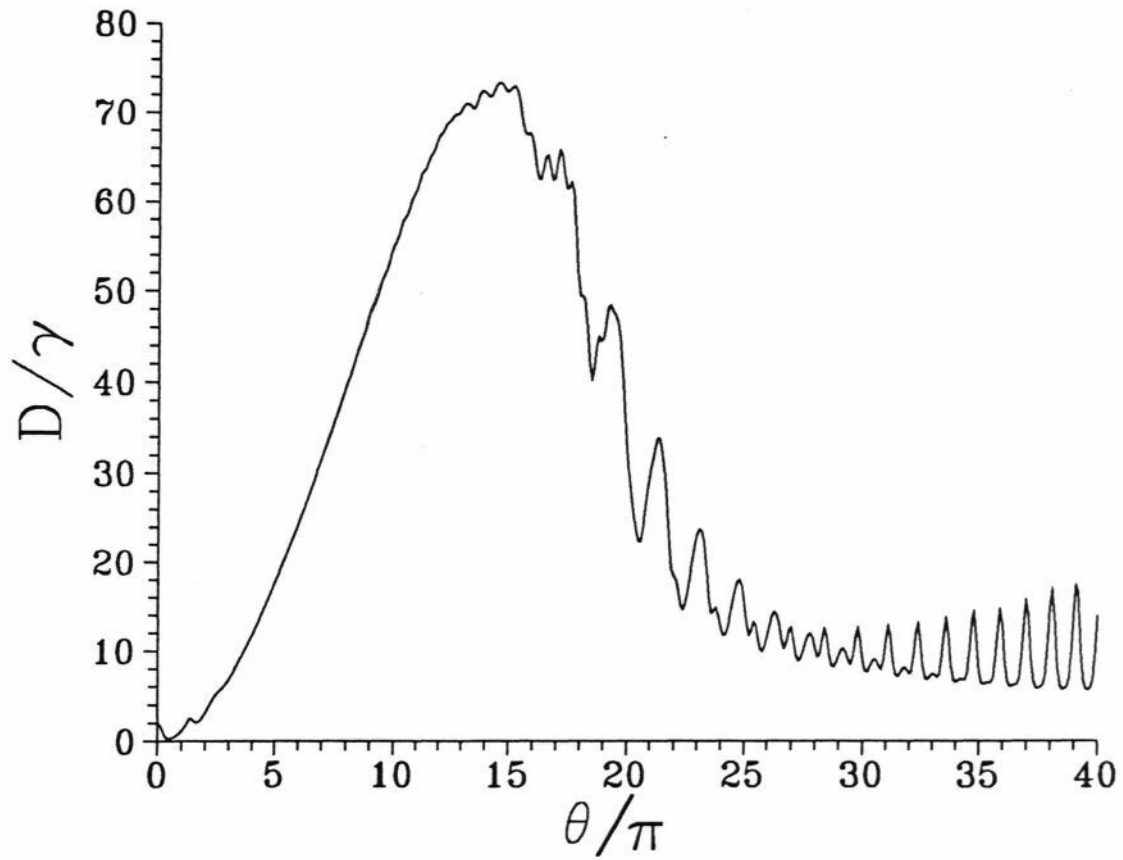


Figure 5.3: Exact numerical linewidth D/γ as a function of the pump parameter $\theta = \sqrt{N}g\tau$ for $N = 20$ and $n_b = 1$.

time. In figure 5.3 we show the behaviour of the linewidth of the spectrum $\mathcal{G}(\omega - \omega_c)$ as a function of the pump parameter $0 = \sqrt{N}g\tau$. The linewidth increases with increase in 0 over a very wide range. For large 0 , it exhibits oscillatory character which is associated with the existence of the trapping states [28]. The behaviour of the spectrum and the linewidth is determined by the eigenvalues $\lambda_{\alpha}^{(2)}$ (Eq. (5.35)) and their weight factors. In Fig.5.4 we show the behaviour of some of the eigenvalues as a function of the transit time and the excitation rate. For the chosen parameters, the eigenvalues are real in the range of 6 values displayed in Fig.5.4. In Fig.5.5 we show the weight factors contributing to the spectrum for different values of gr . Clearly, the intensity-intensity correlation, in general, has contributions from *many different eigenvalues* depending on the magnitude of gr . For small gr only the lowest eigenvalue contributes [29]. In Fig.5.6 we show the time domain behaviour of the intensity correlation $\mathcal{G}(t)$. The time dependent behaviour is determined from (5.35) directly. Multi-exponential character of such correlations is evident which may be compared with the corresponding behaviour reported in Ref. [4,5]. Following the method of Ref. [16,17], we can derive an approximate expression for the linewidth D for large mean photon numbers:

$$\begin{aligned} D &= 2\langle -\mathcal{A}_{n+1}^{(2)} - \mathcal{B}_n^{(2)} - \mathcal{C}_{n-1}^{(2)} \rangle \\ &\approx \langle 4r \sin^2 \left(\frac{gr}{2\sqrt{n}} \right) \rangle + 2\langle \frac{\gamma(2n_b + 1)}{4} \rangle. \end{aligned} \quad (5.40)$$

In Fig.5.7 we give a comparison of approximate and exact linewidths. The general features are the same.

We next examine the correlation $\mathcal{I}(t)$. A typical behaviour is shown in Fig.5.8. This figure shows that for $gr = 1$, there are intervals such that $2(t) - 2(0) > 0$, i.e.,

$$\langle \hat{a}^\dagger(0)\hat{a}^\dagger(t)\hat{a}(t)\hat{a}(0) \rangle > \langle \hat{a}^{\dagger 2}(0)\hat{a}^2(0) \rangle. \quad (5.41)$$

Thus the intensity correlation $\mathcal{I}(t)$ for the micromaser field exhibits *antibunching* property. This is because for a classical system the Cauchy-Schwarz inequality would imply that

$$|\langle \mathcal{I}(t)\mathcal{I}(0) \rangle| < \langle \mathcal{I}^2(0) \rangle. \quad (5.42)$$

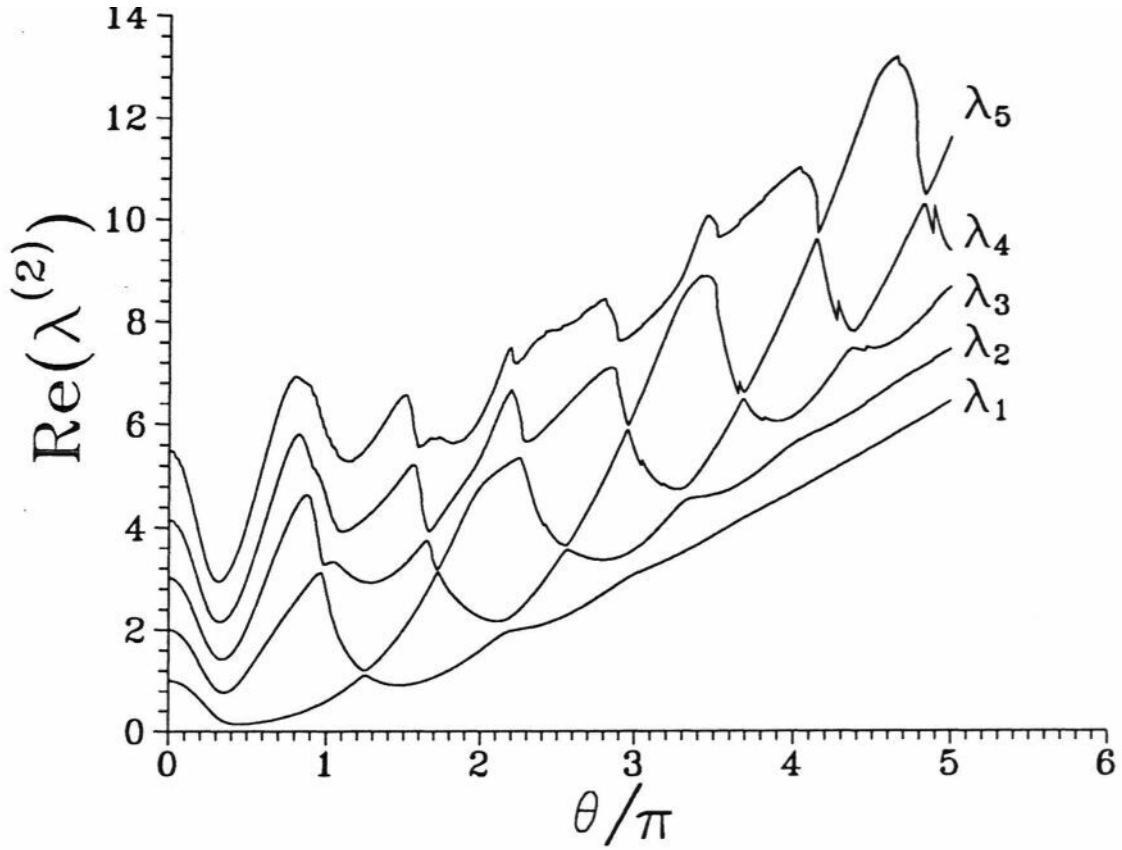


Figure 5.4: Real part of the first five eigenvalues of (5.18) corresponding to the correlation function $\mathcal{G}(t)$ (5.23) as a function of the pump parameter $\theta = \sqrt{N}g\tau$ for $N = 20$ and $n_b = 1$.

Chapter 5. Intensity-Intensity Correlations for Micromaser

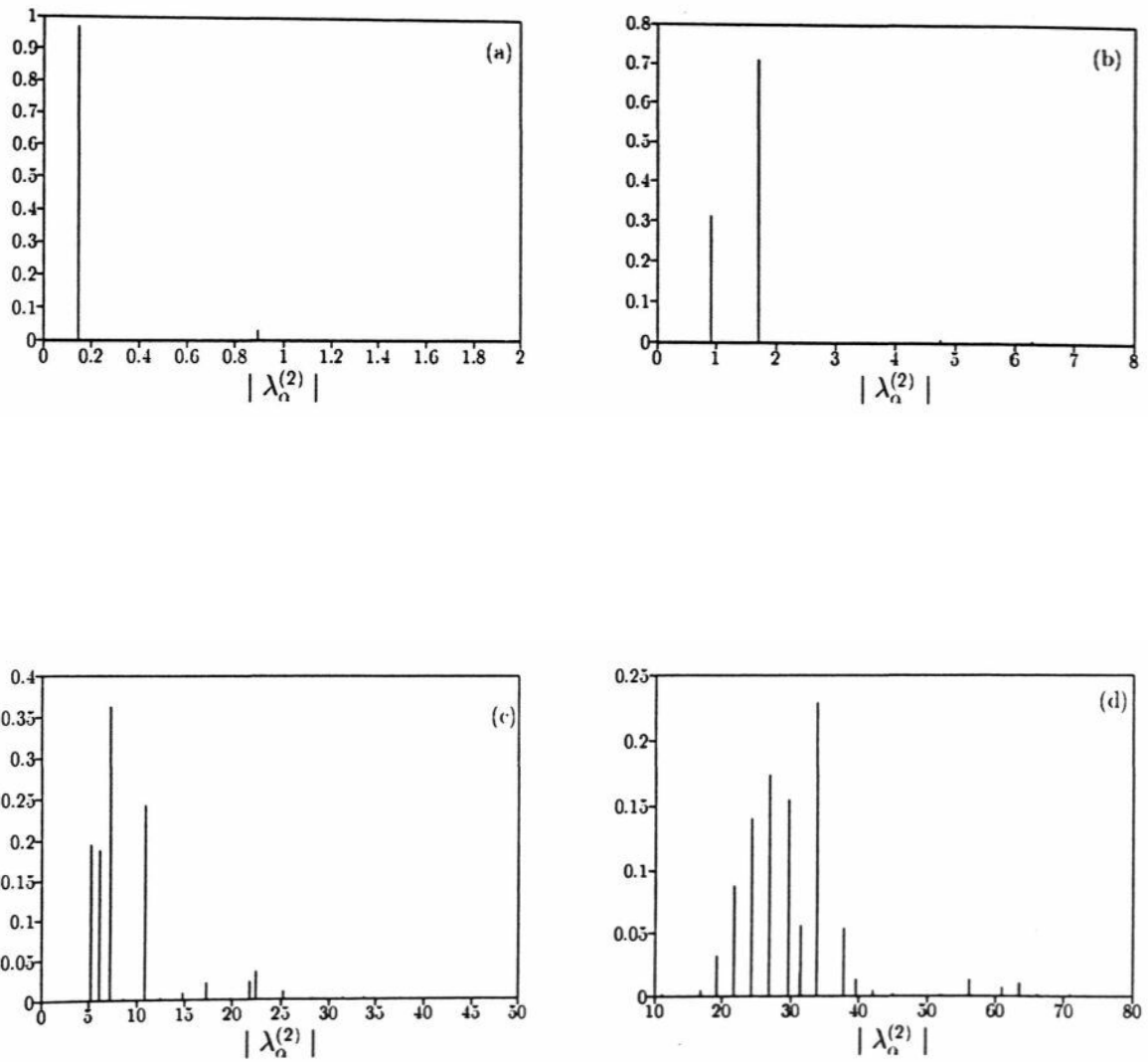


Figure 5.5: Weights ($|W_\alpha|$) of the eigenvalues contributing to the spectrum $\mathcal{G}(\omega - \omega_c)$ for $N = 20, n_b = 1$, (a) $g\tau = 0.3$, (b) $g\tau = 1$, (c) $g\tau = 3$ and (d) $g\tau = 7$.

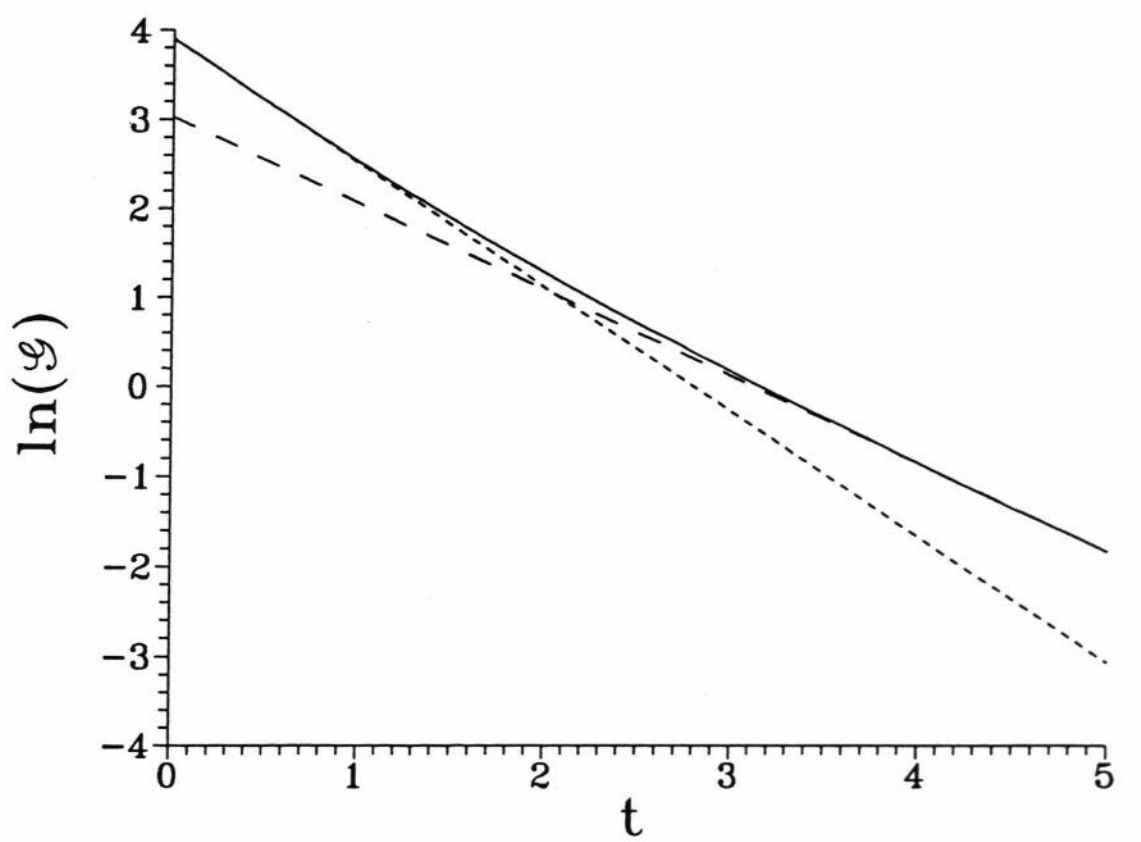


Figure 5.6: Time dependence of the logarithm of the correlation function $\mathcal{G}(t)$ for $N = 20$, $n_b = 1$ and $g\tau = 1$. The dashed curves correspond to the two eigenvalues (cf Fig. 5.5(b)).

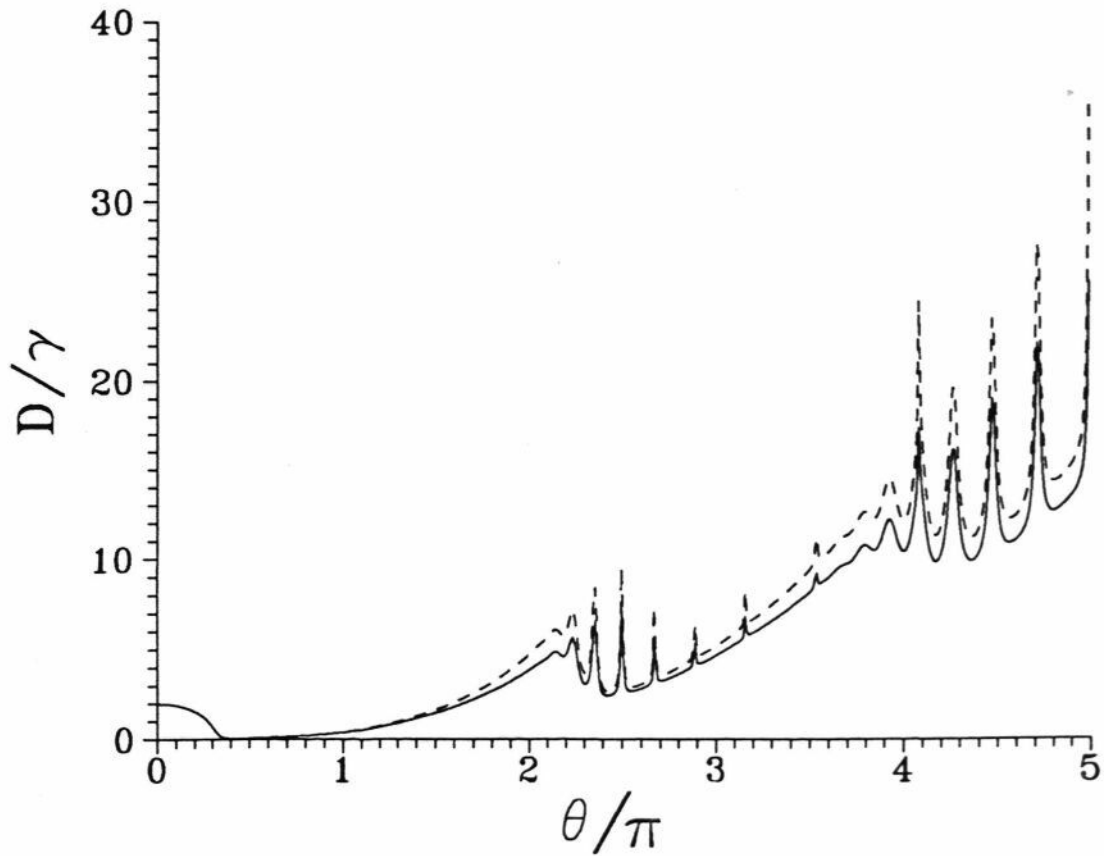


Figure 5.7: Comparison between the exact linewidth D/γ (solid curve) and the approximate analytical expression (5.40) (dashed curve), for $N = 50$ and $n_b = 10^{-4}$.

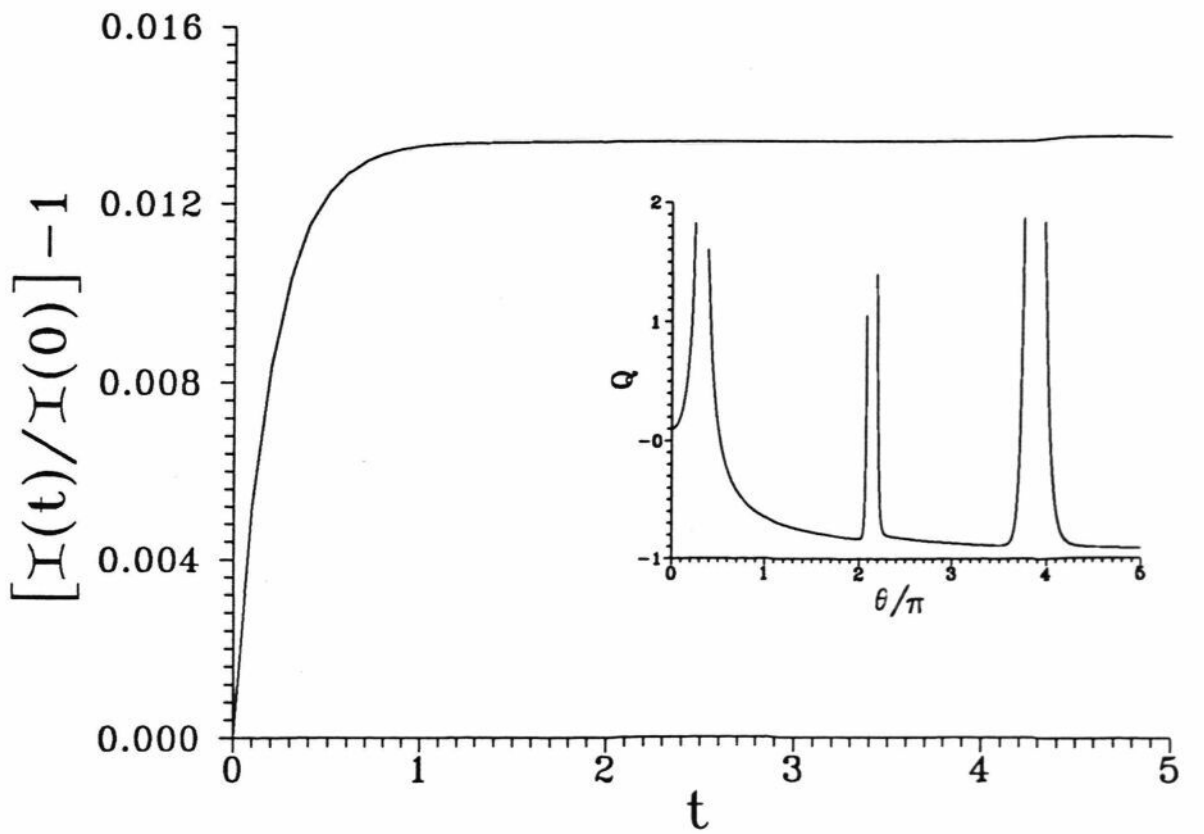


Figure 5.8: Time dependence of the quantity $[I(t)/I(0)] - 1$ for $N = 200$, $n_b = 0.1$ and $\theta = 1.5\pi$. Inset shows the Mandel's Q-parameter, $Q = (\langle \hat{a}^{\dagger 2} \hat{a}^2 \rangle - \langle \hat{a}^{\dagger} \hat{a} \rangle^2) / \langle \hat{a}^{\dagger} \hat{a} \rangle$, plotted as function of the pump parameter θ for the same parameters N and n_b .

For long times, $\mathcal{I}(t) \longrightarrow \langle \hat{a}^\dagger \hat{a} \rangle^2$ and hence $(\mathcal{I}(t)/\mathcal{I}(0)) - 1$ will be positive if the θ value were to correspond to sub-Poissonian statistics of the micromaser field. For completeness the inset in figure 5.8 shows the sub-Poissonian property of the field for the same parameters. In Fig. 5.9 we also display the behaviour of the eigenvalues which determine the correlation $\mathcal{I}(t)$; the eigenvalues are real in the range shown. On a comparison of the figures 5.4 and 5.9 it is clear that the eigenvalues that determine the dynamical behaviour of $\mathcal{I}(t)$ are different from the ones which determine $\mathcal{G}(t)$.

5.4 Probe of the intensity correlations for the micromaser field

We next consider the question of how the correlations like $\mathcal{G}(t)$ and $\mathcal{I}(t)$ for the micromaser field can be probed. As mentioned before the field characteristics can only be probed by examining the dynamical properties of the atoms [11,12]. The correlation function $T(i)$ can be, in principle, probed by examining the probability of finding two consecutive atoms in excited state in an interval t .

To probe $\mathcal{G}(t)$ we consider the following situation—we use a probe beam of atoms such that the frequency of the micromaser field can cause a resonant *two-photon transition*. We will now show how the two-photon absorption rate of the probe atoms is related to $\mathcal{G}(t)$. Consider the interaction Hamiltonian for a two-level atom interacting with a quantised radiation field in the dipole approximation (neglecting the term proportional to A^2),

$$H_{\text{int}}(t) = \frac{\hat{\mathbf{p}}(t) \cdot \mathbf{A}(t)}{mc}, \quad (5.43)$$

where $\hat{\mathbf{p}}(t)$ is the momentum of the atom and $\mathbf{A}(t)$ is the vector potential of the field at the location of the atom. The modal expansion of the vector potential \mathbf{A} is given by

$$\vec{A}(t) = \sqrt{\frac{\hbar c^2}{2V}} \sum_{\mathbf{k}} \frac{1}{\sqrt{\omega_{\mathbf{k}}}} \mathbf{e}_{\mathbf{k}} (\hat{a}_{\mathbf{k}} e^{-i\omega_{\mathbf{k}} t} + \hat{a}_{\mathbf{k}}^\dagger e^{i\omega_{\mathbf{k}} t}), \quad (5.44)$$

where $\mathbf{e}_{\mathbf{k}}$, $\omega_{\mathbf{k}}$ and $\hat{a}_{\mathbf{k}}$ are the polarisation vector, frequency and the annihilation operator corresponding to the k -th mode of the field. The time evolution operator in the interaction

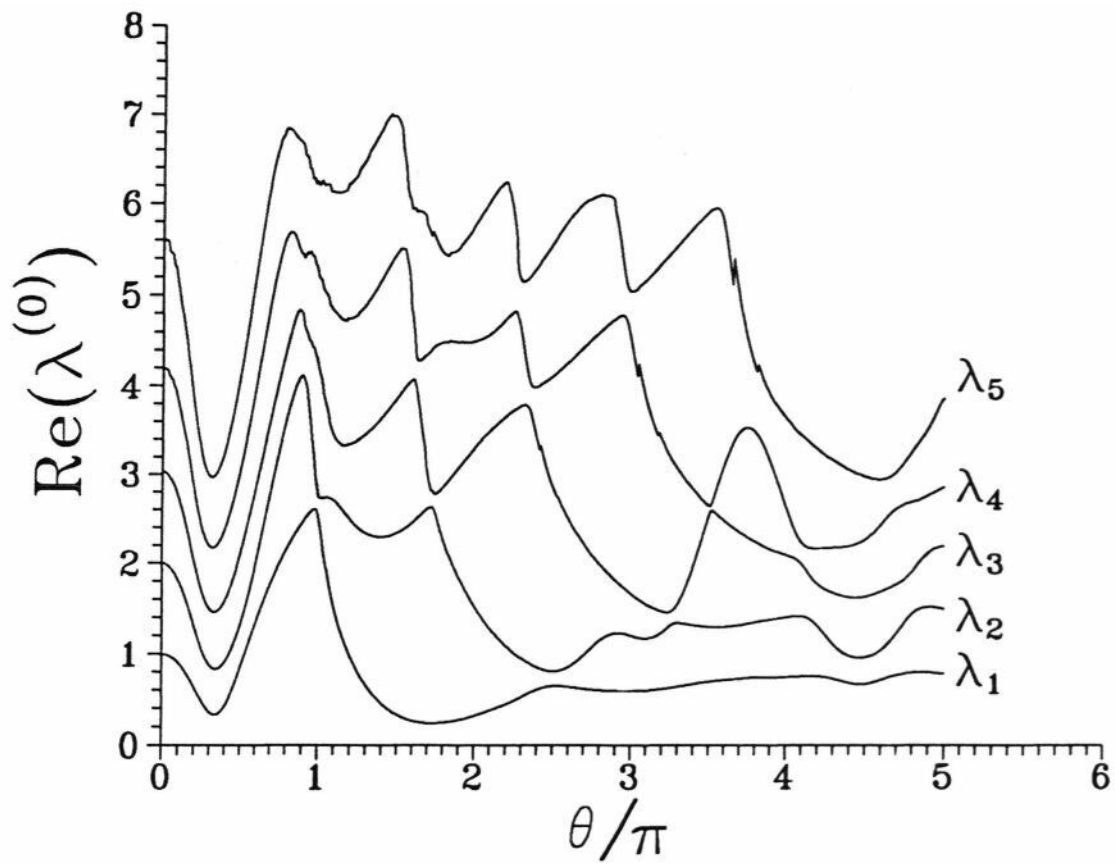


Figure 5.9: Same as Fig.5.4, but corresponding to the correlation function $X(\tau)$ (5.24).

picture is given by

$$\hat{U}(t) = \mathbf{1} - \frac{i}{\hbar} \int_0^t dt' \hat{H}_{\text{int}}(t') - \frac{1}{\hbar^2} \int_0^t \int_0^{t'} dt_1 dt_2 \theta(t_1 - t_2) H_{\text{int}}(t_1) H_{\text{int}}(t_2) \quad (5.45)$$

where the definition of the theta function

$$\theta(\tau) = \begin{cases} 1 & \text{if } \tau \geq 0 \\ 0 & \text{if } \tau < 0 \end{cases} \quad (5.46)$$

has been used. Let initially the atom be in the ground state $|g\rangle$ and the field be in an arbitrary pure state $|\psi\rangle$. The probability at time t , of the atom to be excited as result of the interaction is

$$P(t) = \sum_{\phi} |\langle \phi | \langle e | \hat{U}(t) | g \rangle | \psi \rangle|^2, \quad (5.47)$$

where the summation runs over all possible field states $|\phi\rangle$. We are interested only in transitions caused by two-photon processes. We assume that the transition frequencies of the probe atoms are far detuned from the frequency of the micromaser field so that the probe atoms do not perturb the micromaser field appreciably. The analysis gets complicated if the probe atoms have a resonance with some other mode of the cavity. In this case one has the possibility of transfer of energy through probe atoms to another mode of the cavity. Such a situation should ideally be avoided. We now allow the summation to extend over all the field states and retain only terms which are to second order in the expansion (5.45). Introducing a function \mathcal{L} , which is entirely dependent on the probe atoms and not the field

$$\mathcal{L}(t_1, t_2) = \theta(t_1 - t_2) \left(\frac{e}{\hbar m c} \right)^2 \langle e | p(t_1) p(t_2) | g \rangle \quad (5.48)$$

$$= \theta(t_1 - t_2) \left(\frac{e}{\hbar m c} \right)^2 \sum_{\epsilon_j} p_{\epsilon_j} p_{jg} e^{-i(\omega_j)t_1 + i\omega_j t_2}, \quad (5.49)$$

the probability of two-photon absorption, $P_2(t)$ becomes

$$P_2(t) = \iiint dt'_1 dt'_2 dt_1 dt_2 \mathcal{L}^*(t'_1, t'_2) \mathcal{G}(t'_1, t'_2; t_1, t_2) \mathcal{L}(t_1, t_2), \quad (5.50)$$

where $\mathcal{G}(t'_1, t'_2; t_1, t_2)$ is the second-order field correlation function. Expressing the probability in terms of the Fourier components, we have

$$P_2(t) = \int \int d\omega' d\omega g^*(\omega') \left\{ \frac{1}{(2\pi)^2} \int \int \int \int dt'_1 dt'_2 dt_1 dt_2 e^{-i(\omega_e - \omega')t'_1 - i\omega' t'_2 + i(\omega_e - \omega)t_1 + i\omega t_2} \right\} \quad (5.51)$$

where

$$g(\omega) = \left(\frac{e}{\hbar mc} \right)^2 \sum_j p_{ej} p_{jg} \frac{1}{\omega - \omega_j + i\epsilon}. \quad (5.52)$$

The probability of two photon absorption by the atom can be expressed in terms of the second-order spectral correlation function

$$\mathcal{G}(\omega'_1, \omega'_2; \omega_1, \omega_2) = \int \int \int \int dt'_1 dt'_2 dt_1 dt_2 e^{-i\omega'_1 t'_1 - i\omega'_2 t'_2 + i\omega_1 t_1 + i\omega_2 t_2} \mathcal{G}(t'_1, t'_2; t_1, t_2) \quad (5.53)$$

as

$$P_2 = \iint d\omega' d\omega g^*(\omega') \mathcal{G}(\omega_e - \omega', \omega'; \omega_e - \omega, \omega) g(\omega). \quad (5.54)$$

The steady state field in a micromaser is a stationary field. A stationary field is one whose statistical properties are independent of the choice of the origin of time. The second-order field correlation function thus satisfies

$$\mathcal{G}(t'_1, t'_2; t_1, t_2) = \mathcal{G}(t'_1 + \tau, t'_2 + \tau; t_1, t_2), \quad \forall \tau \quad (5.55)$$

For a stationary field, the two photon transition rate has been derived by Mollow [30] to be

$$\mathcal{R} = 2g^*(\omega_c) \left[\int_{-\infty}^{\infty} dt e^{-i(\omega_p - 2\omega_c)t - \Gamma|t|} \right] g(\omega_c) \quad (5.56)$$

$$= \int_{-\infty}^{\infty} dt \mathcal{G}(t) e^{-i\omega_p t + 2i\omega_c t - \Gamma|t|}, \quad (5.57)$$

where ω_p and Γ are respectively the frequency and linewidth of the two-photon transition. We can write (5.57) as

$$\mathcal{R} = 2\text{Re } \mathcal{G}(\Gamma + i(\omega_p - 2\omega_c)). \quad (5.58)$$

Thus the spectrum calculated in Sec. 5.2 can be studied by examining two-photon absorption by a probe atomic beam.

In conclusion, we have shown the unusual properties of the micromaser field as reflected in higher-order correlation functions of the field. We have provided evidence for the antibunching characteristics of such a field. We have further shown how the two-photon correlations can be probed by using atomic characteristics.

Appendix 5A

Eigenvalue method

In this appendix the eigenvalue method is described. The equation of motion of the off-diagonal density matrix elements $\rho_{n,n+2}$ can be written in matrix form

$$\boldsymbol{\rho} = \mathbf{A}\boldsymbol{\rho}, \quad (5A.1)$$

where the column vector ρ is

$$\boldsymbol{\rho} = \begin{pmatrix} \rho_{02} \\ \rho_{13} \\ \rho_{24} \\ \vdots \\ \rho_{n,n+2} \\ \vdots \end{pmatrix}. \quad (5A.2)$$

The matrix A is of tridiagonal form, given by

$$\mathbf{A} = \begin{pmatrix} A_{00} & A_{01} & & & \\ A_{10} & A_{11} & A_{12} & & \\ & A_{21} & A_{22} & A_{23} & \\ & & \ddots & \ddots & \ddots \\ & & & A_{n,n-1} & A_{n,n} & A_{n,n+1} \\ & & & & \ddots & \ddots & \ddots \end{pmatrix}, \quad (5A.3)$$

where the non-zero matrix elements are

$$A_{n,n-1} = r \sin(g\tau\sqrt{n}) \sin(g\tau\sqrt{n+2}) + \gamma n_b \sqrt{n(n+2)} \quad (5A.4)$$

Appendix 5A. *Eigenvalue method*

$$A_{n,n} = -r[\cos(g\tau\sqrt{n+1})\cos(g\tau\sqrt{n+3})],$$

$$-\gamma(n+1)(n+2), \quad (5A.5)$$

$$A_{n,n+1} = \gamma(n+1)\sqrt{(n+1)(n+3)} \quad (5A.6)$$

The solution to (5A.1) can be formally written down as

$$\rho_{n,n+2}(t_0 + t) = \sum_{m=0}^{\infty} (e^{At})_{nm} \rho_{m,m+2}(t_0). \quad (5A.7)$$

The matrix A can be diagonalised as

$$A = P\Lambda P^{-1}, \quad (5A.8)$$

where $\Lambda (= \text{diag}(\lambda_0, \lambda_1, \dots))$ is a diagonal matrix of eigenvalues of the matrix A and P is the matrix of eigenvectors of the matrix A . Thus, $(e^{At})_{nm}$ can be written as

$$(e^{At})_{nm} = (Pe^{\Lambda t}P^{-1})_{nm} \quad (5A.9)$$

$$= \sum_{k=0}^{\infty} P_{nk} e^{\lambda_k t} P_{km}^{-1}. \quad (5A.10)$$

On comparing (5.29), (5A.7) and (5A.10), we have

$$\langle \hat{a}^{\dagger 2}(t_0 + t) \hat{a}^2(t_0) \rangle = \sum_{n,m} \sqrt{(n+1)(n+2)(m+1)(m+2)} \left(\sum_{k=0}^{\infty} P_{nk} e^{\lambda_k t} P_{km}^{-1} \right) \rho_{n,n+2}(t_0). \quad (5A.11)$$

Appendix 5B

Green's function approach

In this appendix the steps involved in the computation of $G(s)$ (equation (5.34)) are given. We have to evaluate the quantity $\mathcal{G}(s)$, defined as

$$\mathcal{G}(s) = \sum_{n=0}^{\infty} \sum_{m=0}^{\infty} \sqrt{(n+1)(n+2)(m+1)(m+2)} G_{nm}^{(2)}(s) p_{m+2}. \quad (5B.1)$$

The problem is to obtain the elements of the matrix $G_{nm}^{(2)}(s)$:

$$\left(G_{nm}^{(2)}(s) \right) = \begin{pmatrix} G_{00}^{(2)} & G_{01}^{(2)} & G_{02}^{(2)} & \dots \\ G_{10}^{(2)} & G_{11}^{(2)} & G_{12}^{(2)} & \dots \\ G_{20}^{(2)} & G_{21}^{(2)} & G_{22}^{(2)} & \dots \\ \vdots & \vdots & \vdots & \ddots \end{pmatrix} \quad (5B.2)$$

Eventhough the dimension of this matrix is infinite, for numerical purposes we restrict its dimension to be decided by the distribution p_n . It is typically around 250 to 300.

Let us now make the following definitions

$$\psi_n = G_{n,m}^{(2)}(s) \quad (5B.3)$$

$$\psi_{n-1} = G_{n-1,m}^{(2)}(s) \quad (5B.4)$$

$$\psi_{n+1} = G_{n+1,m}^{(2)}(s) \quad (5B.5)$$

Equation (5.36) can then be written as

$$(s - \mathcal{A}_n)\psi_n - \mathcal{B}_n\psi_{n-1} - \mathcal{C}_n\psi_{n+1} = \delta_{nm}. \quad (5B.C)$$

In the above equation, we have used the fact that

$$G_{nm}^{(2)}(t=0) = \delta_{nm}. \quad (5B.7)$$

Appendix 5B. Green's function approach

For rotational simplicity the superscript (2) is not written for A_n, B_n and C_n . For $n > m$ let us define the following ratios:

$$S_{n+1} \equiv \frac{\psi_{n+1}}{\psi_n} \quad (5B.8)$$

$$S_n \equiv \frac{\psi_n}{\psi_{n-1}}, \quad (5B.9)$$

and for $n < m$,

$$T_{n+1} \equiv \frac{\psi_{n+1}}{\psi_n} \quad (5B.10)$$

$$T_n \equiv \frac{\psi_n}{\psi_{n-1}}. \quad (5B.11)$$

Let us consider the first column in the matrix (5B.5), i.e., $m = 0$. Then for $n > m$, we have

$$s - \mathcal{A}_n - \frac{B_n}{S_n} - C_n S_{n+1} = 0. \quad (5B.12)$$

Solving for S_n , we have

$$S_n = \frac{B_n}{s - \mathcal{A}_n - C_n S_{n+1}}. \quad (5B.13)$$

Similarly, we have

$$S_{n+1} = \frac{B_{n+1}}{s - \mathcal{A}_{n+1} - C_{n+1} S_{n+2}} \quad (5B.14)$$

$$\begin{aligned} & \vdots \\ S_{n+l} &= \frac{B_{n+l}}{s - \mathcal{A}_{n+l} - C_{n+l} S_{n+l+1}} \\ & \vdots \end{aligned} \quad (5B.15)$$

Combining the above equations, we thus have a continued fraction for the quantity S_n

$$S_n = \frac{B_n}{s - \mathcal{A}_n - \frac{C_n B_{n+1}}{s - \mathcal{A}_{n+1} - \frac{C_{n+1} B_{n+2}}{s - \mathcal{A}_{n+2} - \dots}}}. \quad (5B.16)$$

Consider the following continued fraction

$$f_n = b_0 + \frac{a_1}{b_1 + \frac{a_2}{b_2 + \frac{a_3}{b_3 + \dots}}} \quad (5B.17)$$

Appendix 5B. Green 5 function Approach

The n -th convergent of this continued fraction is given by the ratio p_n/q_n , where the numerator and denominator are obtained from the recursion formula

$$p_n = b_n p_{n-1} + a_n p_{n-2} \quad (5B.18)$$

$$q_n = b_n q_{n-1} + a_n q_{n-2} \quad (5B.19)$$

with $p_{-1} = 1, p_0 = b_0, q_{-1} = 0$ and $q_0 = 1$. Thus given the dimension, n , of the matrix (5B.2), one can determine the ratio S_n by evaluating the continued fraction (5B.1G) to the required accuracy. From the knowledge of S_n the ladder of ratios S_{n-1} to S_1 can be obtained using the relation

$$S_{n-1} = \frac{B_{n-1}}{s - \mathcal{A}_{n-1} - C_{n-1} S_n}. \quad (5B.20)$$

Now consider the element $m = 0, n = 0$. Equation (5B.6) then yields

$$\psi_0 = \frac{1}{s - \mathcal{A}_0 - C_0 S_1}. \quad (5B.21)$$

All the other terms in the column can then be obtained by using the definitions of the ratios S_n (5B.8) or (5B.9).

Consider the second column, i.e., $m = 1$. For $n = 0$, we have

$$T_1 = \frac{s - \mathcal{A}(0)}{C(0)}, \quad (5B.22)$$

where

$$T_1 = \frac{\psi_1}{\psi_0}. \quad (5B.23)$$

For $n = m = 1$, equation (5B.6) then yields,

$$\psi_1 = \frac{1}{s - \mathcal{A}(1) - \frac{B(1)}{T_1} - C(1) S_2}. \quad (5B.21)$$

Using (5B.10) or (5B.11) one can then determine ψ_0 and using (5B.8) or (5B.9) one can determine ψ_2 to ψ_n . This procedure can now be generalised to any column. First we must determine both the ratios S_l and T_l . Then, from the diagonal element we must determine ψ_l . Once ψ_l is obtained we can use one of the equations from ((5B.8) to (5B.11)) to obtain the remaining matrix elements.

References

- [1] E.T. Jaynes and F.W. Cummings, Proc. IEEE 51, 89 (1963).
- [2] R. Hanbury Brown and R.Q. Twiss, Nature 177, 27 (1956).
- [3] L. Mandel and E. Wolf, Rev. Mod. Phys. 37, 231 (1965).
- [4] S. Chopra and L. Mandel, IEEE J. Quant. Elec. QE-8, 324 (1972).
- [5] *Coherence and Quantum Optics*, ed. L. Mandel and E. Wolf, (Plenum Publishing Corporation, New York, 1972).
- [6] H.J. Carmichael and D.F. Walls, J. Phys. B: Atom. Molec. Phys. 9, L43 (1976).
- [7] H.J. Kimble and L. Mandel, Phys. Rev. A 13, 2123 (1976).
- [8] D.F. Walls and P. Zoller, Phys. Rev. Lett. 10, 709 (1981).
- [9] M.J. Collett and D.F. Walls, Phys. Rev. Lett. 61, 2442 (1988).
- [10] Z.Y. Ou, S.F. Pereira and H.J. Kimble, Phys. Rev. Lett. 70, 3239 (1993).
- [11] G. Rempe, F. Schmidt-Kaler and H. Walther, Phys. Rev. Lett. 64, 2783 (1990).
- [12] G. Rempe and H. Walther, Phys. Rev. A 42, 1650 (1990).
- [13] P. Filipowicz, J. Javanainen and P. Meystre, Phys. Rev. A 34, 3077 (1986).
- [14] L. Lugiato, M.O. Scully and H. Walther, Phys. Rev. A 36, 740 (1987).
- [15] M.O. Scully, H. Walther, G.S. Agarwal, T. Quang and W. Schleich, Phys. Rev. A 44, 5992 (1991).
- [16] T. Quang, G.S. Agarwal, J. Bergou, M.O. Scully, H. Walther, K. Vogel and W. Schleich, Phys. Rev. A 48, 803 (1993).
- [17] K. Vogel, W.P. Schleich, M.O. Scully and H. Walther, Phys. Rev. A 48, 813 (1993).
- [18] C. Wagner, R.J. Brecha, A. Schenzle and H. Walther, Phys. Rev. A 46, R535C (1992).
- [19] **C. Wagner, R.J. Brecha, A. Schenzle and H. Walther, Phys. Rev. A 47, 5068 (1993)**

References

- [20] Ning Lu, *Phys. Rev. A* **47**, 1317 (1993).
- [21] S. Arun Kumar and G.S. Agarwal, *Phys. Rev. A* **50**, 680 (1994).
- [22] F.W. Cummings, *Phys. Rev.* **140**, 1051 (1965).
- [23] J.H. Eberly, N.B. Narozhny and J.J. Sanchez-Mondragón, *Phys. Rev. Lett.* **44**, 1323 (1980).
- [24] D. Meschede, H. Walther and G. Müller, *Phys. Rev. Lett.* **54**, 551 (1985).
- [25] M. Brune, J.M. Raimond, P. Goy, L. Davidovich and S. Haroche, *Phys. Rev. Lett.* **59**, 1899 (1987).
- [26] H. Risken, *The Fokker-Planck Equation* (Springer-Verlag, Berlin Heidelberg, 1984), Chapter 9, pp. 196-228.
- [27] M. Abramowitz and I. Stegun, *Handbook of Mathematical Functions* (Dover, New York, 1965).
- [28] P. Meystre, G. Rempe and H. Walther, *Opt. Lett.* **13**, 1078 (1988).
- [29] H. Risken, *Progress in Optics*, Vol. VIII, ed. E. Wolf, (North-Holland Publishing Co., Amsterdam, 1970).
- [30] B.R. Mollow, *Phys. Rev.* **175**, 1555 (1968).
- [31] G.S. Agarwal, *Phys. Rev. A* **1**, 1445 (1970).

Chapter 6

Quasiprobability distributions for the micromaser field

In this chapter, we continue the study of nonclassical features of the micromaser field. In section 6.1 a general introduction to quasi-probability distributions is given. In section 6.2, a discussion about the trapping states, which characterise the very low temperature behaviour of a micromaser and results on the study of quasiprobability distributions for the micromaser field are presented.

6.1 Quasiprobability distributions

Quasiprobability distributions were the result of an effort to obtain distributions analogous to classical phase space distributions. They are useful for evaluating expectation values of operators in a form similar to classical averages over a phase space [1]. In addition to being useful as computational tools they also provide insights into the relation between quantum and classical physics. But unlike classical probability distributions, these may not be positive definite or may not exist as simple functions. Many quasiprobability distributions have been described and used in the literature [1]. Each of these different types of quasiprobability functions map averages of operators ordered according to specific prescriptions to classical-like averages over phase space. The most common ones among these distributions are the Q-function [2-4], the Wigner function [5] and the Glauber-Sudarshan P -function [6,7].

6.1.1 Q-function

The Q-function is defined as the diagonal coherent state expectation value of the density operator [2-4],

$$Q(\alpha) = \frac{1}{\pi} \langle \alpha | \hat{\rho} | \alpha \rangle \quad (6.1)$$

where $|\alpha\rangle$ represents a coherent state and $\hat{\rho}$ the density operator. It satisfies the property that

$$\int d^2\alpha Q(\alpha, \alpha^*) = 1, \quad (6.2)$$

This is so since the density operator is normalised:

$$\text{Tr}\{\hat{\rho}\} = 1 \quad (6.3)$$

$$= \text{Tr}\left\{\frac{1}{\pi} \int d^2\alpha |\alpha\rangle \langle \alpha| \hat{\rho}\right\} \quad (6.4)$$

$$= \frac{1}{\pi} \int d^2\alpha \langle \alpha | \hat{\rho} | \alpha \rangle. \quad (6.5)$$

Alternatively, it is also defined as the Fourier transform of the quantum characteristic function as [8,9]

$$Q(\alpha) = \frac{1}{\pi^2} \int C_Q(\lambda, \lambda^*) \exp(\alpha \lambda^* - \alpha^* \lambda) d^2\lambda, \quad (6.6)$$

where

$$C_Q(\lambda, \lambda^*) = \text{Tr}\left\{\hat{\rho} e^{-\lambda^* \hat{a}} e^{\lambda \hat{a}^\dagger}\right\}. \quad (6.7)$$

Here a and a^\dagger are the annihilation and creation operators of the field, respectively. The quantum characteristic function $C_Q(\lambda, \lambda^*)$ has the property that the normal ordered moments of operators are obtained from its derivatives evaluated at $\lambda = 0$. Thus,

$$\langle \hat{a}^{\dagger m} \hat{a}^n \rangle = (-1)^n \frac{\partial^{m+n}}{\partial^m \lambda \partial^n \lambda^*} C_Q(\lambda, \lambda^*)|_{\lambda=0} \quad (6.8)$$

The Q-function is used to calculate expectation values of anti-normally ordered operators. It is unique among the quasi-probability distributions in that it always exists for any state of the field and is strictly positive definite and hence is truly a probability distribution.

Chapter 6. Quasiprobability distributions for the micromaser field

6.1.2 Wigner function

Wigner first introduced the idea of quasiprobability distributions by constructing a function which is now called the Wigner distribution function [5]. He constructed a joint distribution which would resemble a classical probability for the two conjugate variables x and p . He had originally developed it to study quantum corrections to classical statistical mechanics. In the quantum domain the Wigner function plays the role of a phase space distribution and hence serves as a bridge between classical and quantum physics. The only way it differs from classical phase space distribution is that it can assume negative values for some states. In terms of the quantum characteristic function $C_W(\lambda, \lambda^*)$, it is defined as [8,9]

$$W(\alpha) = \frac{1}{\pi^2} \int C_W(\lambda, \lambda^*) \exp(\alpha \lambda^* - \alpha^* \lambda) d^2 \lambda, \quad (6.9)$$

where

$$C_W(\lambda, \lambda^*) = \text{Tr} \left\{ \hat{\rho} \exp(\lambda \hat{a}^\dagger - \lambda^* \hat{a}) \right\}. \quad (6.10)$$

The following is a summary of the properties of the Wigner function. The Wigner function always exists for any given state. Its value is restricted to between -2 and $+2$. The averages of symmetrically ordered products of a and a^\dagger are calculated from the moments of the Wigner function. Symmetrical ordering (or Weyl order) of operators consists of the average of all possible ways of arranging the operators involved. Thus,

$$\{\hat{a}^2 \hat{a}^{\dagger 2}\}_{sym} = \frac{1}{6} \left[\hat{a}^{\dagger 2} \hat{a}^2 + \hat{a}^\dagger \hat{a} \hat{a}^\dagger \hat{a} + \hat{a}^\dagger \hat{a}^2 \hat{a}^\dagger + \hat{a} \hat{a}^{\dagger 2} \hat{a} + \hat{a} \hat{a}^\dagger \hat{a} \hat{a}^\dagger + \hat{a}^2 \hat{a}^{\dagger 2} \right]. \quad (6.11)$$

6.1.3 Glauber-Sudarshan P-function

In chapter 1 the Glauber-Sudarshan P-function was introduced. The moments of this function are related to normally ordered combinations of a and \hat{a}^\dagger . These normally ordered operator averages are the ones which are measured in photodetectors. For non-classical states this function may become highly singular and it can be understood only

Chapter 6. Quasiprobability distributions for the micromaser field

in the sense of generalised functions. But precisely this property is used as an indicator of purely nonclassical states (cf. chapter 1). Various other types of distributions, like the Drummond-Gardiner positive-P distribution, have also been defined over the years in order to overcome the non-positive nature of the P-function [10]. A unified approach to quasi-probability distributions corresponding to various operator orderings was given by Agarwal and Wolf [11-13] and by Cahill and Glauber [14,15].

6.2 Trapping states and quasiprobability distributions for the micromaser field

Consider a single-mode cavity through which an atomic beam passes such that at the most only one atom exists within the cavity at a given time. The very low temperature behaviour of the micromaser field shows numerous resonances which are a signature of trapping states [16,17]. The trapping condition is achieved whenever $\sqrt{n+1}g\tau = q\pi$, for some integer q . These are the states of the micromaser field for which the atoms execute $2q\pi$ Rabi oscillations during their interaction with the cavity field. At higher temperatures, these resonances get washed out due to thermal fluctuations.

In this section we present the results of a numerical study of quasiprobability distributions for the micromaser field. In particular, we concentrate on the first order phase transition and the very low temperature trapping regimes of the micromaser field. The Wigner function becomes negative and shows oscillations for a wide range of the pump parameter.

The field associated with the micromaser is known to manifest important nonclassical properties. Several manifestations of these strictly quantum properties have been studied both theoretically [18,19] and experimentally [20-22]. The most important among these characteristics is the prediction and verification of the sub-Poissonian nature of the field [21,22]. The antibunching property of the field has also been studied [23]. As discussed in chapter 1, these properties refer to expectation values of the two-time correlation function involving the number operator of the field [24]. Even the phase sensitive correlation

properties are very different compared to the usual laser systems [25,26].

It is then clear that one should examine the nonclassical properties in their totality. As mentioned in section 6.1 the quasiprobability distributions like the Wigner function and the Q -function can provide quite useful information on the statistical character of the quantum field.

The standard model of the micromaser has shown that in the steady state the off-diagonal elements of the density matrix of the field are zero [18]. The diagonal elements are given by

$$p_n = p_0 \prod_{j=1}^n \left(\frac{n_b}{n_b + 1} + \frac{N \sin(g\tau \sqrt{j})}{(n_b + 1)j} \right), \quad (6.12)$$

where n_b is the mean thermal photon number in the cavity, N is the average number of Rydberg atoms passing through the cavity during the cavity life time, r is the interaction time (time of flight) of the Rydberg atoms with the cavity field and g is the coupling strength of the atoms with the cavity field. The quantity p_0 is fixed by normalisation requirements. Since the steady state micromaser field density matrix is diagonal, (6.1) yields,

$$Q(\alpha) = \frac{1}{\pi} \sum_n \exp(-|\alpha|^2) \frac{|\alpha|^{2n}}{n!} p_n, \quad (6.13)$$

where p_n is given by (6.12).

A micromaser field does not evolve into a coherent state, unlike conventional masers and lasers. Moreover, for increasing values of the pump parameter ($\theta = \sqrt{N}g\tau$), the micromaser shows many abrupt transitions in addition to the initial maser transition [18] (see Fig.6.1). Around $\theta = 1$, there is the first maser transition and there is a sharp rise in the mean photon number. Following this transition, the mean photon number falls gradually and reaches a minimum around $\theta = 2\pi$. At approximately $\theta = 2\pi$ and multiples thereof, the field shows further abrupt rise in the mean photon number. These transitions, unlike the one occurring at $\theta = 1$ which has the characteristics of a continuous phase transition, are first order phase transitions [18]. The photon number distribution splits and shows a double peaked structure in the first order phase transition regions (see

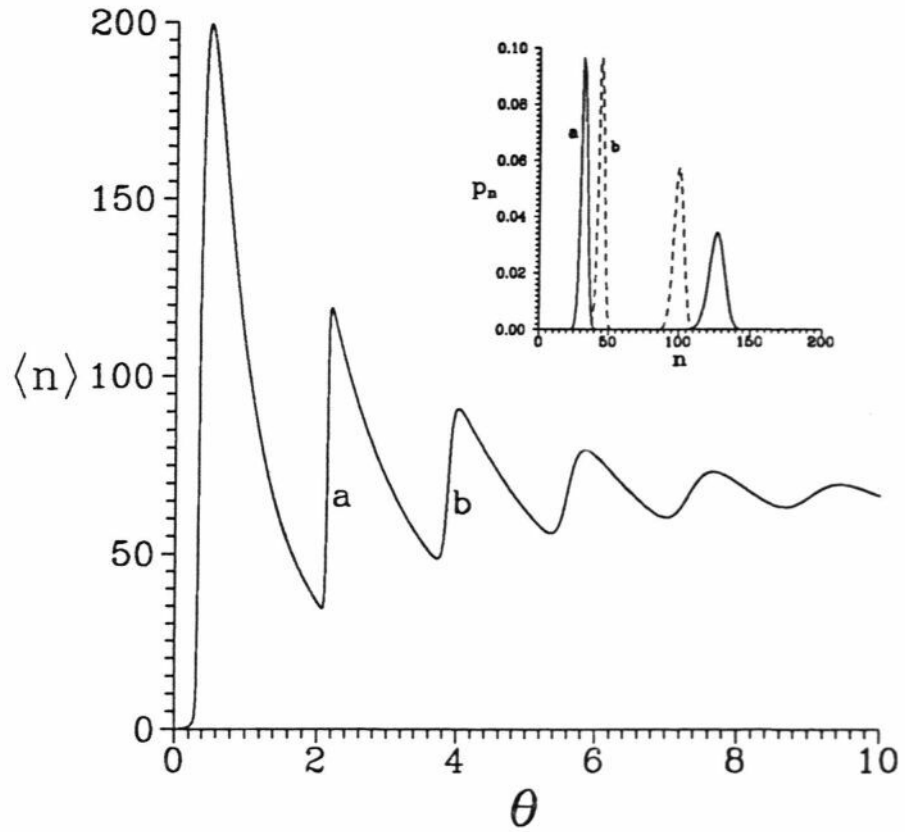


Figure 6.1: Mean photon number $\langle n \rangle$ versus the pump parameter θ in units of p for $n_b = 0.1$ and $N = 200$. Inset shows the photon number distribution, p_n for values of the pump parameter corresponding to the labels a ($\theta = 2.14$) and b ($\theta = 3.88$) in the main figure.

the inset in Fig. 6.1). This is due to the fact that the excited atoms after executing integer number of Rabi oscillations may or may not get de-excited as they leave the cavity.

Filipowicz et al [18] and Guzman et al [30] have constructed a semi-classical theory of the micromaser. For large values of N and n_b not too small, this approach reproduces almost all the results provided by the exact microscopic theory. They introduced a Fokker-Planck equation for the photon statistics

$$\frac{\partial P(\nu, \tau)}{\partial \tau} = -\frac{\partial}{\partial \nu} [q(\nu) P(\nu, \tau)] + \frac{1}{2N} \frac{\partial^2}{\partial \nu^2} [g(\nu) P(\nu, \tau)], \quad (6.14)$$

where

$$\nu = \frac{n}{N} \quad (6.15)$$

$$q(\nu) \sim -\nu + \sin^2(\theta \sqrt{\nu + \frac{1}{N}}) \quad (6.16)$$

$$g(\nu) \sim \nu + 2n_b \nu + \sin^2(\theta \sqrt{\nu + \frac{1}{N}}). \quad (6.17)$$

Here, the terms $\frac{n_b}{N}$ have been dropped, for if this approximation is to be **valid**, $N \rightarrow \infty$.

Under steady state conditions, we have

$$\frac{\partial P}{\partial \tau} = 0. \quad (6.18)$$

The semi-classical rate equation is given by

$$\frac{d\langle \nu \rangle}{d\tau} = q(\langle \nu \rangle) \quad (6.19)$$

$$= -(\langle \nu \rangle - \frac{n_b}{N}) + \sin^2(\theta \sqrt{\langle \nu \rangle + \frac{1}{N}}). \quad (6.20)$$

For steady state conditions, we have

$$\langle \nu \rangle = \frac{n_b}{N} + \sin^2(\theta \sqrt{\langle \nu \rangle + \frac{1}{N}}) \approx \sin^2(\theta \sqrt{\langle \nu \rangle + \frac{1}{N}}). \quad (6.21)$$

Solving for the roots of this equation we obtain the semiclassical steady state mean photon number.

In the Fokker-Planck approach the abrupt rise in the mean photon number in the cavity at multiples of $2p$ for the value of the pump parameter can be understood as due to the occurance of two attractive minima for the effective potential $V(\nu)$, where

$$V(\nu) = - \int_0^\nu d\nu' \frac{q(\nu')}{g(\nu')} = - \int_0^\nu d\nu' \frac{\sin^2(\sqrt{\nu'}\theta) - \nu'}{\sin^2(\sqrt{\nu'}\theta) + \nu' + 2\nu'n_b}. \quad (6.22)$$

The photon number distribution tends to accumulate near the minima of the effective potential $V(\nu)$. In these transition regions the global minimum of the effective potential gets replaced by the next minimum. Because of this increased number fluctuations the statistics is super-Poissonian as is shown by the Maudel's Q-parameter, defined as (cf chapter 1)

$$Q = \frac{\langle \hat{n}^2 \rangle - \langle \hat{n} \rangle^2}{\langle \hat{n} \rangle} - 1 \quad (6.23)$$

(see Fig.6.2, solid curve). Eventhough the Mandel's Q-parameter is positive for those values of the pump parameter q , it does not imply that the field is not nonclassical. Agarwal and Tara [27,28] have generalised the criterion for nonclassicality by constructing the matrix

$$m^{(n)} = \begin{pmatrix} 1 & m_1 & m_2 & \dots & m_{n-1} \\ m_1 & m_2 & m_3 & \dots & m_n \\ m_2 & m_3 & m_4 & \dots & m_{n+1} \\ \vdots & \vdots & \vdots & \ddots & \vdots \\ m_{n-1} & m_n & m_{n+1} & \dots & m_{2n-2} \end{pmatrix} \quad (6.24)$$

where $m_n = \langle (\hat{a}^\dagger)^n \hat{a}^n \rangle$. For $n = 2$, the determinant of $m^{(2)}$ is just $\langle \hat{a}^{\dagger 2} \hat{a}^2 \rangle - \langle \hat{a}^\dagger \hat{a} \rangle^2$, which by dividing with $\langle \hat{a}^\dagger \hat{a} \rangle$ one gets the definition of Mandel's Q-parameter. Note that for a classical state, the determinant of the matrix $m^{(n)}$ is positive definite. If for any state the determinant is negative, then the state is a nonclassical state. In particular, for a coherent state, $\det m^{(n)} = 0$, whereas for a Fock state, which is a highly nonclassical state, it is negative. By defining a matrix $m^{(n)}$ with the terms $\mu_n = \langle (\hat{a}^\dagger \hat{a})^n \rangle$ replacing

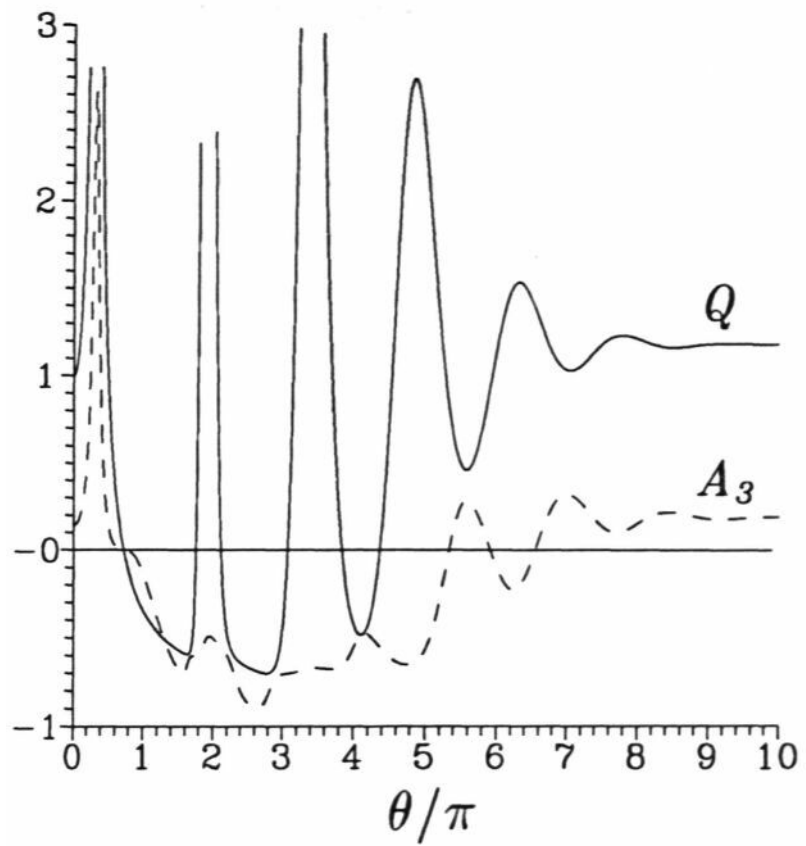


Figure 6.2: Mandel's Q -parameter (solid curve) and the A_3 parameter (dashed curve) as functions of the pump parameter θ with $n^b = 1$ and $N = 100$.

Chapter 6. Quasiprobability distributions for the micromaser field

the terms m_n in (6.21) and defining a parameter A_n

$$A_n = \frac{\det m^{(n)}}{\det \mu^{(n)} - \det m^{(n)}}, \quad (6.25)$$

we have a general criterion for nonclassicality — a state is nonclassical if $A_n < 0$ for some n . The nonclassicality of the micromaser field is shown by the parameter A_3 (see Fig.6.2, dashed curve) in the regions where the Mandel's Q -parameter fails to show any. In the regions following the first order transitions the photon number distribution is single-peaked, narrow and shows sub-Poissonian statistics.

The time development of the field in the first-order transition regions also shows many interesting features. In a recent work [29], it has been experimentally shown that in these regions spontaneous jumps or slow transitions between the two metastable states occur depending on the parameter values. Hysteretic behaviour of the field was also observed. In Fig.6.3 we plot the normalised mean photon number (ν) versus the pump parameter δ (the pump parameter is varied, with N, g and T remaining fixed) corresponding to the experiment [29]. The solid curve corresponds to the micromaser theory and the dashed one to semi-classical theory. In Fig.6.4, the Q and the Wigner functions for the second first-order transition regime for the points marked in Fig.6.3 are plotted. The Wigner function, besides being a doublet, exhibits oscillations quite characteristic of states like Fock states.

In Fig.6.5 we plot mean value of the photon number versus the pump parameter for a range which shows the trapping states. As in [17], the resonances have been labeled as $(n + 1/2, q)$, where n indicates the trapping state and q represents the number of 2π oscillations that the atoms execute in the cavity. In Fig.6.6, we show the photon number distribution, the Q -function and the Wigner function for the various points indicated by the labels in Fig.6.5. Corresponding to the points b, d, f and h of Fig.6.5, the number distribution is bistable and it is reflected in the Q - and the Wigner functions. The points a, c, e, g and i correspond to the trapping states. The distributions are narrow and single peaked with the exception of a and i. This is due to the fact that there are two trapping states corresponding to $q = 1$ and $q = 2$ for these pump parameter values. It

is seen from Fig.6.6. that the average behaviour of the Wigner function is very similar 1
 P_n .

In conclusion, we have studied the quasiprobability distributions of the micromaser field which manifests many nonclassical features. The Q - and the Wigner functions show a double peaked structure for the phase transition regimes of the micromaser. The Q -function is much broader than the Wigner function and the Wigner function takes on negative values for certain ranges of the argument and has oscillatory behaviour for lower values of θ . For the low-temperature trapping regime also the Q - and the Wigner functions show double peaked structures.

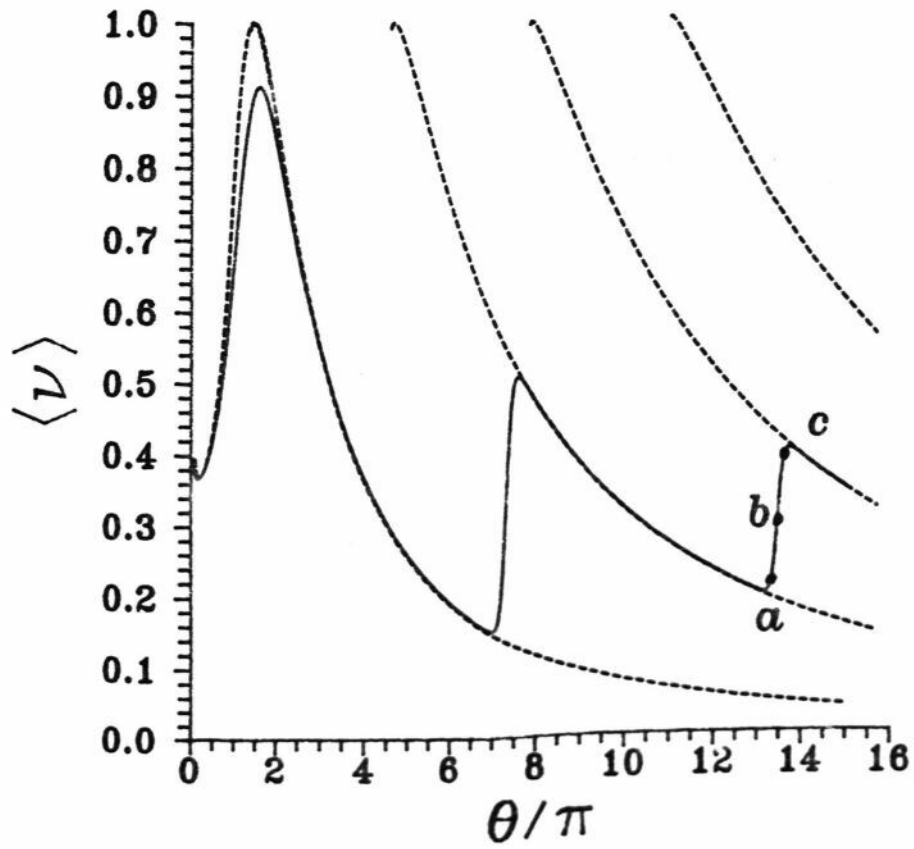


Figure 6.3: Normalised mean value of the photon number versus the pump parameter. The pump parameter is varied through N . The dashed curve is from the semi-classical theory and the solid curve is from the micromaser theory calculated for $g = 18$ KHz and $\tau = 35\mu s$.

Chapter 6. Quasiprobability distributions for the micromaser field

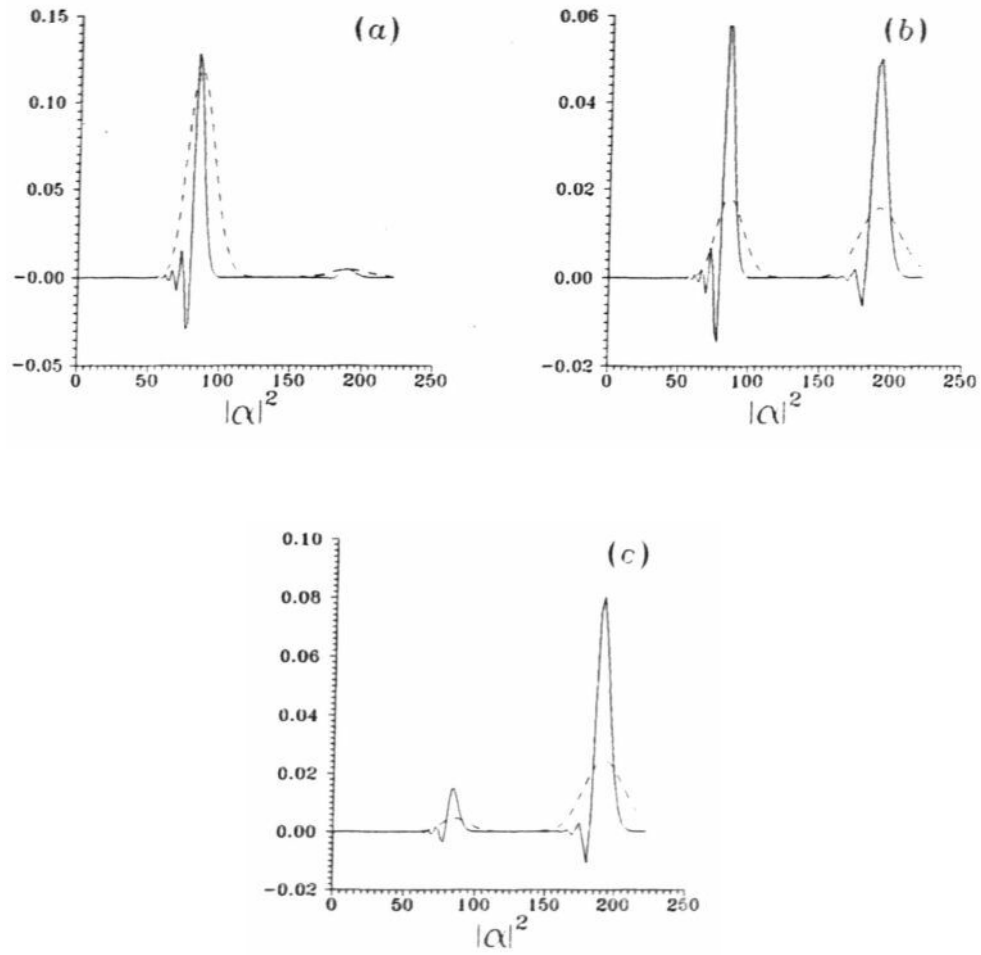


Figure 6.4: The Q-function (dashed curve) and the Wigner function (solid curve) corresponding to the three points (marked *a*, *b*, *c*) of Fig.6.3.

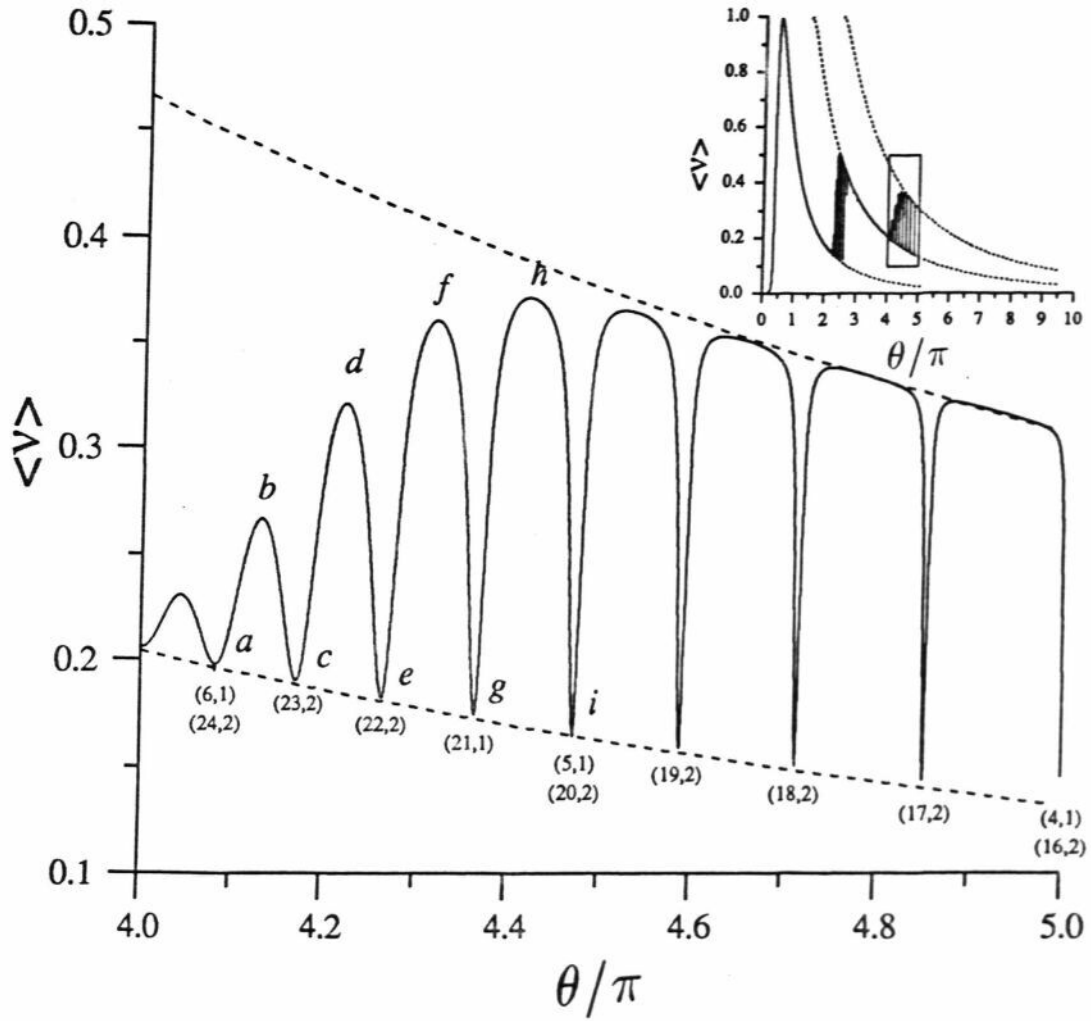


Figure 6.5: Normalised mean value of the photon number versus the pump parameter for a range which shows the trapping states ($n_b = 10^{-7}$, $N = 100$). Inset shows the phase transition region, a magnification of the boxed portion of which is shown in the main figure. The dashed curves are calculated from the semi-classical theory.

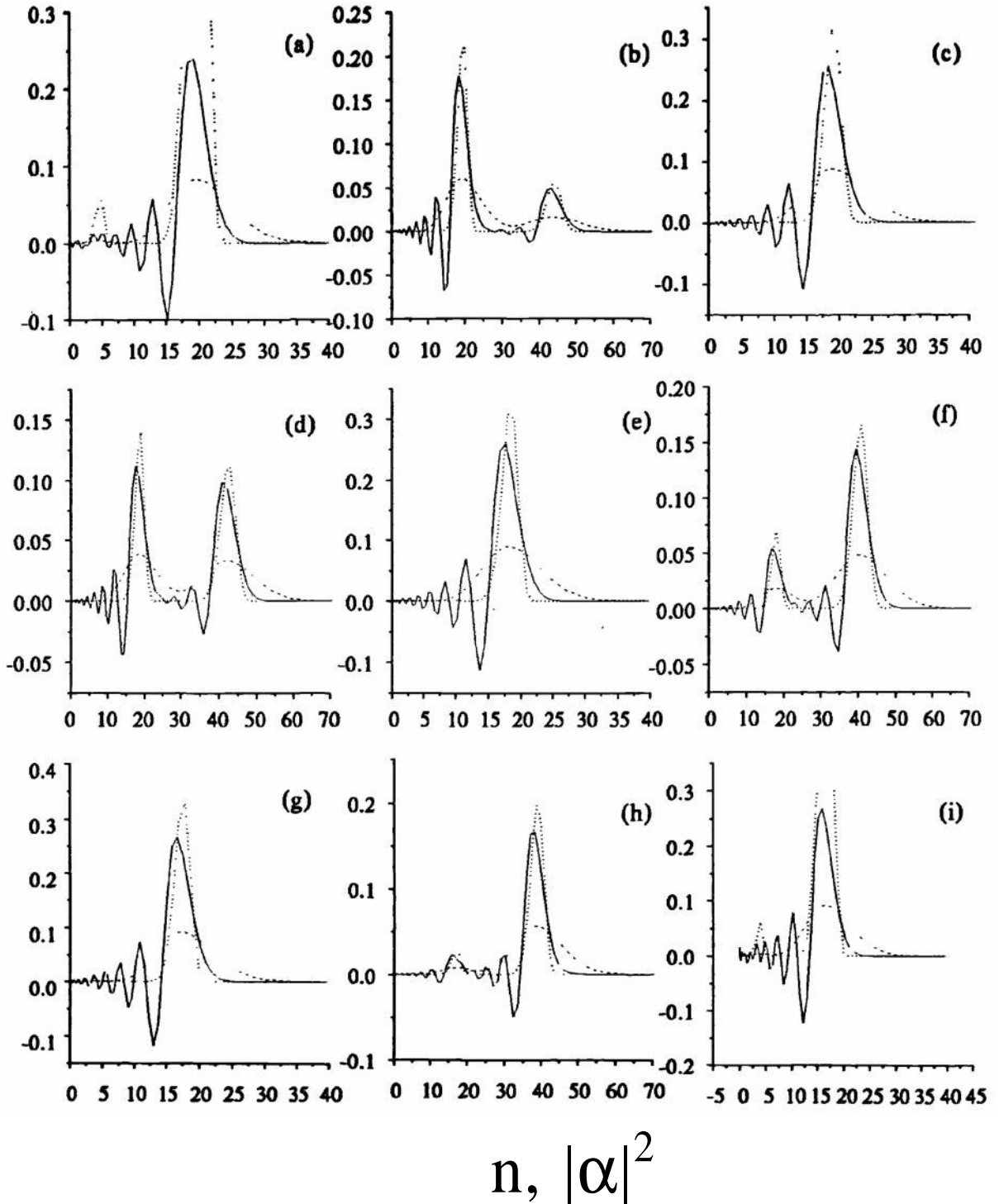


Figure 6.6: The Q-function (dashed curve) and the Wigner function (solid curve) as functions of $|\alpha|^2$, and p_n as a function of n (dotted curve) for various points indicated by the labels (a-i) in the Fig.6.4. To highlight the peaks corresponding to the trapping state with $9 = 1$, five times the value of the photon number distribution, p_n is plotted in plots (a) and (i).

References

- [1] M. Hillery, R.F. O'Connell, M.O. Scully and E.P. Wigner, Phys. Rep. 106, (1984).
- [2] Y. Kano, J.Phys. Soc. Jan. 19, 1555 (1964).
- [3] Y. Kano, J. Math. Phys. 6, 1913 (1965).
- [4] C.L. Mehta and E.C.G. Sudarshan, Phys. Rev. 138, 274 (1965).
- [5] E. Wigner, Phys. Rev. 40, 749 (1932).
- [6] R.J. Glauber, Phys. Rev. Lett, 10, 84 (1963).
- [7] E.C.G. Sudarshaa, Phys. Rev. Lett, 10, 277 (1963).
- [8] C.W. Gardiner, *Quantum Noise*, (Springer, Heidelberg, 1991).
- [9] W.H. Louisell, *Quantum Statistical Properties of Radiation*, (Wiley, New York, 1973).
- [10] P.D. Drummond and C.W. Gardiner. J. Phys. A: Math. Gen. 13, 2353 (1980).
- [11] G.S. Agarwal and E. Wolf, Phys. Rev. D 2, 2161 (1970).
- [12] G.S. Agarwal and E. Wolf, Phys. Rev. D 2, 2187 (1970).
- [13] G.S. Agarwal and E. Wolf, Phys. Rev. D 2, 2206 (1970).
- [14] K.E. Cahill and R.J. Glauber, Phys. Rev. 177, 1857 (1969).
- [15] K.E. Cahill and R.J. Glauber, Phys. Rev. 177, 1882 (1969).
- [16] P. Filipowicz, J. Javanainen and P. Meystre, J. Opt. Soc. Am. B 3. 906 (1986).
- [17] P. Meystre. G. Rempe and H. Walther. Opt. Lett. 13. 1078 (1988).
- [18] P. Filipowicz, J. Javanainen and P. Meystre, Phys. Rev. A 34, 3077 (1986).
- [19] L. Lugiato. M.O. Scully and H. Walther, Phys. Rev. A 36, 740 (1987).
- [20] G. Rempe, H. Walther and N. Klein, Phys. Rev. Lett, 58, 353 (1987).
- [21] G. Rempe. F. Schmidt-Kaler and H. Walther, Phys. Rev. Lett. **64**. 2783 (1990).

References

- [22] G. Rempe and H. Walther, Phys. Rev. A 42, 1G50 (1990).
- [23] G. Rempe and H. Walther, *Recent Developments in Quantum Optics*, (Proceedings of the International Conference on Quantum Optics, Hyderabad, 1991), edited by R. Inguva, (Plenum, New York, (1993)).
- [24] S. Arun Kumar and G.S. Agarwal, Phys. Rev. A 50, 680 (1994).
- [25] C. Wagner, R.J. Brecha, A. Schenzle and H. Walther, Phys. Rev. A 46, R5350 (1992).
- [26] C. Wagner, R.J. Brecha, A. Schenzle and H. Walther, Phys. Rev. A 47, 5068 (1993).
- [27] G.S. Agarwal and K. Tara, Phys. Rev. A 46, 485 (1992).
- [28] K. Tara, Ph.D. Thesis, submitted to the University of Hyderabad, 1993 (unpublished).
- [29] O. Benson, G. Raithel and H. Walther, Phys. Rev. Lett. 72, 3506 (1991).
- [30] A.M. Guzman, P. Meystre and E.M. Wright, Phys. Rev. A 40, 2471 (1989).